THE UNIVERSITY
of EDINBURGH

Investigating the role of a novel Type IV secretion system in *Legionella pneumophila*

Kate Mathers

MSc (by Research) Infection and Immunity

The University of Edinburgh

2015

Postgraduate research thesis declaration

I declare that this thesis has been composed solely by myself and that it has not been submitted, in whole or part, in any previous application for a degree. Except where stated otherwise by reference or acknowledgement, the work presented is entirely my own.

Abstract

A novel Type IV secretion system (T4SS) was identified in *Legionella pneumophila* isolates from the Edinburgh Legionnaires' disease outbreak in 2012. A phylogenetic reconstruction of the isolates shows four distinct clades, two of which share a region thought to encode the novel T4SS. In a *Galleria mellonella* infection model, strains with this T4SS caused more rapid killing than those without it. Furthermore, patients infected with isolates containing the novel T4SS required more clinical care intervention. This project aims to dissect the role of the novel T4SS in intracellular survival. Bioinformatic analysis showed that the T4SS is closely related to the *Legionella* genomic island-associated T4SS (LGI-T4SS) of *L. longbeachae.* Other bioinformatic tools were used to identify neighbouring genes predicted to encode T4SS-secreted effector proteins. The expression of these genes was then detected during broth culture and intracellular growth using RT-PCR. A range of techniques were employed in order to compare the intracellular survival, replication and virulence of representative isolates from each of the four clades. Macrophage-like cells were infected in a gentamicin protection assay to compare intracellular replication. DNA extracted from the infected cells at four time points was quantified by qPCR to measure replication of the bacteria over time. In addition, the level of host cell death and autophagy was compared in macrophage-like cells infected with representative isolates from each clade. The results indicate that the region encoding the novel T4SS originated in *L. longbeachae* and encodes at least one putative T4SS effector protein. Although no difference was observed in host cell death and autophagy during infection with representative isolates, the presence of the novel region correlates with a reduced rate of intracellular replication.

Lay summary

Type IV secretion systems (T4SSs) are protein structures used by bacterial cells to transfer genes and proteins into host cells. A novel T4SS was identified in *Legionella pneumophila* isolates from the Edinburgh Legionnaires' disease outbreak in 2012. It was previously shown that isolates with this T4SS cause more rapid killing than those without it. Furthermore, patients infected with isolates containing the novel T4SS required more clinical care intervention. This project aims to dissect the role of the novel T4SS in the intracellular survival of *L. pneumophila*. Bioinformatic analysis showed that the T4SS is closely related to a T4SS found in another species, *Legionella longbeachae.* A range of techniques were employed to compare the survival of isolates with and without the novel T4SS. Although no difference was observed in host cell death during infection with the different isolates, the presence of the novel T4SS appears to reduce the rate of replication inside host cells.

Contents

Chapter 1: Introduction

Legionnaires' disease

The first known outbreak of Legionnaires' disease occurred at an American Legion convention in Philadelphia in 1976 (Fraser *et al.*, 1977). Of 182 recorded cases, 29 were fatal and 147 required hospital care. The causative agent, *L. pneumophila* was isolated the following year from samples taken from the patients' lungs (McDade *et al*., 1977). Although more than 50 species of *Legionella* have now been identified, *L. pneumophila* is associated with more than 90% of Legionnaires' disease cases worldwide (Jarraud *et al.*, 2013).

Human infection by *L. pneumophila* occurs through the inhalation of contaminated aerosols from artificial aquatic environments such as air conditioning systems, cooling towers and hot tubs (Bartram, 2007). As water temperatures of 25 to 42°C are optimal for *Legionella* growth, these water systems can promote the rapid amplification of *Legionella* to high concentrations, thereby increasing the risk of infection (Kozak *et al*., 2013).

Once inside the human lung, *L. pneumophila* can cause acute alveolitis and bronchiolitis (Swanson and Hammer, 2000). However, human monocytes activated by the inflammatory cytokine interferon-γ can inhibit intracellular multiplication of the bacterium by overriding the ability of the bacteria to evade the lysosomal degradation pathway (Santic *et al.*, 2005). Therefore the majority of people exposed to *L. pneumophila* either do not become ill or suffer only a mild self-limiting infection (Newton *et al*., 2010).

The clinical symptoms of Legionnaires' disease include fever, non-productive cough, headache, breathing difficulties and diarrhoea (TSAI *et al.*, 1979). As these symptoms are indistinguishable from those of other forms of pneumonia, diagnostic tests must be carried out in order to establish the causative agent (Bartram, 2007). Most cases are now identified by urinary antigen tests, although cultures of either sputum or bronchoalveolar lavage may also be used (European Centre for Disease Prevention and Control, 2015).

The majority of individuals who develop Legionnaires' disease are elderly or immunocompromised (Berrington and Hawn, 2013). For example, 81% of European cases in 2013 occurred in people over 50 years of age (European Centre for Disease Prevention and Control, 2015). Further risk factors for the disease include cigarette smoking, immunosuppressant treatment and chronic lung disease (Swanson and Hammer, 2000). In Europe, the overall case-fatality rate is approximately 12%, although this varies considerably according to the severity of disease, the quality and time of treatment and other risk factors (Bartram, 2007).

Between 1994 and 2008, almost 54,000 cases were reported across 30 European countries (Joseph and Ricketts, 2010). The largest outbreak to date originated from the cooling towers of a city hospital in Murcia, Spain in 2001, where 449 cases were confirmed (García-Fulgueiras *et al.*, 2003).

Models of Legionnaires' disease

Early evidence for the effective treatment of Legionnaires' disease was provided using a guinea pig model of infection (Edelstein *et al.*, 1984). Intratracheal inoculation resulted in lung histopathology and bacteriology that was almost identical to that caused by Legionnaires' disease in humans. In this model, fatality rates were significantly reduced by treatment with either erythromycin, rifampicin, doxycycline or cotrimoxazole. More recently, the two antimicrobials fluoroquinolone and azithromycin were recommended for the treatment of human infections by the Infectious Diseases Society of America in 2007 (Mandell *et al.*, 2007).

A guinea pig model of infection was also used to test the efficacy of immunisation with the major secretory protein (MSP) of *L. pneumophila* (Blander and Horwitz, 1991b). This protein is a Zn^{2+} metalloprotease encoded by the *mspA* gene (Szeto and Shuman, 1990). Although the MSP is the most abundant protein in culture supernatants of the bacteria, it is not required for intracellular growth or destruction of human macrophages. Nevertheless, immunisation with the MSP was shown to induce significant protective immunity against aerosolised *L. pneumophila* in the guinea pig model (Blander and Horwitz, 1991b). Additionally, immunisation by aerosolised *L. pneumophila* membranes was also shown to induce protective immunity in the guinea pig model (Blander and Horwitz, 1991a). The guinea pig infection model has also been used to study host immune defences and to measure the relative virulence of different *Legionella* strains (Edelstein, 2013).

More recently, a DNA vaccine has been shown to protect the A/J mouse against *L. pneumophila* infection (Xu *et al*., 2012). This vaccine encodes a 29 kDa outer membrane protein and the Type IV pili protein (PilE) of *L. pneumophila*.

Legionella pneumophila

Legionella pneumophila is an aerobic, Gram-negative coccobacillus which multiplies inside freshwater and soil amoebae (Newton *et al.*, 2010, Chien *et al.*, 2004). The bacterium evades lysosomal degradation inside these cells through the formation of a specialised phagosomal compartment, known as the *Legionella*-containing vacuole (LCV) (Allombert *et al.*, 2013). This

mechanism also enables *L. pneumophila* to survive within alveolar macrophages, causing Legionnaires' disease (Brüggemann *et al.*, 2006). Outbreaks result from the inhalation of contaminated aerosols from various water sources, making *L. pneumophila* an opportunistic and accidental pathogen of humans (Bartram, 2007).

L. pneumophila replicates intracellularly in over 13 species of amoebae, including several species of *Acanthamoeba, Hartmannella* and *Naegleria* (Fields, 1996). During its life cycle in both amoebae and macrophages, *L. pneumophila* alternates between several distinct phenotypic forms (Garduno *et al.*, 2002). The replicative form (RF) is non-motile, thin walled and acid tolerant, whereas the mature intracellular form (MIF) is motile and resilient for survival in the extracellular environment (Dalebroux *et al.*, 2010). Furthermore, MIFs can resist detergent-mediated lysis and high pH conditions (Garduno *et al.*, 2002). The viable but non-culturable (VBNC) form is a dormant phenotype which enables the bacteria to survive in unfavourable environmental conditions (Al-Bana *et al.*, 2014).

L. pneumophila is taken up into host cells by phagocytosis (Newton *et al.*, 2010). Once inside the host cell phagosome, the bacterium initiates formation of the LCV (*Figure 1*) (Allombert *et al.*, 2013). This compartment resists fusion with lysosomes, protects the bacterium from immune detection and provides nutrients for intracellular replication (Xu and Luo, 2013, Horwitz, 1983b). Within the LCV, the bacteria differentiate into the RF (Swanson and Hammer, 2000). As the nutrients inside the LCV become depleted over time, the bacteria differentiate into the MIF, which is able to infect a new host cell.

In order to form the LCV, *L. pneumophila* recruits host cell mitochondria and endoplasmic reticulum (ER) vesicles to the surface of the phagosome within 5 minutes of internalisation (Tilney *et al.*, 2001). Next, the ER-derived membranes fuse with the LCV and the resulting LCV membrane gradually accumulates other materials from the host cell, including ribosomes, ubiquitinated proteins and vacuolar ATPases (Xu and Luo, 2013, Hubber and Roy, 2010). As a result of these modifications, the LCV membrane resembles that of the rough ER by approximately 4 hours post-infection (Horwitz, 1983a).

The outer surface of the LCV membrane is characterised by the accumulation of the membrane lipid phosphatidylinositol 4-phosphate (PI(4)P) and secreted bacterial proteins (Allombert *et al.*, 2013). As PI(4)P is a marker of the Golgi membrane, this feature favours the fusion of additional ER vesicles with the LCV membrane. Furthermore, phosphatidyl phosphoinositides act as anchors for several effector proteins secreted by the Dot/Icm T4BSS, as discussed below.

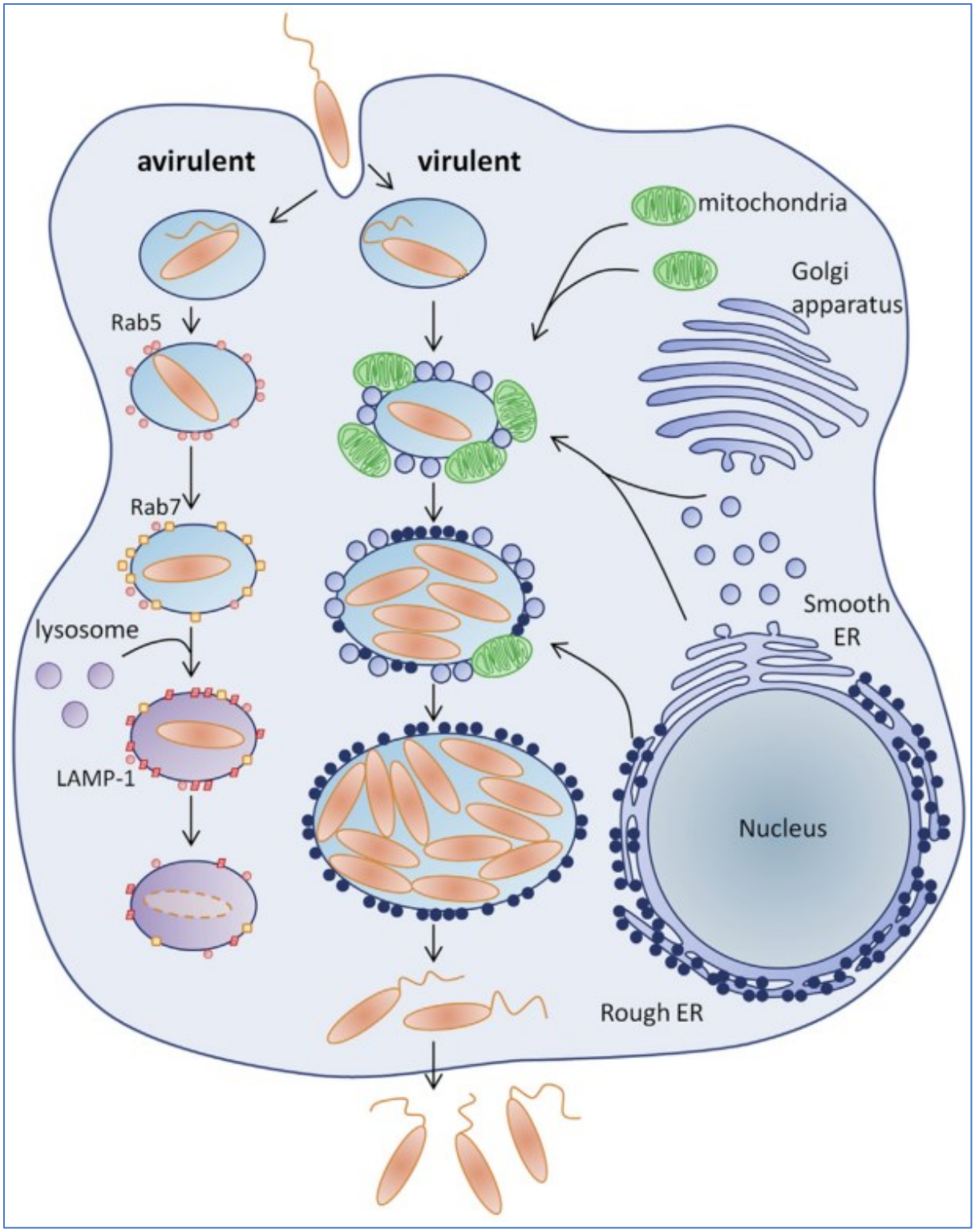

Figure 1 *LCV biogenesis by L. pneumophila (Allombert et al., 2013). Once inside the host cell, avirulent L. pneumophila are cleared via the endosomal pathway and fusion with lysosomes. In contrast, virulent L. pneumophila form the LCV by recruitment of mitochondria, ER-derived smooth vesicles and ribosomes. Inside the LCV, L. pneumophila escape lysosomal degradation and undergo replication.*

Host cell response

The autophagy pathway is activated as an immediate response to *Legionella* during infection of macrophages (Amer and Swanson, 2005). During autophagy, intracellular bacteria are packaged into double membrane-bound phagosomes, which undergo maturation before fusing with lysosomes (Xie and Klionsky, 2007). This fusion results in degradation of the bacteria by lysosomal hydrolases.

During autophagy, a protein called Atg8 undergoes a modification at its C-terminus, and is then covalently attached to the lipid phosphatidylethanolamine on the phagosome membrane (Ichimura *et al.*, 2000). This process has been shown to be essential to the autophagy pathway. However, some *L. pneumophila* strains secrete a cysteine protease called RavZ which inhibits the autophagy pathway by removing Atg8 from the membrane and removing the C-terminus modification necessary for lipid conjugation (Choy *et al.*, 2012).

Most inbred mouse strains are resistant to *L. pneumophila* infection (Hori and Zamboni, 2013). However, a murine model of Legionnaires' disease has been developed with mice of the A/J strain, which do support the growth of *L. pneumophila* (Brieland *et al.*, 1994). This variation in resistance is caused by different alleles encoding a Nucleotide-binding Oligomerisation Domain Leucine-Rich Repeat (NOD-LRR) protein called Neuronal Apoptosis Inhibitory Protein 5 (NAIP5) (also called Birc1e), a component of the NAIP5-NLRC4 inflammasome (Diez *et al.*, 2003).

In resistant macrophages, a 35-amino acid region of the *L. pneumophila* protein flagellin triggers activation of the inflammasome and the consequent proteolytic activation of caspase-1 (Lightfield *et al.*, 2008). Together with the NOD-like receptor (NLR) protein NLRC4 (also called Ipaf), NAIP5 is required for this flagellin-induced caspase-1 activation (Amer *et al.*, 2006). NAIP5 and caspase-1 both contribute to the activation of caspase-7, which promotes fusion of the LCV with the lysosome (Akhter *et al.*, 2009).

Active caspase-1 also induces a pro-inflammatory form of cell death called pyroptosis (Bergsbaken *et al.*, 2009). During pyroptosis, pores are formed in the plasma membrane, causing osmotic lysis and release of lactate dehydrogenase (Silveira and Zamboni, 2010). In addition, the pro-inflammatory cytokines IL-1β and IL-18 are activated and released from the cell (Bergsbaken *et al*., 2009).

In contrast, in human macrophage-like U937 cells, the transcriptional regulator NF-κB induces the up-regulation of anti-apoptotic genes in response to *L. pneumophila* infection (Losick and Isberg, 2006). The resulting anti-apoptotic pathway promotes survival of the host cell. Furthermore, the

secreted effector protein SidF specifically interacts with and inhibits two apoptotic proteins, BNIP3 and Bcl-rambo (Banga *et al.*, 2007).

Genetics

Approximately 66% of the *L. pneumophila* genome is differentially expressed during intracellular growth compared to growth in laboratory media (Faucher *et al.*, 2011). The number of genes expressed gradually increases during the first 18 hours of infection. Genes induced intracellularly include those involved in amino acid biosynthesis, amino acid uptake, iron uptake and glycerol catabolism.

Although all of the sequenced *L. pneumophila* strains contain a single circular chromosome between 3.3Mb and 3.5Mb in length, the gene content specific to each of four strains (Paris, Corby, Philadelphia and Lens) was found to be as high as 11% (Gomez-Valero *et al.*, 2009). This high level of plasticity between the genomes of different strains has been linked to frequent recombination events and horizontal gene transfer (Gomez-Valero *et al.*, 2011). For example, the horizontal transfer of *Legionella* chromosomal virulence genes by conjugal DNA transfer has been demonstrated between two *L. pneumophila* strains (Miyamoto *et al.*, 2003).

Another key feature of the *L. pneumophila* genomes is the presence of many genes encoding eukaryotic-like proteins and domains (Newton *et al.*, 2010). This suggests that the functional mimicry of eukaryotic pathways is a major survival strategy of these bacteria (Lomma *et al.*, 2009). Genes for these eukaryotic-like proteins are thought to have been acquired by horizontal transfer from their protozoan host cells (Cazalet *et al.*, 2004). This theory is supported by the fact that *L. pneumophila* is naturally competent for DNA transformation (Stone and Kwaik, 1999). Further evidence of horizontal gene transfer is the presence of a G+C bias in *Legionella* genes with eukaryotic motifs compared to other *L. pneumophila* genes (de Felipe *et al.*, 2005). This bias is indicative of genes that have been acquired from another species.

Virulence factors

The first *L. pneumophila* gene that was shown to be necessary for optimal infection of human macrophage-like cells was named the macrophage infectivity potentiator (*mip*) (Cianciotto *et al.*, 1989). This gene encodes a 24 kDa surface protein with peptidyl-prolyl *cis/trans* isomerase (PPIase) activity which catalyses the *cis/trans* isomerisation of prolyl peptide bonds in oligopeptides (Fischer *et*

al., 1992). The Guinea pig infection model has shown that the Mip protein contributes to the dissemination of *L. pneumophila* within the lung and to the spleen (Wagner *et al*., 2007). Mip was also shown to bind specifically to collagen and enables the bacteria to cross a barrier of lung epithelial cells and extracellular matrix.

Another cause of tissue damage during Legionnaires' disease is the release of the extracellular metalloprotease MSP, which causes tissue necrosis and acute pulmonary damage in guinea pigs (Baskerville *et al*., 1986). In addition, this protease has been shown to inhibit neutrophil chemotaxis (Rechnitzer and Kharazmi, 1992).

A Type I secretion system (T1SS) was recently shown to be required for host cell entry by *L. pneumophila* (Fuche *et al*., 2015). Furthermore, this secretion system was found to export the repeats-in-toxin (RTX) protein RtxA, which is involved in adherence, cytotoxicity and pore formation (Cirillo *et al.*, 2001). A Type II secretion system (T2SS) is also required for growth in the lungs of A/J mice (McCoy-Simandle *et al*., 2011). The *L. pneumophila* T2SS has been shown to export multiple effectors and to reduce the cytokine response of infected host cells (Tyson *et al*., 2013). Proteins secreted via the T2SS are required for the infection of macrophages and the amoeba *Acanthamoeba castellanii*.

Type IV secretion systems

Type IV secretion systems (T4SSs) are multi-subunit protein structures found in several species of pathogenic Gram-negative bacteria (Christie *et al.*, 2005). They span both bacterial cell membranes and the cell wall, enabling them to facilitate horizontal gene transfer and the secretion of effector proteins into eukaryotic cells. They are ancestrally related to bacterial conjugation systems, which transfer DNA through the mating pair formation (Mpf) complex (Christie, 2001). However, the T4SSs are unique among bacterial secretion systems due to their ability to transfer both proteins and nucleoprotein complexes (Juhas *et al.*, 2008). The translocation machinery comprises a set of 26 proteins, encoded by 26 genes across two loci (Ensminger and Isberg, 2009, Gomez-Valero *et al.*, 2009). In addition, most T4SSs have three ATPases that power the secretion machinery (Fronzes *et al.*, 2009).

The T4SS genes are named using either the prefix *vir* after those on the *Agrobacterium tumefaciens* Ti plasmid or *tra* after those on the *Escherichia coli* F plasmid (Juhas *et al.*, 2008). For example, the *virB4/traC* gene encodes the VirB4/TraC protein, the only subunit found in all T4SSs to date (Alvarez-Martinez and Christie, 2009).

Several species of pathogenic bacteria use T4SS-secreted effector proteins to subvert host cell physiology through a variety of distinct mechanisms (Christie, 2001). For example, the *A. tumefaciens* T4SS (Figure 2) mediates the transfer of a segment of bacterial oncogenic plasmid into recipient plant cells (Vergunst *et al.*, 2000). In *Helicobacter pylori*, the protein CagA is translocated through a T4SS into the mammalian host cell, where it triggers cytoskeletal rearrangements (Segal *et al.*, 1999a). The pertussis toxin is secreted through a T4SS in *Bordetella pertussis* called the pertussis toxin exporter (Ptl) (Locht *et al.*, 2011). Inside the mammalian host cell, this five-subunit toxin catalyses ADP-ribosylation of G proteins, thereby interfering with host cell signalling pathways and metabolism.

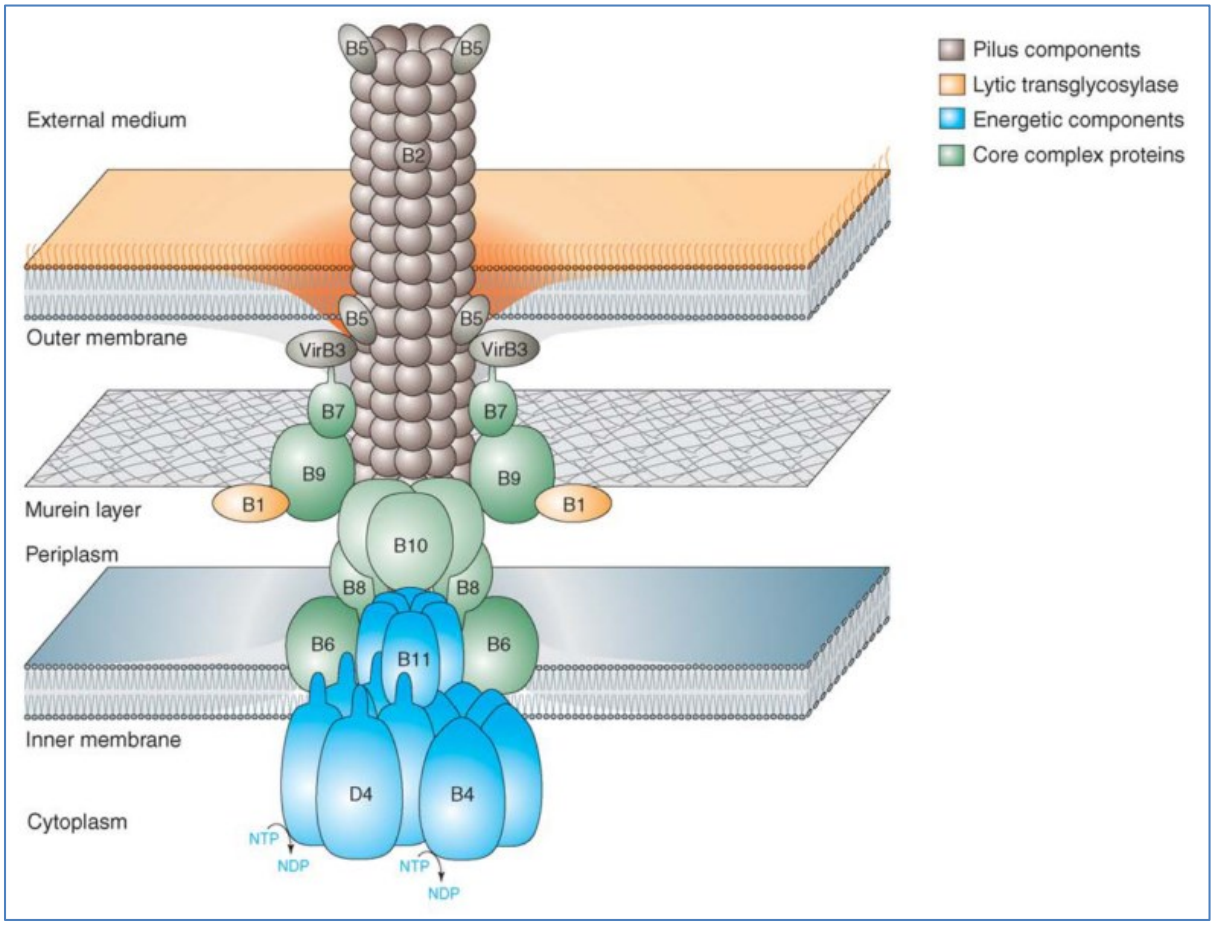

Figure 2 *Structure of the prototypical A. tumefaciens VirB/D4 T4ASS (Backert and Meyer, 2006). The subunits VirB2 and VirB5 form an extracellular pilus (Fronzes et al., 2009). The membrane proteins VirB6, VirB8 and VirB10 are thought to form the inner membrane channel. The ATPases VirB4, VirB11 and VirD4 power the translocation of substrates.*

Each of the sequenced *L. pneumophila* strains contain multiple T4SSs from three main classes: Type IVA (T4ASS), Type IVB (T4BSS) and genomic island-associated (GI-T4SS) (Table 1) (Isberg *et al*., 2009). T4ASSs are related to the archetypal *A. tumefaciens* VirB/D4 T4ASS (Vergunst *et al.*, 2000). The F-type and P-type T4ASSs encode conjugative pili that facilitate mating *(Gomez-Valero et al.*, 2014).

The F-type T4ASS encodes long, flexible pili, whereas the P-type T4ASS encodes short, rigid pili (Lawley *et al*., 2003). The remaining secretion systems are described below.

Type IV secretion systems		Type IVB	Type IVA			GI-type
Chromosome		Dot/Icm	P-type	F-type	Lvh	
L. pneumophila	Paris	1	-	-	1	2
	Lens	1	-	-	1	1
	Philadelphia	1	-	1	1	1
	Corby	1	2	-	-	2
	Lorraine	1	1	-	-	1
	HL06041035	1	-	-	1	2
	130b	1	1		2	2
L. longbeachae	NSW-150	1	1	1	-	-
L. longbeachae	D-4968	1	-	1	1	1
L. hackeliae	ATCC35250	1	-	-	-	1
L. micdadei	ATCC33218	1	-	-	1	1
L. micdadei	02/42	1	1	-	1	-
L. fallonii	ATCC700992	1	-	1	-	1

Table 1 *Type IV secretion systems present in 13 Legionella genomes (Gomez-Valero et al., 2014).*

Lvh Type IVA secretion system

The *L. pneumophila* Lvh T4ASS is encoded by 11 *lvh* (*Legionella vir* homologue) genes and 5 *lvr* (*Legionella vir* region) genes (Figure 3) (Segal *et al.*, 1999b). This secretion system has been identified in 147 of 217 *L. pneumophila* strains, including Philadelphia-1, Paris and Lens (Cazalet *et al.*, 2008).

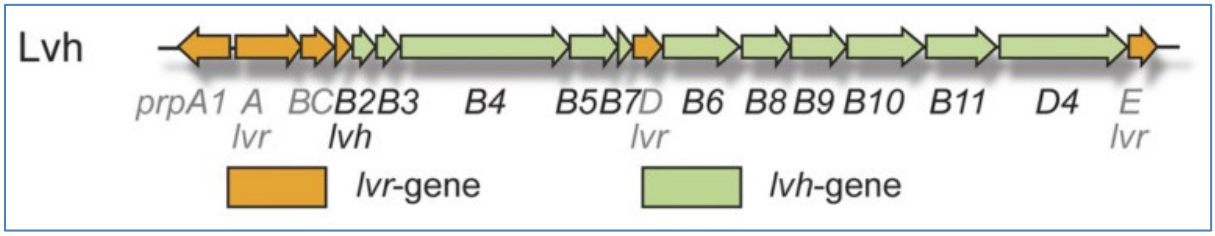

Figure 3 *Genetic organisation of the L. pneumophila Lvh T4ASS (Schroeder et al., 2010). The T4ASS subunits are encoded by lvr genes (lvrA, -B, -C, -D and –E) and lvh genes (lvhB2, -B3, -B4, -B5, -B7, -B6, -B8, -B9, -B10, -B11 and -D4). The gene prpA1 encodes a putative phage repressor protein (Samrakandi et al., 2002).*

Although the Lvh T4ASS is not essential for multiplication within macrophages, it has been found more frequently in strains associated with human disease (Hilbi *et al.*, 2001, Samrakandi *et al.*,

2002). This secretion system is also required for entry and intracellular multiplication in *dot/icm* mutants following conditions designed to mimic the spread of *L. pneumophila* from water and amoebae (Bandyopadhyay *et al*., 2007).

In the Philadelphia-1 strain, the *lvh* region is found in a plasmid-like element of 45kb that is present either within the chromosome or in circular episomal form (Chien *et al.*, 2004). Similarly, in the Paris strain, the *lvh* region is encoded in a 36kb region that is either integrated in the chromosome or excised as a multicopy plasmid (Cazalet *et al*., 2004). One study found that the chromosomal integration of the plasmid was growth-phase dependent, occurring during the exponential phase (Doléans-Jordheim *et al*., 2006).

Dot/Icm Type IVB secretion system

The Dot/Icm T4BSS has been described as the essential virulence determinant of *L. pneumophila* (Harding *et al*., 2012). It is encoded by the *dot/icm* genes, which were characterised by two different groups between 1992 and 1993 (Figure 4) (reviewed in Rolando and Buchreiser, 2014). The *dot* (defective in organelle trafficking) locus was shown to be crucial for intracellular growth, organelle recruitment and inhibition of phagosome-lysosome fusion (Berger and Isberg, 1993). Similarly, the *icm* (intracellular multiplication) locus is necessary for intracellular replication in human macrophages (Marra *et al.*, 1992). Since then, the *L. pneumophila* Dot/Icm T4BSS has also been shown to be required for LCV biogenesis and the secretion of many effector proteins into the host cell (Allombert *et al*., 2013).

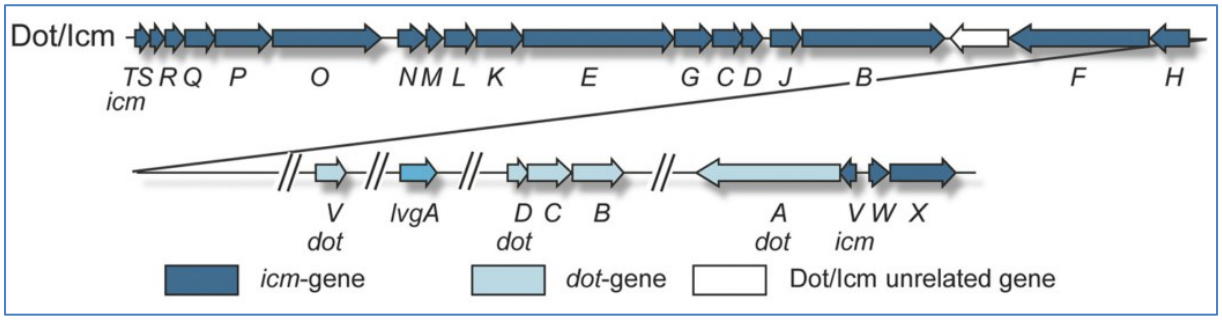

Figure 4 *Genetic organisation of the L. pneumophila Dot/Icm T4BSS (Schroeder et al., 2010). The T4BSS subunits are encoded by icm genes (icmT, -S, -R, -Q, -P, -O, -N, -M, -L, -K, -E, -G, -C, -D, -J, -B, -F, -H, -V, -W and -X) and dot genes (dotV, -D, -C, -B and -A). These are located at 5 loci across 2 distinct regions of the chromosome. The gene lvgA is thought to encode a virulence protein (Edelstein et al., 2003).*

The genes encoding the Dot/Icm T4BSS are constitutively expressed by *L. pneumophila* inside human macrophages and when cultured in AYE broth (Faucher *et al.*, 2011). However, the genes

encoding several translocated effector proteins are strongly induced inside human cells, as 64% of the known Dot/Icm effector proteins are induced during intracellular growth.

Dot/Icm T4BSS-secreted effector proteins

At least 275 bacterial effector proteins are secreted via the *L. pneumophila* Dot/Icm T4BSS (reviewed in Prashar and Terebiznik, 2015). Some of these Dot/Icm effector proteins associate with the LCV and recruit host proteins involved in trafficking (Newton *et al.*, 2010). For example, SidM (also called DrrA) is a Dot/Icm effector involved in the recruitment of ER-derived vesicles to the LCV membrane (Prashar and Terebiznik, 2015). After translocation into the host cell, SidM becomes anchored to PI(4)P on the cytoplasmic face of the LCV membrane (Brombacher *et al.*, 2009). It then binds specifically to the host protein Rab1 and catalyses Rab1 activation (Ninio and Roy, 2007). As Rab1 regulates vesicle trafficking from the ER to the Golgi, this interaction mediates the fusion of the ER and LCV membranes (Prashar and Terebiznik, 2015).

Ankyrin B (AnkB) is the only Dot/Icm effector that has been shown to be essential for *L. pneumophila* proliferation inside both macrophages and protozoan host cells (Price *et al.*, 2009). AnkB anchors to the cytosolic face of the LCV membrane, where it interacts with the host SCF1 ubiquitin ligase complex to generate polyubiquitinated proteins (Price *et al.*, 2010). The ubiquitin-proteasome system then recognises the ubiquitin chains and degrades the associated proteins, generating amino acids for intracellular bacterial proliferation (Price *et al.*, 2011).

After translocation into the host cell, the Dot/Icm effector SidK specifically interacts with the catalytic unit of the host vacuolar ATPase, the enzyme responsible for organelle acidification (Xu *et al.*, 2010). This interaction inhibits ATP hydrolysis and proton translocation, thereby preventing acidification of the LCV.

RomA (also called LegAS4) is a Dot/Icm effector with methyltransferase activity that modifies the epigenetic state of host cell chromatin (Li *et al.*, 2013). This effector contains an evolutionarily conserved eukaryotic motif called the SET domain, found in proteins that modulate gene activity (Jenuwein *et al.*, 1998). Inside the host cell, RomA localises to the nucleus, where it methylates lysine 14 (K14) of histone H3, thereby repressing gene expression (Rolando *et al.*, 2013). Nearly 5,000 H3K14 methylated promoter regions have been identified, including those involved in innate immunity. Furthermore, RomA deletion mutants show significantly reduced replication in host cells (Rolando *et al.*, 2013).

Other host cell targets of the effector proteins include GTPases, protein translation and ubiquitination pathways (Newton *et al*., 2010, Isberg *et al*., 2009). However, there is thought to be considerable functional redundancy among the effectors as inactivation of individual effector genes rarely causes a severe defect in intracellular replication (Newton *et al*., 2010).

Genomic island-associated T4SS

Genomic islands are large chromosomal regions that form mobile genetic elements and are thought to play an important role in the evolution and adaptation of bacteria as they enable new traits to be acquired rapidly (Dobrindt *et al*., 2004). It has been suggested that these elements may have evolved from bacteriophages or plasmids. Some are referred to as pathogenicity islands as they are found more frequently in pathogenic variants than non-pathogenic variants (Dobrindt *et al.*, 2004).

GI-T4SSs are located within genomic islands and encode the conjugation machinery required for transfer of the associated element (Wee *et al.*, 2013). Therefore they enable genomic islands to mobilise and spread through a bacterial population, playing a key role in bacterial virulence, evolution and adaptation (Juhas *et al.*, 2008). Despite strong conservation of the GI-T4SS, there are significant differences in the mobility and expression of the genomic islands harbouring these genes.

The GI-T4SS was first identified on the genomic island ICE*Hin*1056, a vector encoding antibiotic resistance in *Haemophilus influenza* (Juhas *et al.*, 2007). This GI-T4SS forms a conjugative pilus that is responsible for the transfer of the genomic island. GI-T4SSs have since been found in several other species, including *Pseudomonas aeruginosa*, *Salmonella enterica* and *Salmonella bongori* (Juhas *et al.*, 2008).

In *P. aeruginosa,* the genomic island pKLC102 contains a cluster of *pil* genes, which encode Type IV thin sex pili (Klockgether *et al.*, 2004). The virulent *P. aeruginosa* strain PA14 also contains a pathogenicity island called PAPI-1 (Harrison *et al.*, 2010). This encodes a Type IVB pilus that transfers PAPI-1 into recipient *P. aeruginosa* strains during co-culture (Carter *et al.*, 2010).

The *S. enterica* serovar Typhi has a pathogenicity island called SPI-7 which contains an operon encoding Type IV pili (Zhang *et al.*, 2000). These pili are used for entry into human intestinal epithelial cells. A related genomic island called ICE*Sb*1 has been identified in *S. bongori* (Seth-Smith *et al.*, 2012). ICE*Sb*1 also contains genes responsible for replication, Type IV pili, conjugation and integration.

Legionella GI-T4SS

Legionella GI-T4SSs (LGI-T4SSs) are substantially divergent from other GI-T4SSs and represent a novel clade of GI-T4SSs only found in this genus (Wee *et al.*, 2013). Nevertheless, they are highly conserved across *Legionella* strains. LGI-T4SSs were found in eight of the nine *Legionella* genome sequences publicly available in 2013, including those of *L. pneumophila*, *L. longbeachae* and *L. drancourtii*. Furthermore, the genomes of *L. pneumophila* Paris, Corby and 130b were found to encode two distinct LGI-T4SSs, denoted LGI-1 and LGI-2. The LGI-T4SS gene cluster was found to be associated with several cargo genes, including those encoding antibiotic resistance and virulence factors.

The LGI-T4SS cluster consists of 24 genes, designated *lvrRABC* and *lgiA-T* (*Figure 5*) (Wee *et al.*, 2013). At the 5' end of the LGI-T4SS cluster, the first four genes (*lvrRABC*) form a regulatory module unique to *Legionella*. This sequence of genes is also present upstream of the Lvh, P-type and F-type T4ASSs in *Legionella,* suggesting a role in coordinating the T4SS expression.

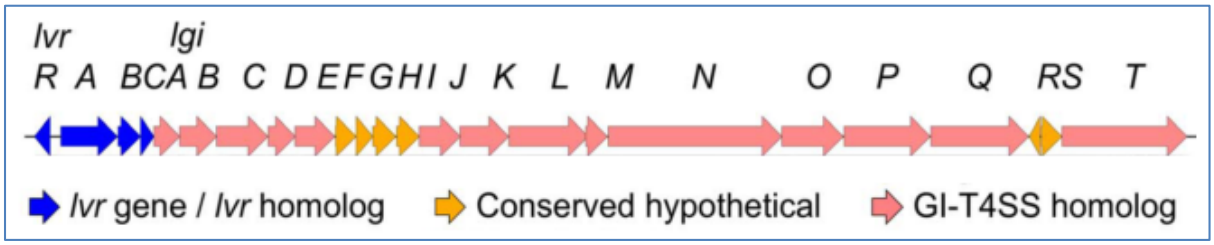

Figure 5 *Genetic organisation of the LGI-T4SS (Wee et al., 2013).*

The *lvrR* gene encodes domains that are homologous to those involved in the regulation of SOS-response genes in *Escherichia coli* (Wee *et al.*, 2013). In addition, the protein encoded by *lvrC* is a homologue of CsrA, a protein that regulates the change between the expression of replicative and transmissive traits (Gomez-Valero *et al.*, 2011, Molofsky and Swanson, 2003). This suggests that the associated genomic island may be excised during a specific growth phase or in response to certain conditions.

A continuous stretch of 20 genes (*lgiA-T*) is well conserved across all 14 LGI-T4SS clusters (Wee *et al.*, 2013). Thirteen of these *lgi* genes are homologous to genes found in other previously characterised GI-T4SSs such as ICE*Hin*1056, and the gene order is largely conserved. Of these homologous genes, only nine shared some sequence similarity with genes encoding well characterised T4SS subunit proteins: PilL, TraG, TraW, TraB, TraC, TraU, PilT, TraG and TraD. These nine subunits play important roles in the formation and stabilisation of the conjugative pilus, as well as providing an energy source via ATPases for the assembly of the T4SS complex.

The LGI-T4SSs are all located on genomic islands, where they are flanked by variable genomic regions (Wee *et al.*, 2013). This indicates multiple insertion, deletion and translocation events, typical of genomic islands and other mobile genetic elements. The LGIs are all found within hypervariable regions of the genome, adjacent to tRNA genes, which are typical recognition sites for site-specific recombinases such as integrases and transposases, suggesting that these regions are hotspots for the acquisition of horizontally acquired DNA.

The conservation of the LGI-T4SS cluster as a predominantly intact stretch of at least 20 genes suggests that it plays an important role in the life cycle of *Legionella* (Wee *et al.*, 2013). To show that these genes are being maintained by selection, rather than evolving neutrally, selection analyses have been performed on alignments of 15 conserved genes, estimating the ratio of the rate of non-synonymous substitutions per non-synonymous site (dN) to the rate of synonymous substitutions per synonymous site (dS) for each gene (Wee *et al.*, 2013). Genes that are evolving neutrally, suggesting that they are not beneficial, are expected to have a dN/dS ratio of one or close to one, whereas genes that are evolving under selection pressures, suggesting that they are beneficial, should have a dN/dS ratio of significantly less than one. It was found that all 15 genes in the LGI-T4SS clusters have a dN/dS that is significantly less than one ($p<0.01$). This provides further evidence that the LGI-T4SSs have been evolving under selection pressures, and may therefore be beneficial to the survival of *Legionella*.

The LGI-T4SS of *L. pneumophila* strain Corby is located on a *Legionella* genomic island (LGI-2) that can undergo horizontal transfer by conjugation and is integrated into a specific site of the recipient genome (Lautner *et al.*, 2013). These findings indicate that this LGI-T4SS encodes a functional conjugation system.

Edinburgh 2012 Legionnaires' disease outbreak

From May to June 2012, there were 50 confirmed and 49 suspected cases during an outbreak of Legionnaires' disease in Edinburgh (McCormick *et al.*, 2012). Of these cases, 3 were fatal and 71 required hospital care. Although the source of the outbreak has not been established, it is thought to have originated from nearby cooling towers. The 2012 Edinburgh outbreak was caused by several genetic subtypes of *L. pneumophila* Sg1, mAb subgroup Knoxville, sequence type (ST)191 (McAdam *et al.*, 2014). Whole genome sequencing and phylogenetic reconstruction revealed four distinct subtypes (A to D) among the isolates from 15 patients (Figure 6). For patients 10, 11 and 15 the multiple isolates obtained from each were identical, suggesting that the short incubation periods did not support extensive within-host diversification. The short timescale between exposure to and isolation of the

pathogen during the outbreak and the lack of person-to-person transmission for *L. pneumophila* strongly suggest that the genetic subtypes of ST191 existed in the outbreak source prior to release. Therefore it is likely that the subtypes evolved from a recent progenitor within the water reservoir by a combination of gene mutation, recombination and horizontal gene transfer.

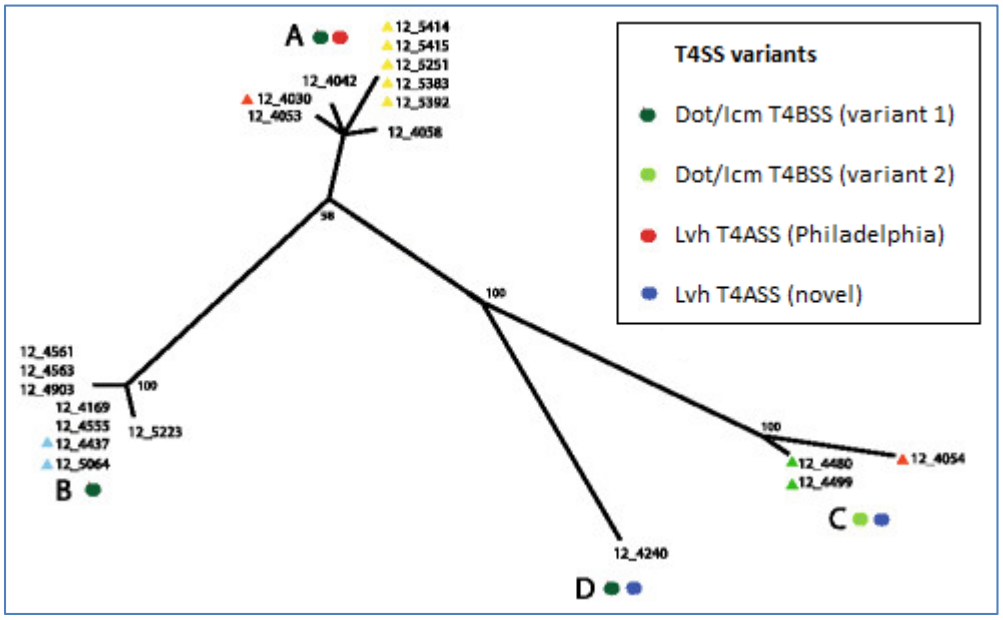

Figure 6 *Maximum likelihood un-rooted radial phylogeny of outbreak isolates, showing the distribution of T4SS variants across subtypes A to D (McAdam et al., 2014). Maximum likelihood bootstrap values are displayed for each node. Coloured triangles indicate multiple isolates from the same patient.*

Several regions of difference were identified among the isolates examined, including three genetic elements encoding T4SSs (McAdam *et al.*, 2014). The authors found that all nine isolates in one clade contained an Lvh T4ASS which shared 100% nucleotide identity with a genetic element in the genome of the Philadelphia 1 strain, derived from the original Legionnaire's disease outbreak in Philadelphia in 1976. However, isolates belonging to clades C and D had a novel T4SS-like region not present in the genomes of the other outbreak isolates (Figure 7). This region contains 46 predicted coding sequences, including homologues of *lvrA, lvrB, lvrC* and *virB*, suggesting a possible role as a novel T4SS. Additionally, all isolates contained a copy of the T4BSS encoding the Dot/Icm system, but a high density of polymorphic sites at the *dotA/icmVWX* locus differentiated the Dot/Icm T4BSS into two distinct variants.

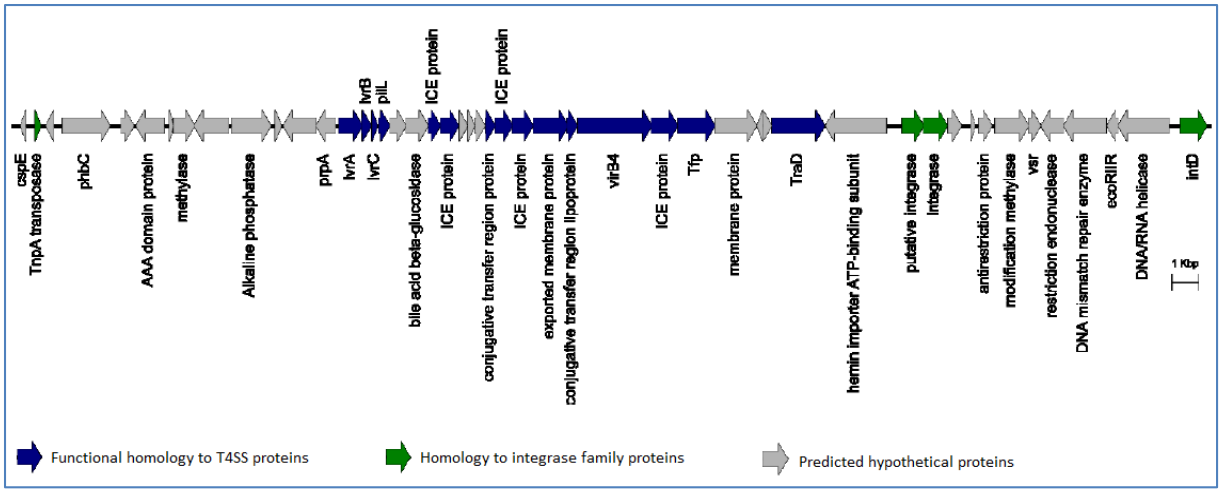

Figure 7 *Schematic diagram of the novel T4SS region present in isolates from clades C and D (McAdam et al., 2014). Arrows represent predicted coding sequences.*

Variation in the complement of T4SSs encoded by different genetic subtypes was shown to correlate with virulence in a *Galleria mellonella* model of infection (Figure 8) (McAdam *et al.*, 2014). Considerable strain-dependent variation in *G. mellonella* host survival was observed after infection, and a significant difference in killing capacity was identified between groups of isolates with unique combinations of T4SSs. In particular, strains with the novel putative T4SS resulted in more rapid killing of *G. mellonella* larvae than strains without it. There was no significant difference between isolates containing different variants of the Dot/Icm T4SS

The small number of patients infected with the subtype containing the novel T4SS was not sufficient for a robust statistical analysis and there was no statistically significant difference in clinical disease indicators between patients infected with strains containing the novel T4SS and those infected with strains lacking the novel T4SS (McAdam *et al.*, 2014). However, patients with the novel T4SS required more clinical care intervention, including higher intensive care unit (ICU) admission, a higher proportion requiring mechanical ventilation, and fewer ICU-free days.

The molecular mechanisms underlying the virulence of strains harbouring the novel T4SS are unknown. This project aims to address the hypothesis that this system provides *L. pneumophila* with an intracellular survival benefit compared to strains lacking this system.

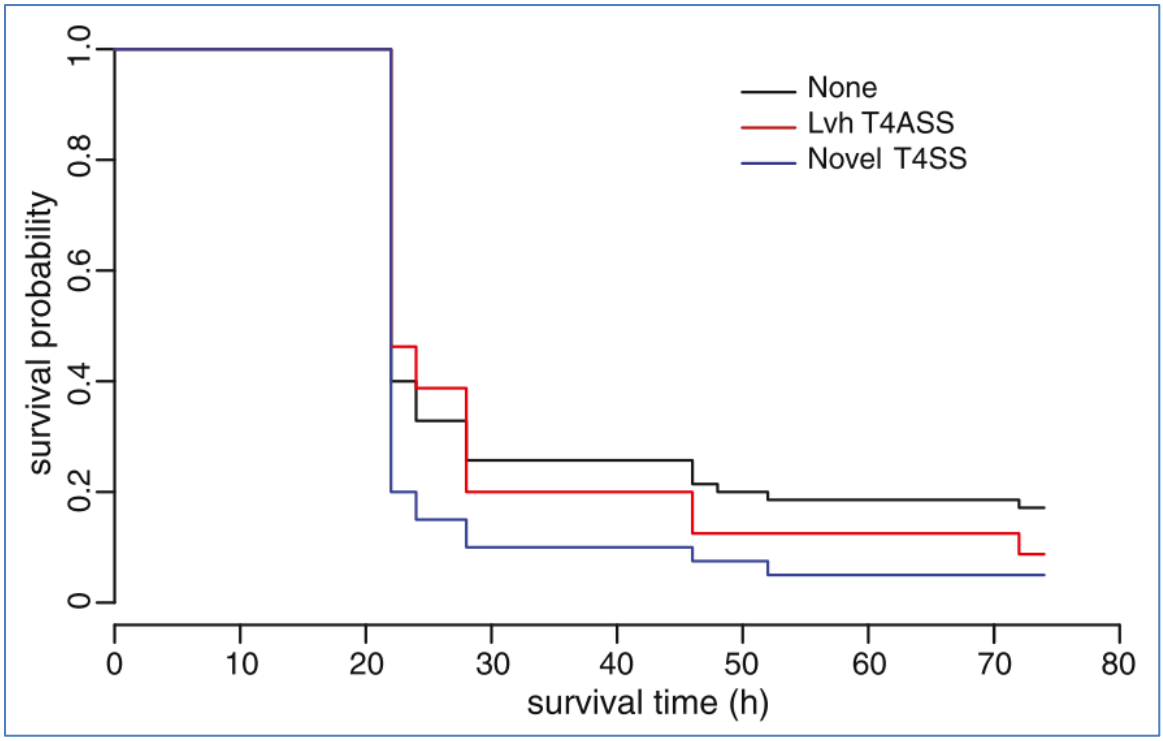

Figure 8 *Virulence of outbreak isolates in G. mellonella model of infection (McAdam et al., 2014). Survival curves represent the mean for isolates grouped according to the presence of each T4SS. Larvae infected with isolates encoding the novel T4SS had a lower survivability to those infected with other isolates (P = 0.04).*

Aims and objectives

Aim: To determine the role of a novel Type IV secretion system in the increased virulence of clade C and D *L. pneumophila* isolates.

A novel Type IV Secretion System (T4SS) was identified in patient isolates from the Edinburgh Legionnaire's disease outbreak in 2012 (McAdam *et al.*, 2014). A phylogenetic reconstruction of the isolates shows four distinct subtypes, two of which share a region thought to encode a novel T4SS. In a *Galleria mellonella* infection model, the presence of this T4SS correlated with increased virulence. This project aims to dissect the role of the novel T4SS in intracellular survival using a macrophage model of infection.

Objectives:

- Perform a bioinformatics analysis of the novel genes to identify possible origins and functions.
- Detect the expression of novel genes in broth culture and infected macrophage-like cells.
- Compare intracellular replication rates of *Legionella* from each clade.
- Compare rate of cell death in macrophage-like cells infected with *Legionella* from each clade.

Chapter 2: Materials and methods

Bioinformatics

Identification of genes unique to clades C and D

Orthologous genes between the representative isolates listed below were defined using the OrthoMCL algorithm (Li *et al.*, 2003) with the following parameters: minimum 80% coverage in BLAST pairwise alignments, minimum 85% sequence identity in BLAST query/subject pairs, filtered by 50% length difference within clusters. Unique genes were mapped to the genome of clade D strain 12_4240 using the DNAPlotter application (Carver *et al.*, 2009).

Clade	Representative isolate	Accession number
A	12_5415	NZ_CCZU00000000
B	12_5064	NZ_CCZP01000000
C	12_4499	NZ_CDCY00000000
D	12_4240	NZ_CCZI00000000

Analysis of the novel T4SS

Pairwise nucleotide sequence identity analyses of the T4SS and 39-kb region were performed using the Basic Linear Alignment Search Tool (BLASTn) (http://www.ncbi.nlm.nih.gov/blast) (Altschul *et al.*, 1990). Linear comparison figures were generated using EasyFig (Sullivan *et al.*, 2011). The LGI-T4SS phylogenetic tree was constructed using the BLAST tree view (http://www.ncbi.nlm.nih.gov/blast/treeview/treeView.cgi). The strains used are listed below.

Species	Strain	Accession number	LGI-T4SS	LGI-T4SS locus tags
L. pneumophila	Paris	CR628336.1	LGI-1	lpp1075 - lpp1055
	12_4240	NZ_CCZI00000000	39-kb region	PROKKA_00671 – PROKKA_00693
L. longbeachae	D-4968	NZ_ACZG01000001.1		LLB_1169 – LLB_1191

Species	Strain	Accession number	LGI-T4SS	*lgiN* locus tag
L. pneumophila	Alcoy	CP001828	LGI-1	lpa_01507
	Corby	CP000675	LGI-1	LPC_2290
			LGI-2	LPC_1874
	Philadelphia 1	AE017354	LGI-1	lpg0989
	Paris	CR628336.1	LGI-1	lpp1059 - lpp1060
			LGI-2	lpp2392
	12_4240	NZ_CCZI00000000	39-kb region	PROKKA_00687
			50-kb region	PROKKA_01789
L. longbeachae	D-4968	NZ_ACZG01000001.1		LLB_1185

Prediction of T4SS-secreted effector proteins and eukaryotic-like motifs

The classifier T4EffPred was used to predict whether or not each of the 31 genes unique to clade C and D encode T4SS effector proteins (http://bioinfo.tmmu.edu.cn/T4EffPred/prediction.html) (Zou *et al.*, 2013). The eukaryotic linear motif resource ELM was used to identify any eukaryotic motifs present in the seven predicted T4SS effector proteins (http://elm.eu.org) (Dinkel *et al.*, 2013).

Bacteriology

Growth of representative *L. pneumophila* isolates

The *L. pneumophila* isolates were resuscitated from frozen glycerol stocks on BCYE agar plates (CYE agar plates with *Legionella* BCYE growth supplement (VWR Chemicals)) at 37°C for 48 hours, then cultured in broth (0.5% yeast extract, 1% bovine serum albumin and *Legionella* BCYE growth supplement) at 37°C with shaking.

Triton X-100 assay

A broth culture of *L. pneumophila* Paris was diluted in broth to an OD_{600} of 0.5 (approximately 10^9 bacteria/ml) using the Utrospec 2100 pro UV/visible spectrophotometer (Amersham Biosciences), then further diluted in broth to approximately 10^6 bacteria/ml. 1ml of the diluted culture was added to 3 microcentrifuge tubes, then centrifuged at 13,000 x g for 1 minute. The resulting pellets were resuspended in 1ml of either 0%, 0.05% or 0.1% Triton X-100 in PBS. After incubation for 5 minutes at room temperature, each suspension was serially diluted in PBS, then 10µl of each dilution was plated on BCYE agar. The plates were incubated at 37°C until colonies were visible.

Growth curve in broth culture

L. pneumophila isolates from glycerol stocks were resuscitated on CYE agar plates with *Legionella* BCYE growth supplement (VWR Chemicals) at 37°C for 48 hours, then 3 colonies from each strain were cultured in broth at 37°C for 48 hours. OD_{600} was adjusted to 0.02 in broth or DMEM using the Utrospec 2100 pro UV/visible spectrophotometer (Amersham Biosciences). 200µl of each diluted sample was added to a 96-well tissue culture plate. Growth was quantified hourly for 4 days by OD_{600}

using the FLUOstar Omega microplate reader (BMG LabTech) set at 37°C and shaking. Data was analysed by the student's 2-sample t-test using Minitab® 17 statistical software.

Molecular methods

CTAB extraction of L. pneumophila genomic DNA

Genomic DNA from a representative strain of each clade was extracted. For each strain, 1.5ml of overnight culture was centrifuged at 13,000 x g for 5 minutes. After removal of the supernatant, the cells were vortexed in 567µl Tris-EDTA buffer (10mM Tris-HCl (pH 8.0) and 1mM EDTA (pH 8.0)). The cells were then incubated with 30µl 10% SDS and 3µl 20mg/ml proteinase K at 37°C for 2 hours. The sample was mixed with 100µl 5M NaCl and 80µl CTAB/NaCl solution (0.7M NaCl and 274mM hexadecyltri-methyl ammonium bromide; filter sterilised), then incubated at 65°C for 10 minutes. The sample was mixed with 750µl phenol:chloroform:isoamyl alcohol then centrifuged at 13,000 x g for 30 minutes. The aqueous supernatant was mixed with 750µl phenol:chloroform:isoamyl alcohol then centrifuged at 13,000 x g for 25 minutes. The aqueous supernatant was mixed with 750µl phenol:chloroform:isoamyl alcohol then centrifuged at 13,000 x g for 15 minutes. The aqueous supernatant was mixed with 450µl isopropanol then centrifuged at 13,000 x g for 10 minutes. After removal of the supernatant, the pellet was centrifuged with 400µl 70% ethanol at 13,000 x g for 10 minutes. The supernatant was removed and the pellet air dried. The pellet was resuspended in 50µl sterile distilled water. RNase was added to a final concentration of 10µg/ml, then the sample was incubated at room temperature for 20 minutes. The quantity and quality of the resulting DNA samples was assessed using the NanoDrop ND-1000 Spectrophotometer (Thermo Scientific).

PCR validation of primers using genomic DNA

PCR reactions were performed in 20µl volumes using the G-Storm GS001 thermal cycler. The reaction mix contained Phusion HF buffer (Thermo Scientific), 0.2mM deoxynucleotides, 1µM forward primer, 1µM reverse primer, 0.4 units Phusion DNA polymerase (Thermo Scientific) and 0.5ng template DNA in nuclease-free water. After an initial denaturation step at 98°C for 2 minutes, thirty cycles of amplification were performed under the following conditions: denaturation at 98°C for 10 seconds, annealing at 64°C for 20 seconds and extension at 72°C for 10 seconds. The final extension was performed at 72°C for 10 minutes.

Gene	Forward primer	Reverse primer
icmQ	GAAAGATCAACTCTCGGATGAACAAAAAG	CGATTGGCAAGATGAGACTCTGCTTTTAAC
lgiA	GAAATTATTATTTGTTACTTCTCTTGGCTTC	GAATATTTAAGCCACCATTCAA**G**AGCTTGG
lgiD	CTCTATTATTGCAGGCTTATTGATGATTAC	GTTAGTTAGTTCGAGTTTTCGTCTTTCCAC
lgiT	GAGCCATTATCCCGTTGAAAACTTGCT	GATAGCGTTTTATTTTAAATGCCTGAACTC
00662	CAAAATCCAGAATCAGACCGGCAACTTC	CGTCCTAGAGTATAAGTACGATAACCATC
00663	GGATCTAACTATAGACCCTATTACAAAGCG	CATCCTTATTATCAATACCGATTAGTTCTC
00666	GAACAAGATTTGTAAAGTTTCATGGAAGG	CACTTGATGTGGGTAAATAT
00668	GGGATGTATAGCCGAATTTTTGGCATCAG	GTTTTTGTACTGTCCAGATAGTCTTTACCAC
00669	CAAAAATTCAGATTATTTAACGAGCACCCC	GTCCACAGATATGTCTTCGATGTGAAGATTC
00697	GATAGAGTTACTAAAAATTCTAATCTCTTCGG	CTCTGCCGTATGTATGTTCAGGTAAATATC

Extraction of RNA from *L. pneumophila* clade C and D isolates

RNA from isolates 12_4499 and 12_4240 grown in either broth or infected RAW 264.7 cells was isolated using the Reliaprep™ RNA Cell Miniprep System (Promega) according to the product technical manual. The quantity and quality of the resulting RNA samples was assessed using the NanoDrop ND-1000 Spectrophotometer (Thermo Scientific). 8µl of each RNA sample was then incubated with 1µl RNase-free DNase (Promega) and 1µl RNase-free reaction buffer (Promega) at 37°C for 30 minutes. The samples were then incubated with 1µl DNase Stop Solution (Promega) at 65°C for 10 minutes.

Reverse transcription-PCR

Reverse transcription-PCR (RT-PCR) reactions were performed in 50µl volumes using the Access RT-PCR System (Promega) and G-Storm GS001 thermal cycler. The reaction mix contained AMV/*Tfl* reaction buffer, 0.2mM deoxynucleotides, 1µM forward primer, 1µM reverse primer, 1mM $MgSO_4$, 0.1u/µl AMV reverse transcriptase, 0.1u/µl *Tfl* DNA polymerase and 5ng template RNA in nuclease-free water. Reverse transcription was performed at 45°C for 45 minutes, followed by reverse transcriptase inactivation and nucleic acid denaturation at 94°C for 2 minutes. Thirty cycles of amplification were then performed for RNA samples from isolates grown in broth, and 50 cycles were performed for RNA samples from infected RAW 264.7 cells. Templates were denatured at 94°C for 30 seconds, primers annealed at 60°C for 1 minute and extension performed at 68°C for 1 minute. The final extension was performed at 68°C for 7 minutes.

Agarose gel electrophoresis

PCR and RT-PCR products were resolved in a 1.8% agarose gel with 1% Syber safe DNA stain (Invitrogen) in TAE buffer (40mM Tris-acetate and 1Mm EDTA; pH 7.7). A 100bp DNA ladder (Promega) was loaded into one lane and DNA loading dye (Invitrogen) was added to all samples before loading. Electrophoresis was performed in a Bio-Rad Mini-Sub® Cell at a constant voltage of 100V. DNA was visualised using the FluorChem HD2 imaging system (Alpha Innotech).

Extraction of DNA from infected RAW 264.7 cells for qPCR

Each cell pellet was resuspended in 100µl 0.4mg/ml lysozyme in Tris-EDTA with 1.2% Triton X-100 (Sigma-Aldrich), then incubated at 37°C for 30 minutes prior to DNA extraction using the QIAamp® DNA Mini Kit (Qiagen). The quantity and quality of the resulting DNA samples was assessed using the NanoDrop ND-1000 Spectrophotometer (Thermo Scientific).

Real-time qPCR optimisation

Preliminary amplification and dissociation plots were generated to test all possible pairings of primer concentrations for *IcmQ* and *β-actin,* listed below. For each primer pair, qPCR reactions were performed in 10µl volumes containing Brilliant III Ultra-Fast SYBR Green qPCR master mix (Agilent Technologies), 30nM reference dye (Agilent Technologies), 10ng DNA sample in nuclease-free water and both forward and reverse primers at either 0.1µM, 0.2µM or 0.3µM. Fifty cycles of amplification were performed using the Stratagene Mx3000P qPCR system (Agilent Technologies) under the following conditions: denaturation at 95°C for 10 seconds, then annealing, extension and read fluorescence at 60°C for 22 seconds. This was followed by a dissociation curve in which the PCR products were subjected to a stepwise increase in temperature from 60°C to 95°C to determine their melting temperature. Results were analysed using the MxPro qPCR software (Agilent Technologies).

Gene	Forward primer	Reverse primer
icmQ	GAAAGATCAACTCTCGGATGAACAAAAAG	CGATTGGCAAGATGAGACTCTGCTTTTAAC
β-actin	GTTGTAGCCTAGTCCTTTCTCCA	TGCCACAGGATTCCATACCT

Real-time qPCR

qPCR reactions were performed in 10µl volumes containing Brilliant III Ultra-Fast SYBR Green qPCR master mix (Agilent Technologies), 0.2µM (*β-actin*) or 0.3µM (icmQ) forward and reverse primers, 30nM reference dye (Agilent Technologies) and 10ng DNA sample in nuclease-free water. Fifty cycles of amplification were performed using the Stratagene Mx3000P qPCR system (Agilent Technologies) under the following conditions: denaturation at 95°C for 10 seconds, then annealing, extension and read fluorescence at 60°C for 22 seconds. Results were analysed using the MxPro qPCR software (Agilent Technologies) and the student's 2-sample t-test was performed using Minitab® 17 statistical software.

Cell assays

Cell infection assay

At 24 hours prior to infection, 24-well tissue culture plates were seeded with $1x10^6$ RAW 264.7 cells in 10% DMEM (Dulbecco's Modified Eagle's Medium with 10% heat-inactivated fetal calf serum), then incubated at 37°C with 5% CO_2. At 21 hours prior to infection, existing broth cultures of the required *L. pneumophila* strains at stationary phase were diluted in broth to an OD_{600} of 0.1 using the Utrospec 2100 pro UV/visible spectrophotometer (Amersham Biosciences) then incubated at 37°C with shaking.

Immediately prior to infection, each *L. pneumophila* broth culture was adjusted to an OD_{600} of 0.5 (approximately 10^9 bacteria/ml) in broth, then diluted in 10% DMEM to provide the required multiplicity of infection (MOI). DMEM was removed from each well of the tissue culture plates and replaced with the diluted *L. pneumophila* cultures. A gas-permeable membrane was applied to each plate before centrifugation at 20 x g for 5 minutes, then incubation at 37°C with 5% CO_2 for 1 hour. Media was removed from the plates and the wells were washed three times with phosphate-buffered saline (PBS). 100µg/ml gentamicin in 10% DMEM was added to each well before incubation at 37°C for 1 hour. Media was removed from the plates and the wells were washed three times with PBS. 10% DMEM was added to each well before further incubation at 37°C with 5% CO_2 until the required time point was reached.

Gentamicin protection assay with representative *L. pneumophila* isolates for qPCR

As described previously, tissue culture plates seeded with RAW 264.7 cells were inoculated with bacteria at an MOI of 1. A gas-permeable membrane was applied to each plate before centrifugation at 20 x g for 5 minutes, then incubation at 37°C for 30 minutes (0-hour timepoint) or 1 hour (2-, 4- and 24-hour timepoints). After 30 minutes, the media was removed from one plate and 2ml PBS was added to each well. Cells were scraped into suspension, transferred to microcentrifuge tubes and centrifuged at 900 x g for 5 minutes. The supernatant was removed and the pellet (representing the 0.5 hour timepoint) frozen for DNA purification.

After 1 hour, media was removed from the remaining plates and replaced with 100µg/ml gentamicin in 10% DMEM before incubation at 37°C for 1 hour. Media was removed from the remaining plates and the wells were washed three times with PBS. 10% DMEM was added to each well before incubation at 37°C for a further 1, 3 or 23 hours (2-, 4- and 24-hour timepoints, respectively). Media was removed from the plates and 2ml PBS was added to each well. Cells were scraped into suspension, transferred to microcentrifuge tubes and centrifuged at 900 x g for 5 minutes. The supernatant was removed and the pellet frozen for DNA purification.

Cell cytotoxicity assay

As described previously, four 6-well tissue culture plates seeded with $5x10^6$ RAW 264.7 cells per well were inoculated with either representative *L. pneumophila* isolates (MOI = 1) or 10% DMEM (uninfected control). The final incubation step was performed with 2ml 10% phenol red-free DMEM (phenol red-free DMEM with 10% heat-inactivated fetal calf serum) in each well. At 2, 4 and 24 hours post-infection, 200µl 10X Lysis Solution (Promega) was added to one well for 45 minutes (positive control), then 1ml supernatant from each well was transferred to microcentrifuge tubes. These were centrifuged at 300 x g for 4 minutes, then the resulting supernatant was used in the cell cytotoxicity assay. This assay was performed using the CytoTox 96® Non-Radioactive Cytotoxicity Assay (Promega) according the manufacturer's instructions. Absorbance at 490nm was measured using the FLUOstar Optima microplate reader (BMG LabTech). Data was analysed by the student's 2-sample t-test using Minitab® 17 statistical software.

Protein detection methods

Cell lysate samples

As described previously, four 6-well tissue culture plates seeded with $5x10^6$ RAW 264.7 cells per well were inoculated with either representative *L. pneumophila* isolates (MOI = 1) or 10% DMEM (uninfected control). At 2, 4 and 24 hours post-infection, the media was removed and the wells were washed twice with PBS. 50µl BugBuster™ Protein Extraction Reagent (Novagen) was added to each well, then the plates were incubated at room temperature for 10 minutes. The resulting cell lysates were incubated with 10µl reducing sample treatment buffer (RSTB) at 90°C for 10 minutes, then centrifuged at 13,000 x g for 1 minute.

SDS-polyacrylamide gel electrophoresis (SDS-PAGE)

2µl Precision Plus Protein WesternC Protein Standards (Bio-Rad) and 15 µl of each cell lysate sample were loaded into a 12.5% 1.5 mm SDS-polyacrylamide gel. Gels were submerged in running buffer (25 mM Tris-HCL, 192 mM glycine, 0.1% SDS) and run at 150V with Bio-Rad Mini-PROTEAN Tetra Cell apparatus.

	Resolving gel	**Stacking gel**
30% Acrylamide	4.17ml	850µl
2% Bis-acrylamide	500µl	350µl
1M Tris (pH 8.8)	3.75ml	
1M Tris (pH 6.8)		625µl
10% SDS	100µl	50µl
Distilled water	1.5ml	3.25ml
Tetramethylethylenediamine (TEMED)	8.35µl	12.5µl
10% Ammonium persulphate in water	33.35µl	25µl

Western blotting

Protein was transferred from the SDS-polyacrylamide gel to a nitrocellulose membrane (GE Healthcare Life Science) using the Bio-Rad Trans-Blot Turbo transfer system at 25V for 30 minutes in transfer buffer (25mM Tris-HCl, 192mM glycine, 20% methanol). Following transfer, membranes were blocked in PBS with 5% non-fat dry milk for 30 minutes. After 3 washes in PBS with 0.1% Tween 20 (PBS-T), membranes were incubated with primary antibody (0.2µg/ml rabbit anti-LC3 and 0.1µg/ml goat anti-actin (Santa Cruz Biotechnology)) at 4°C overnight. After 3 washes in PBS-T, membranes were incubated with secondary antibody (1µg/ml anti-rabbit^{680} (Cell Signalling Technology) and 1µg/ml anti-goat^{800} (Li-Cor)) at room temperature for 1 hour. The membranes were washed 5 times in PBS-T, then

stored in PBS before imaging with the Li-Cor Odyssey infrared imager and quantification with Li-Cor Image Studio software. Data was analysed by the student's 2-sample t-test using Minitab® 17 statistical software.

Confocal microscopy

Co-staining RAW 264.7 cells infected with *L. pneumophila*

Coverslips from the infection were washed twice with PBS, then cells were permeabilised with 0.5% Triton-X100 (Sigma-Aldrich) in PBS for 15 minutes at room temperature. The coverslips were washed twice with PBS. Next, non-specific binding sites were blocked with BSA/PBS (0.5% bovine serum albumin in PBS with 0.02% sodium azide; filtered through 0.2 µm filter) for 30 minutes at room temperature. Coverslips were transferred onto parafilm on wet tissue paper, then each coverslip was incubated with 50µl 2 µg/ml FITC-conjugated anti-*Legionella* antibody (abcam) for 1 hour at 37°C. Each coverslip was washed in PBS, then incubated with 50µl 2 U/ml Phalloidin 568 for 15 minutes at room temperature. Each coverslip was washed again in PBS, then stained with 9.53 µM DAPI (4',6-diamidino-2-phenylindole). The coverslips were then mounted on glass slides with 5 µl ProLong Gold (Molecular Probes).

Confocal microscopy of RAW 264.7 cells infected with *L. pneumophila*

Coverslips were imaged using a Zeiss LSM 710 confocal microscope and a 40X objective lens. Fluorophores were excited with lasers at 405 nm, 488 nm and 543 nm. Images were processed using Image J and Zen software.

Chapter 3: Analysis of novel *Legionella pneumophila* genes

Introduction

In order to identify the mechanism underlying the increased virulence of the clade C and D *L. pneumophila* strains, the genes unique to these clades were identified and studied using a bioinformatics approach. Some of these unique genes encode the novel T4SS identified by McAdam *et al.* (2014), which was further analysed in order to identify its origin and possible function in the isolates. Predicted T4SS-secreted effectors containing eukaryotic-like linear motifs unique to clades C and D were also identified. The expression of novel T4SS and putative effector genes was determined in *Legionella* total RNA samples from both broth culture and infected macrophage-like cells using reverse transcription-PCR (RT-PCR) to detect mRNA transcripts.

Bioinformatic analysis of novel genes unique to clades C and D

One representative *L. pneumophila* isolate from each of the four clades was chosen for bioinformatic analysis, as listed in *Table 2*. Using the OrthoMCL algorithm (Li *et al.*, 2003), a total of 149 genes present in Clades C and D were found to be absent from Clade B (Figure 9). Of these, 31 genes are also absent from Clade A, and therefore unique to Clades C and D. Orthologous genes were defined with the following parameters: minimum 80% coverage in BLAST pairwise alignments, minimum 85% sequence identity in BLAST query/subject pairs, filtered by 50% length difference within clusters.

Clade	Representative isolate	Accession number
A	12_5415	NZ_CCZU00000000
B	12_5064	NZ_CCZP01000000
C	12_4499	NZ_CDCY00000000
D	12_4240	NZ_CCZI00000000

Table 2 *Representative L. pneumophila isolates used in this study.*

The 39-kb region shown in *Figure 9* was investigated further as it is unique to clades C and D, and may therefore be linked to the increased virulence of these clades in a *Galleria* model (McAdam *et al.*, 2014). This region and the surrounding genome encode several features that are commonly associated with pathogenicity islands, including integrases, transposases and tRNA (Figure 10) (Hacker *et al.*, 1997). Furthermore, the G+C content of the region (37.45%) is slightly lower than that of the rest of the genome (38.94%). These features suggest that the 39-kb region may be a functional pathogenicity island that can undergo integration and excision from the genome.

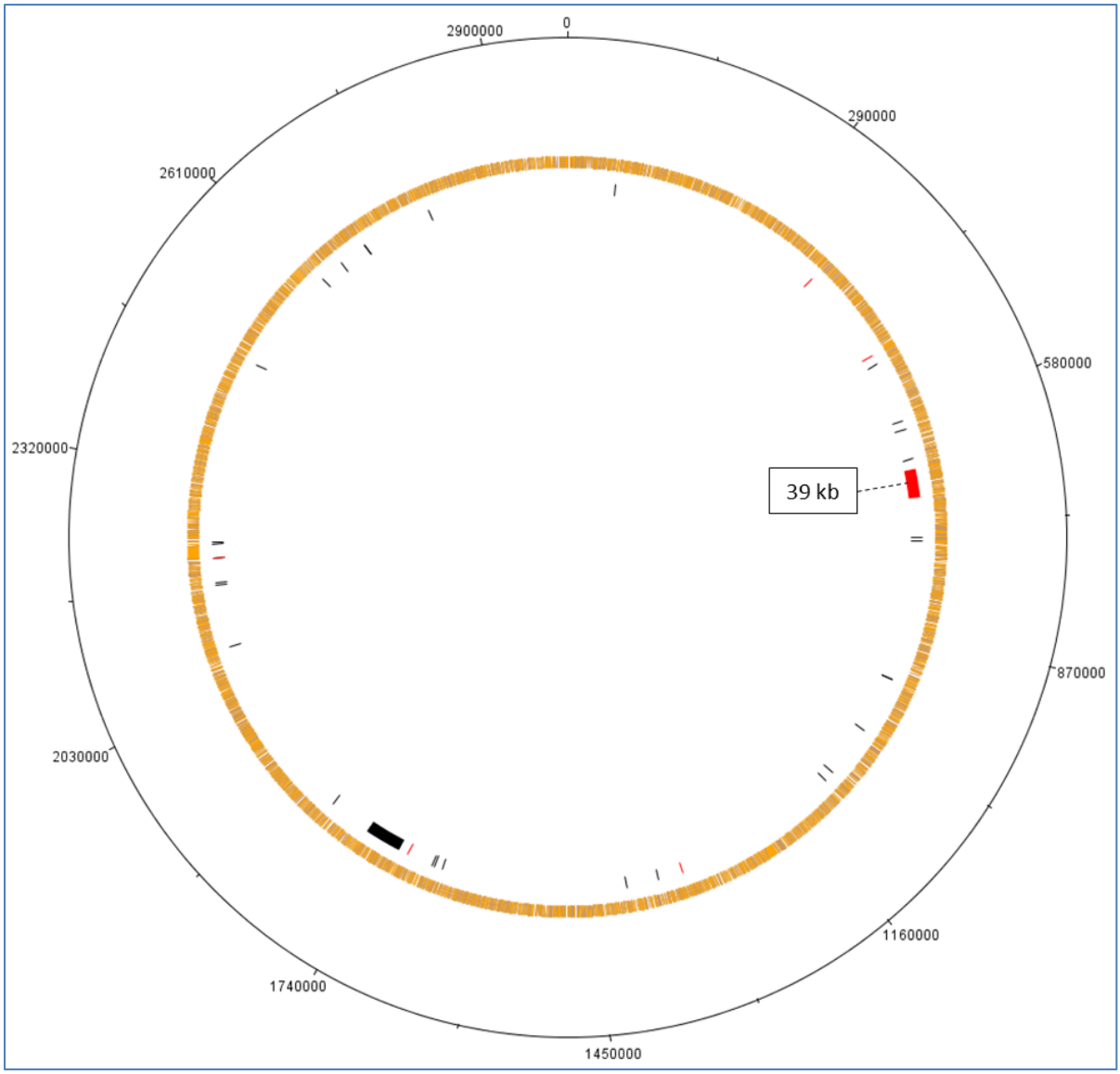

Figure 9 *Distribution of genes absent from Clade B (black) or absent from both Clades A and B (red). Mapped to genome of clade D strain 12_4240 (orange) using the DNAPlotter application (Carver et al., 2009). Label indicates the 39-kb region unique to clades C and D.*

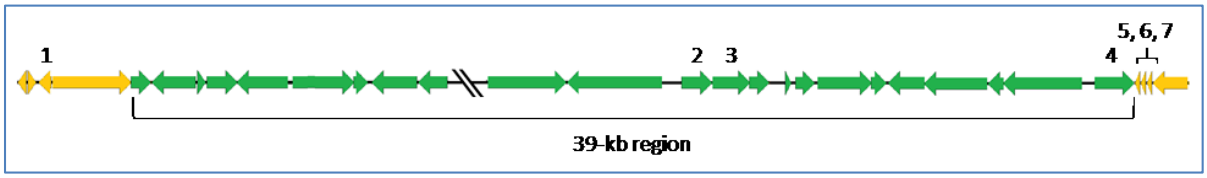

Figure 10 Pathogenicity island features associated with the 39-kb region. Labelled genes encode a transposase (1), integrases (2-4), attR/tRNA-Arg (5) and tRNA-Lys (6-7).

Novel T4SS of clades C and D

The 39-kb region contains the T4SS originally identified by McAdam *et al.* (2014) as a novel Lvh T4ASS (Figure 11). However, pairwise nucleotide sequence identity (BLASTn) analysis revealed that this region encodes a LGI-T4SS (*Figure 12*). The strains and gene clusters used are listed in *Table 3*. Unexpectedly, this LGI-T4SS shares only 75% nucleotide identity and 82% amino acid identity with that of *L. pneumophila* strain Paris, but shares 90% nucleotide identity and 96% amino acid identity with the LGI-T4SS of *L. longbeachae* strain D-4968.

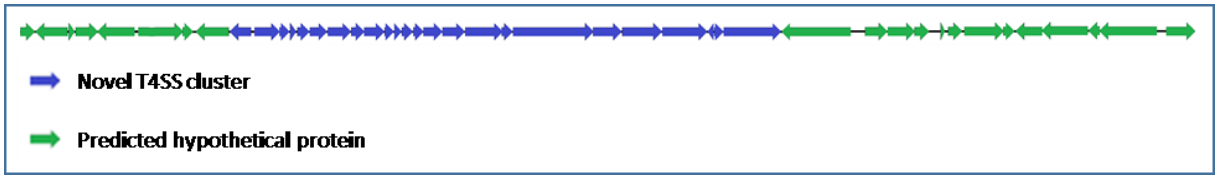

Figure 11 *Schematic diagram of the 39-kb region, including the novel T4SS identified by McAdam et al. (2014). Arrows represent predicted CDSs identified using the Prokka annotation pipeline (Seemann, 2014).*

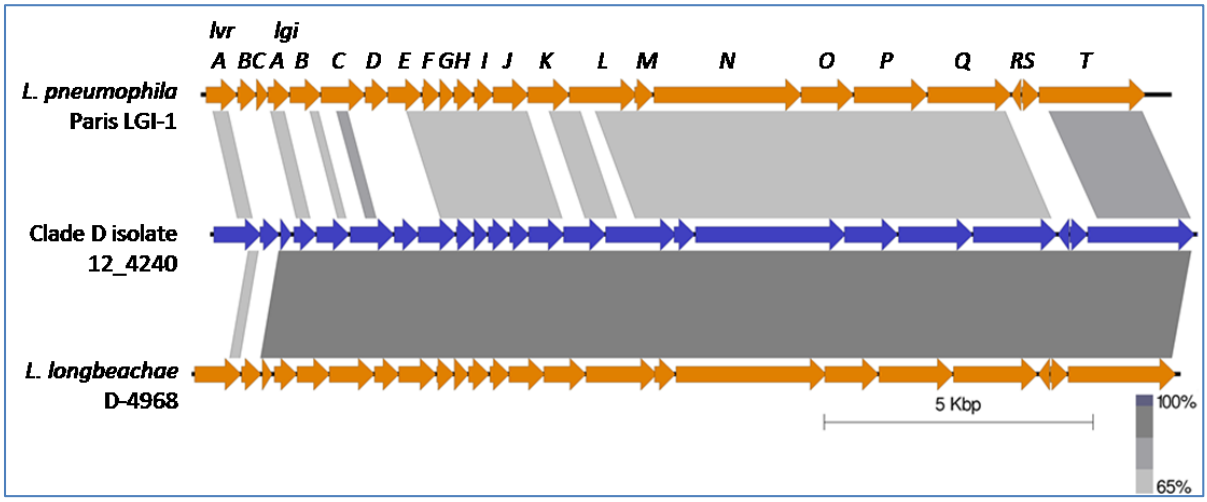

Figure 12 *Linear comparison of LGI-T4SS clusters. Arrows represent coding sequences. Shaded bars between each cluster represent nucleotide sequence identity (BLASTn). Generated using EasyFig (Sullivan et al., 2011).*

Species	Strain	Accession number	LGI-T4SS	LGI-T4SS locus tags
L. pneumophila	Paris	CR628336.1	LGI-1	lpp1075 - lpp1055
	12_4240	NZ_CCZI00000000	39-kb region	PROKKA_00671 – PROKKA_00693
L. longbeachae	D-4968	NZ_ACZG01000001.1		LLB_1169 – LLB_1191

Table 3 *Strains and LGI-T4SS gene clusters used in the BLASTn analysis.*

A phylogenetic tree was constructed using BLAST pairwise alignments of the *lgiN* gene nucleotide sequence, which encodes a putative ATPase within the LGI-T4SS cluster (Figure 13) (Wee *et al.*, 2013). The strains and genes used are listed in *Table 4*. The phylogenetic tree shows that the 39-kb T4SS is closely related to the *L. longbeachae* D-4968 LGI-T4SS. Therefore, the novel T4SS appears to be an LGI-T4SS that has originated from *L. longbeachae*.

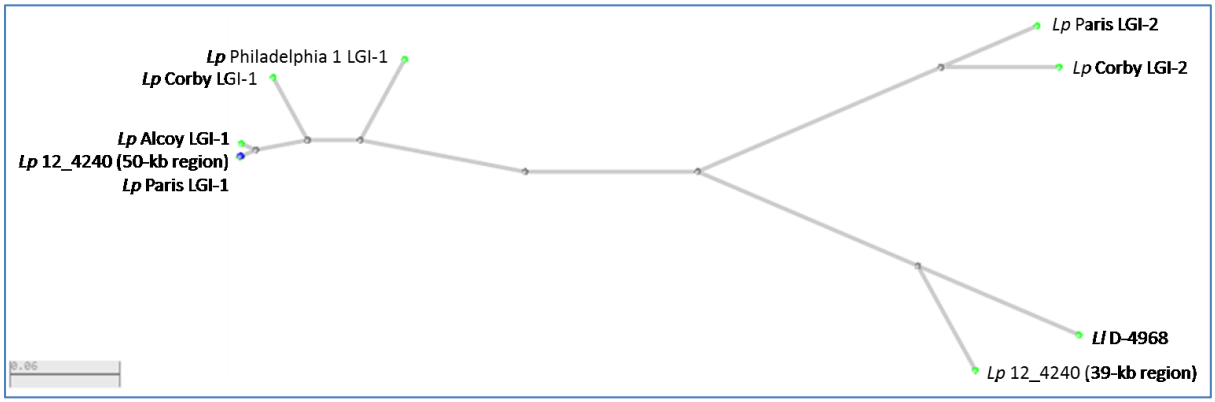

Figure 13 *Unrooted phylogenetic tree of LGI-T4SSs across L. pneumophila (Lp) and L. longbeachae (Ll) genomes listed in Table 4. Tree of lgiN genes using BLASTn pairwise alignments, visualised using the BLAST tree view (http://www.ncbi.nlm.nih.gov/blast/treeview/treeView.cgi).*

Species	**Strain**	**Accession number**	**LGI-T4SS**	***lgiN* locus tag**
L. pneumophila	Alcoy	CP001828	LGI-1	lpa_01507
	Corby	CP000675	LGI-1	LPC_2290
			LGI-2	LPC_1874
	Philadelphia 1	AE017354	LGI-1	lpg0989
	Paris	CR628336.1	LGI-1	lpp1059 - lpp1060
			LGI-2	lpp2392
	12_4240	NZ_CCZI00000000	39-kb region	PROKKA_00687
			50-kb region	PROKKA_01789
L. longbeachae	D-4968	NZ_ACZG01000001.1		LLB_1185

Table 4 *Strains and lgiN genes used to construct the phylogenetic tree.*

Researchers from the Fitzgerald laboratory have access to the *L. longbeachae* genomes of patient and environmental isolates from a Legionnaires' disease outbreak in Scotland in 2013 (Potts *et al.*, 2013). BLASTn analysis showed that the entire 39-kb region shares 94% nucleotide identity with the homologous region in the *L. longbeachae* isolate 13_6619, isolated from a compost sample provided by a patient of the outbreak (Figure 14). Therefore, the full 39-kb region is likely to have originated from *L. longbeachae* and may have been transferred to *L. pneumophila* in the environment.

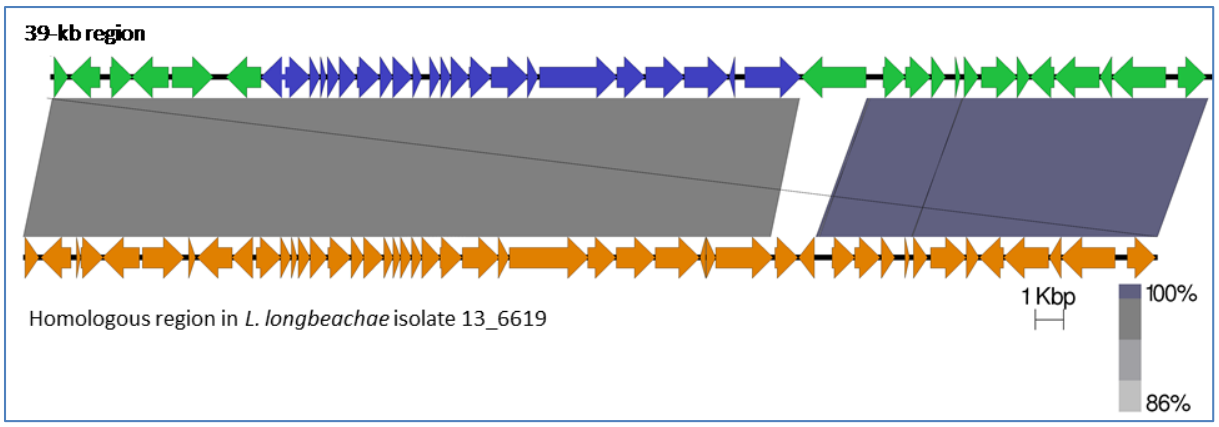

Figure 14 *Linear comparison between the 39-kb region of L. pneumophila clade D isolate 12_4240 (PROKKA_00662 – PROKKA_00706) and the homologous region in the L. longbeachae isolate 13_6619. Shaded bars between each cluster represent nucleotide sequence identity (BLASTn). Generated using EasyFig (Sullivan et al., 2011).*

Prediction of novel T4SS-secreted effector proteins and eukaryotic-like motifs

The classifier T4EffPred was used to predict whether or not each of the 31 genes unique to clade C and D encode T4SS effector proteins (http://bioinfo.tmmu.edu.cn/T4EffPred/prediction.html) (Zou *et al.*, 2013). T4EffPred identifies putative effectors by scoring proteins according to their amino acid composition, dipeptide composition and other distinctive features of T4SS effector proteins. A total of 7 genes were predicted to encode T4SS-secreted effectors, all of which are located adjacent to the *L. longbeachae*-like LGI-T4SS in the 39-kb region (*Figure 15*).

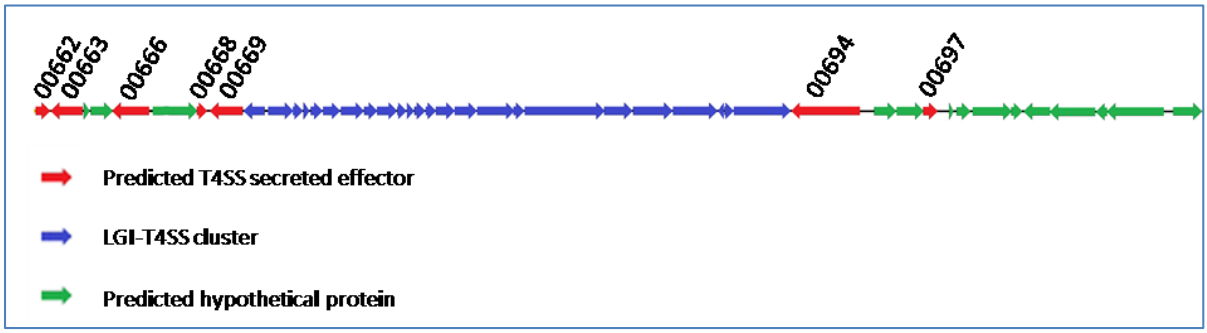

Figure 15 *Schematic diagram of the 39-kb region showing location of predicted T4SS secreted effectors. Arrows represent predicted CDSs identified using the Prokka annotation pipeline (McAdam et al., 2014).*

Secreted effectors interact with host cell proteins via eukaryotic-like domains, which are common features of *Legionella* T4SS effectors (Lomma *et al.*, 2009). These interactions may promote the survival of *Legionella* and could therefore provide a mechanism for the increased virulence of the clade C and D isolates. The eukaryotic linear motif resource ELM was used to identify any eukaryotic motifs present in the seven predicted T4SS effector proteins (http://elm.eu.org) (Dinkel *et al.*, 2013).

Some of the most commonly predicted motifs present in these putative effector proteins are listed in Table 5.

	00662	00663	00666	00668	00669	00694	00697
PDZ-binding motif: PDZ domains are involved in protein targeting and the assembly of protein complexes (Hung and Sheng, 2002). (Interaction domain PF00595)				✓			✓
Clathrin box motif: Binds clathrin heavy chain (Alberts *et al.*, 2008a). Found on cargo adaptor proteins. (Interaction domain PF01394)	✓	✓	✓			✓	
eIF4E binding motif: Binds the dorsal surface of the eukaryotic Translation Initiation Factor 4E (eIF4E) (Marcotrigiano *et al.*, 1999). Blocks assembly of the translation machinery. (Interaction domain PF01652)		✓		✓			
IAP binding motif: Binds Inhibitor of Apoptosis Proteins (IAPs) in apoptotic cells (Vucic and Fairbrother, 2007). (Interaction domain PF00653)	✓		✓				
SH2 domain motif: Binds phosphorylated tyrosine residues (Koch *et al.*, 1991). Involved in signal transduction of receptor tyrosine kinase pathways. (Interaction domain PF00017)					✓	✓	

Table 5 *Selected predicted eukaryotic linear motifs in putative T4SS effector proteins. (P < 0.1).*

Expression of predicted effectors

To determine whether or not the LGI-T4SS and predicted effector proteins are expressed by the isolates in either broth culture or during infection of cultured cells, reverse transcription PCR (RT-PCR) was used to detect mRNA encoding several genes of interest. Bacterial RNA samples were extracted from the representative *L. pneumophila* clade C and D isolates at stationary phase in broth culture and infected RAW 264.7 macrophage-like cells using the ReliaPrep™ RNA Cell Miniprep System (Promega), according to the product technical manual. The quantity and quality of the resulting RNA samples was assessed using the NanoDrop ND-1000 Spectrophotometer (Thermo Scientific).

The RAW 264.7 cells were infected using a gentamicin protection assay (see Chapter 2) at an MOI of 1. At 18 hours post-infection, media was removed from each well and replaced with 1ml PBS. Cells were scraped into suspension then transferred to microcentrifuge tubes and pelleted for RNA extraction.

Several aspects of the RT-PCR protocol were optimised using the gene *icmQ*, which encodes a component of the constitutively expressed Dot/Icm T4BSS (Faucher *et al.*, 2011). For each clade, four wells of a 6-well tissue culture plate with a total of approximately $2x10^7$ RAW 264.7 cells were infected in order to maximise the yield of RNA for *Legionella* gene expression to be detected. Infected RAW 264.7 cells were incubated with 0.4mg/ml lysozyme in Tris-EDTA for 5 minutes prior to RNA extraction to increase the yield of RNA. This incubation step increased the yield by 44%, from 15.94µg to 22.94µg RNA. In addition, the number of RT-PCR cycles was increased from 30 to 50 for reactions with RNA samples from infected cells. This was necessary as these samples also contained RAW 264.7 cell RNA and therefore a smaller quantity of bacterial RNA.

A negative control reaction without reverse transcriptase (RT) was carried out alongside each RT-PCR reaction. This ensured that the PCR reaction only amplified DNA that was produced from the reverse transcription of mRNA. Therefore the assay specifically detected transcribed genes only. In addition, the RNA samples were treated with RNase-free DNase (Promega) in order to reduce the amount of DNA in the negative control reaction (*Figure 16*).

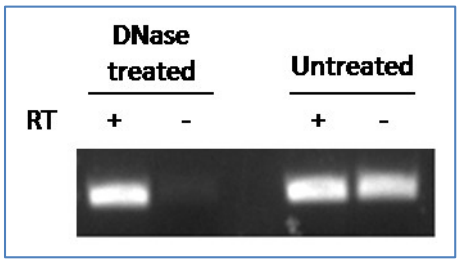

Figure 16 *Optimisation of RT-PCR protocol with DNase treatment. Products of RT-PCR with primers for icmQ and RNA extracted from the representative clade A isolate in broth culture.*

Primers were designed for three LGI-T4SS genes (*lgiA, lgiD* and *lgiT*) and five genes encoding predicted effectors (*00662, 00663, 00666, 00669* and *00697*) (*Figure 17*). Each pair of primers was designed to produce a DNA product of 200bp in length. The primers were validated by PCR on genomic DNA extracted from representative isolates of each clade to ensure specificity to the unique genes of clades C and D (Figure 18).

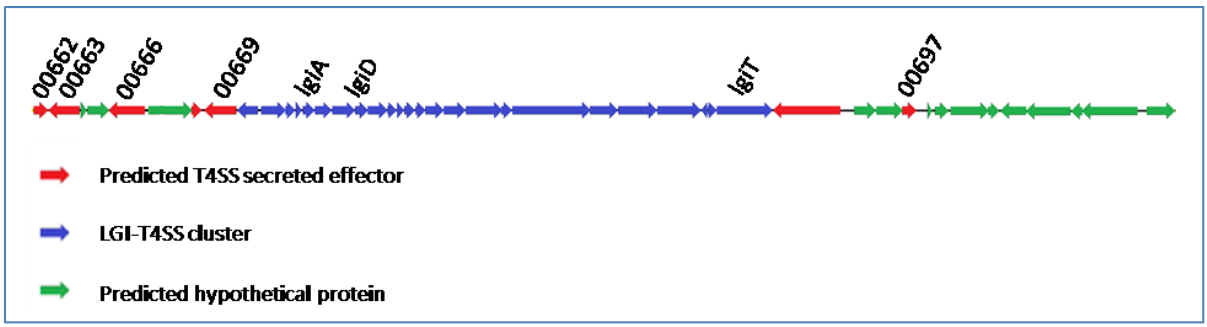

Figure 17 *Location of genes within the 39-kb region that were detected using PCR and RT-PCR.*

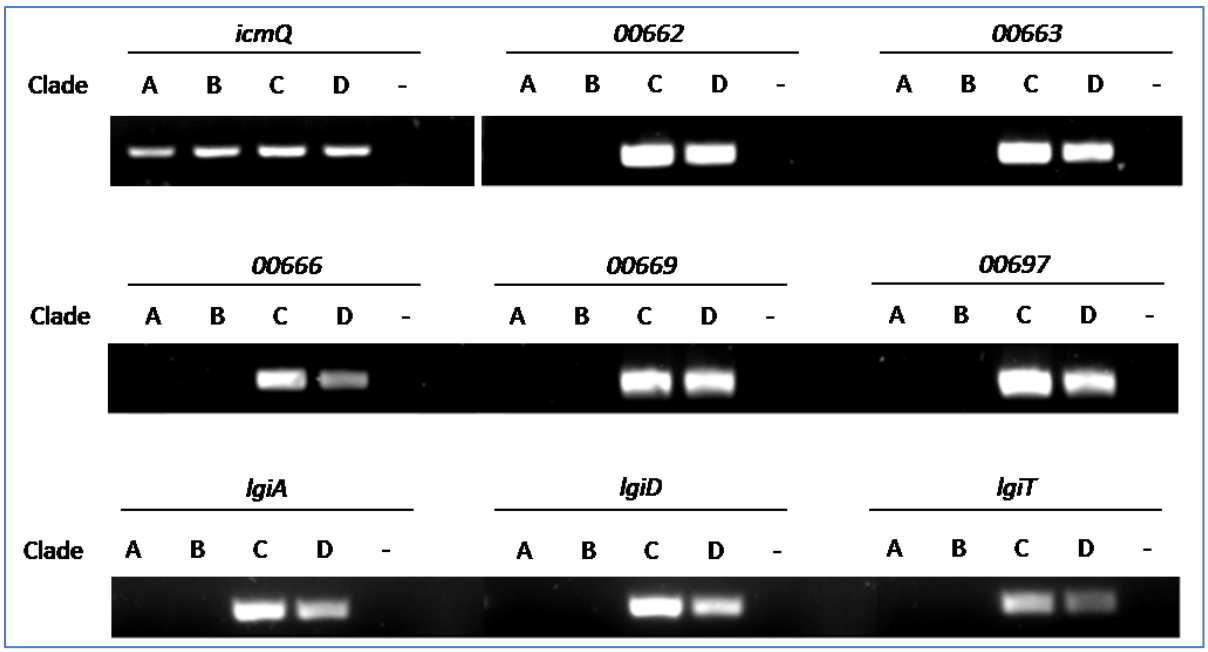

Figure 18 *PCR validation of primers for genes encoding putative effector proteins on genomic DNA from representative L. pneumophila isolates. icmQ is used as a positive control. Negative controls (-) contain no genomic DNA.*

Whilst expression of *icmQ* could be detected, expression of the putative effector genes was not detected in bacteria from broth culture (Figure 19). However, the genes *lgiA, lgiD, lgiT*, *00662* and possibly *00666* appeared to be expressed during intracellular growth (Figure 20). This indicates that expression of the LGI-T4SS and the predicted effectors 00662 and 00666 may be induced during infection, and could therefore play a role in intracellular survival or interaction with the host cell.

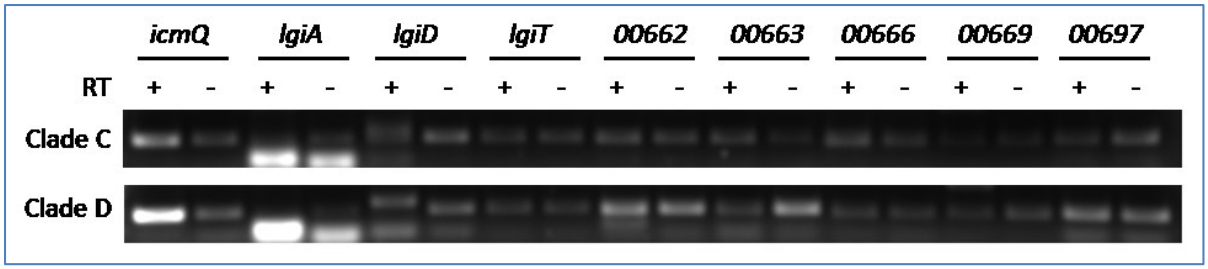

Figure 19 *RT-PCR on RNA extracted from representative Clade C and D isolates grown in broth culture. icmQ was used as a positive control.*

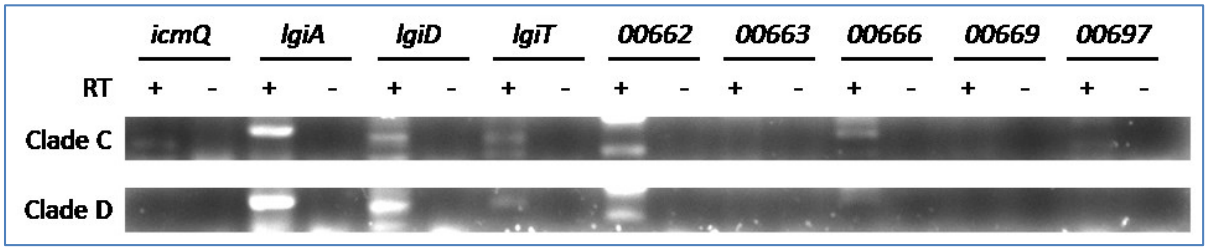

Figure 20 *RT-PCR on RNA extracted from representative Clade C and D isolates from infected RAW 264.7 cells. icmQ was used as a positive control.*

Expression of the positive control gene *icmQ* was not detected in the RNA samples from infected cells (Figure 20). It has been shown previously that the expression of *icmQ* decreases after 3 hours of infection and is only expressed at a low level by 20 hours post-infection (Barysheva *et al.*, 2008). As the RNA samples were extracted at 18 hours post-infection, it is likely that *icmQ* was expressed at a low level that was insufficient for detection by RT-PCR.

Summary

The genes unique to clades C and D were analysed using a bioinformatics approach. The 39-kb region unique to these clades was found to resemble a pathogenicity island and unexpectedly, the novel T4SS identified by McAdam *et al.* (2014) was shown to be a LGI-T4SS originating from L. longbeachae. Five of the genes adjacent to the LGI-T4SS were predicted to encode T4SS-secreted effector proteins and were shown to contain several eukaryotic-like linear motifs. mRNA encoding the LGI-T4SS and predicted effectors 00662 (and possibly 00666) was detected in cells infected with representative clade C and D isolates.

Chapter 4: Comparing growth rates and host cell response

Introduction

In order to assess any requirement of the novel T4SS in the survival of *L. pneumophila*, several techniques were used to determine the replication rate of isolates from each clade. The infection protocol was optimised using *L. pneumophila* Paris and RAW 264.7 macrophage-like cells, which were later infected with representative isolates of each clade. Replication rate in broth culture was compared using a microplate reader and intracellular replication was quantified using qPCR. In addition, two assays were used to compare cytotoxicity and autophagy in RAW 264.7 cells infected with representative isolates from each clade.

Infection optimisation with *L. pneumophila* Paris

A gentamicin protection assay was used to study the intracellular replication of the *L. pneumophila* isolates and the response of infected host cells. The *L. pneumophila* strain Paris was used to optimise the infection protocol before using representative isolates from clades A, B, C and D. The mouse leukemic monocyte macrophage cell line RAW 264.7 was used as a model host cell for infection. At 1 hour post-infection, any remaining extracellular bacteria were killed by incubation with gentamicin. As this antibiotic cannot penetrate eukaryotic cells, this method ensures that only intracellular bacteria survive (Venkataraman *et al.*, 1997).

The efficiency of *L. pneumophila* infection is highest at the transition between the exponential and stationary growth phases of the bacteria (Tiaden *et al.*, 2013). Therefore, *L. pneumophila* broth cultures were diluted to an OD_{600} of 0.1 at 21 hours prior to infection to ensure that they reached the late exponential or early stationary growth phase at the time of infection, as described by Tiaden *et al.* (2003). Tissue culture plates were seeded with RAW 264.7 cells at 24 hours prior to infection, then adherent cells were infected with *L. pneumophila* cultures at the required MOI. The plates were then centrifuged for 5 minutes to bring the bacteria into contact with the cells and synchronise the infection (Harding *et al.*, 2013). After incubation at 37°C for 1 hour, the infected cells were incubated with 100µg/ml gentamicin for 1 hour in order to kill extracellular bacteria. The media was then removed from the plates, the wells were washed three times with PBS and incubated with antibiotic-free media at 37°C until the required time point was reached. This ensured that *L. pneumophila* could survive in the media and infect new host cells after release.

To ensure that the extracellular bacteria were sensitive to gentamicin, the minimum inhibitory concentration (MIC) was determined for *L. pneumophila* Paris and the representative *L. pneumophila*

isolates listed in *Table 6*. The results indicate that the MIC for all strains is 0.125µg/ml, as no bacterial growth was visible at this concentration and above (*Figure 21*). Therefore the gentamicin concentration of 100µg/ml used in the gentamicin protection assay far exceeded the MIC and was sufficient to kill any extracellular bacteria.

Clade	Representative isolate	Accession number
A	12_5415	NZ_CCZU00000000
B	12_5064	NZ_CCZP01000000
C	12_4499	NZ_CDCY00000000
D	12_4240	NZ_CCZI00000000

Table 6 *Representative L. pneumophila isolates used in this study.*

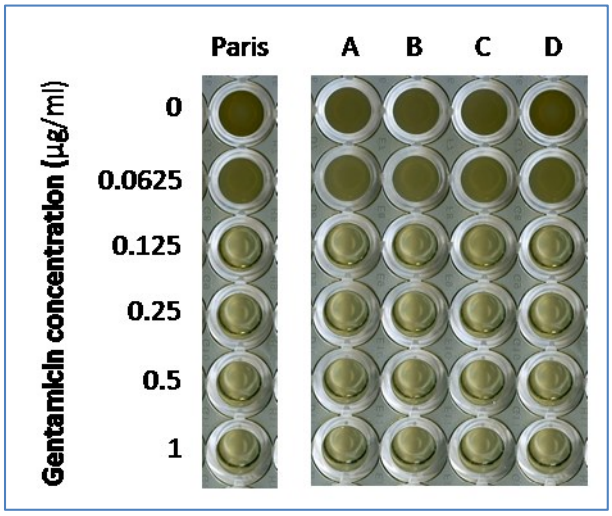

Figure 21 *Minimum inhibitory concentration of gentamicin on L. pneumophila Paris and representative isolates of clades A, B, C and D. Broth cultures of L. pneumophila were diluted to an OD_{600} of 0.02 in broth containing either 0, 0.0625, 0.125, 0.25, 0.5 or 1µg/ml gentamicin. 200µl of each diluted sample was added to a 96-well tissue culture plate. The image was taken after incubation of the plate at 37°C for 1 week.*

In order to achieve the required multiplicity of infection (MOI), the number of colony-forming units (CFUs) in the inoculum was determined by measuring the optical density at 600nm (OD_{600}) of the bacteria in broth culture. A culture with an OD_{600} of 0.5 contains approximately $1x10^9$ CFU/ml. This was confirmed by plating serial dilutions of the inoculum on CYE agar plates and counting the number of visible colonies after incubation at 37°C for up to 4 days.

RAW 264.7 cells were visualised using confocal microscopy after infection with *L. pneumophila* Paris at a range of MOIs, from 1 to 100 (Figure 22). Although a higher MOI resulted in the infection of a higher proportion of the cells, this also caused excessive host cell death, as determined by microscopy. Therefore, an MOI of 1 was used for further experiments.

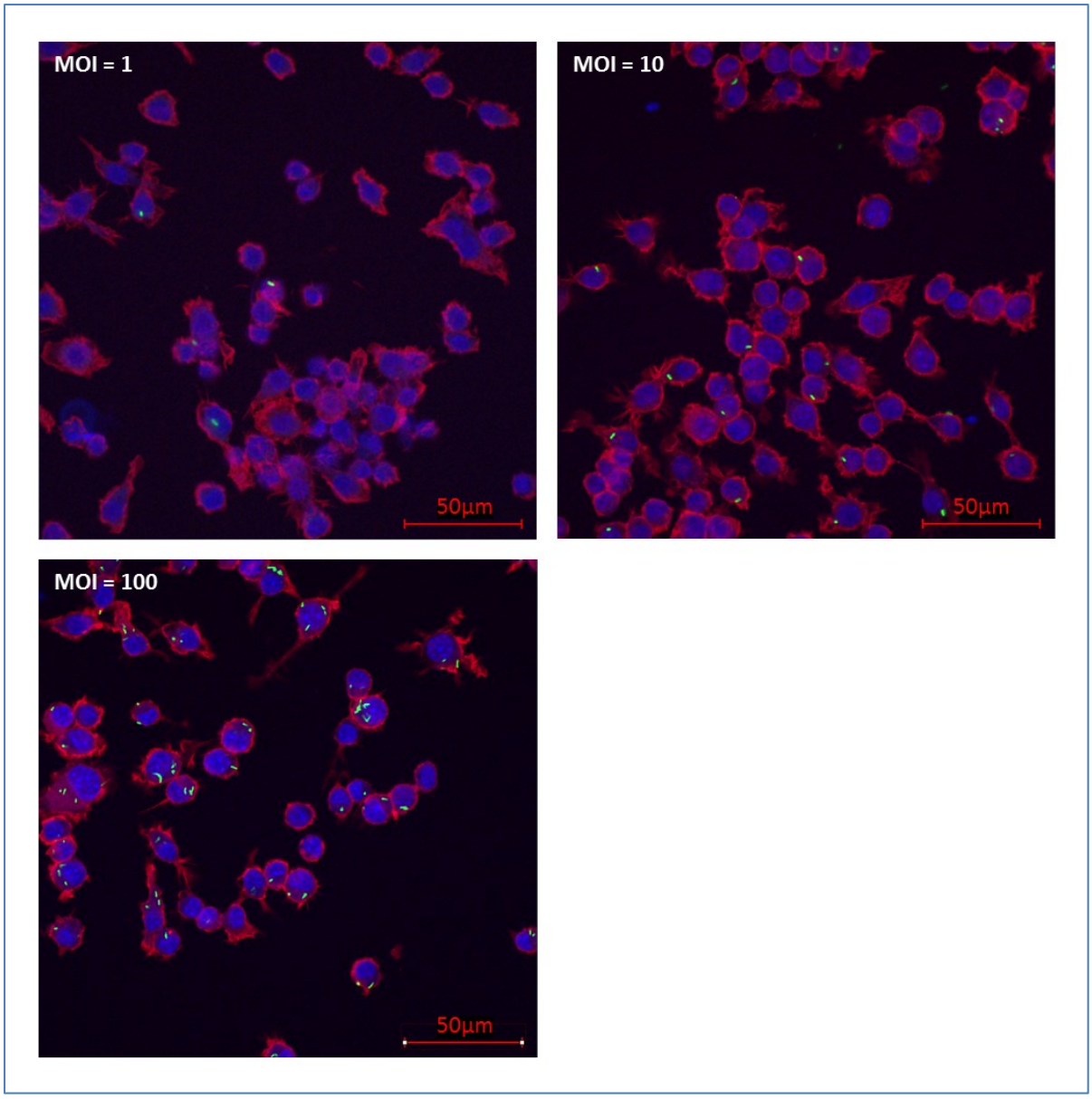

Figure 22 *Representative confocal microscopy images of RAW 264.7 cells infected with L. pneumophila Paris at 2 hours post-infection with MOI of 1, 10 or 100 (labelled). Cells were fixed on 13mm poly-L-lysine glass coverslips with PFA (4% paraformaldehyde in PBS; pH 7.4) for 20 minutes at room temperature. Cells were then permeabilised with 0.5% Triton X100 for 15 minutes at room temperature. Non-specific binding sites were blocked with BSA/PBS for 30 minutes at room temperature. Legionella were stained with FITC-conjugated anti-Legionella antibody (green), F-actin was visualised with Phalloidin 568 (red) and DNA was stained with DAPI (blue).*

An appropriate timescale for the infection was also determined using confocal microscopy. RAW 264.7 cells were visualised after infection with *L. pneumophila* Paris at 24, 48 and 72 hours post-infection (Figure 23). As intracellular bacteria were still visible at 72 hours post-infection, this timescale was used for initial experiments.

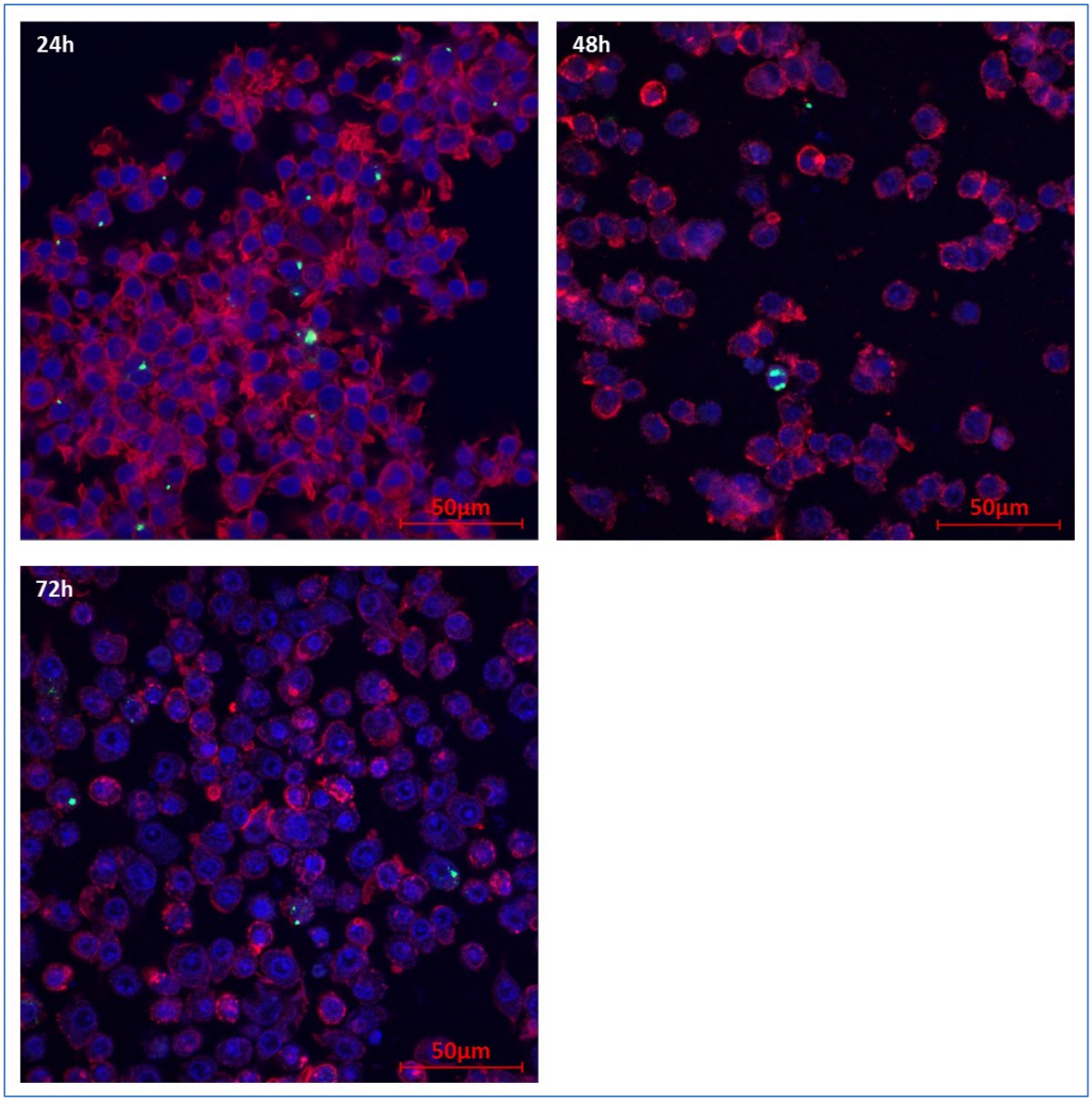

Figure 23 *Representative confocal microscopy images of RAW 264.7 cells infected with L. pneumophila Paris at an MOI of 1. Labels indicate hours post-infection. Cells were fixed on 13mm poly-L-lysine glass coverslips with PFA (4% paraformaldehyde in PBS; pH 7.4) for 20 minutes at room temperature. Cells were then permeabilised with 0.5% Triton X100 for 15 minutes at room temperature. Non-specific binding sites were blocked with BSA/PBS for 30 minutes at room temperature. Legionella were stained with FITC-conjugated anti-Legionella antibody (green), F-actin was visualised with Phalloidin 568 (red) and DNA was stained with DAPI (blue).*

The first aim of the gentamicin protection assays was to measure the intracellular replication of the *L. pneumophila* isolates by quantifying colonies recovered from infected cells at several time points. At 24, 48 or 72 hours post-infection, the media was removed from the tissue culture plates and wells were washed twice with PBS to remove any extracellular bacteria. Next, 100µl 0.05% Triton X-100 (Sigma-Aldrich) in PBS was added to each well for 5 minutes in order to lyse the infected cells.

The resulting lysates were serially diluted in PBS, then 10µl of the tenfold dilutions were plated on BCYE agar plates before incubation at 37°C for 3 days or until colonies were visible.

Although viable colonies were recovered from infected cells at 24 hours post-infection (Figure 24), none were recovered at later time points. This may have been due to the entry of the bacteria into a viable but non-culturable (VBNC) form in response to environmental stress (Oliver, 2010). In this form, the cells are viable but cannot be cultured on laboratory media. *L. pneumophila* may enter the VBNC state in response to starvation, hypochlorite treatment or high temperatures (reviewed in Al-Bana *et al.,* 2014). Therefore, the number of colony-forming units recovered may not accurately reflect the number of intracellular bacteria due to the formation of VBNC cells.

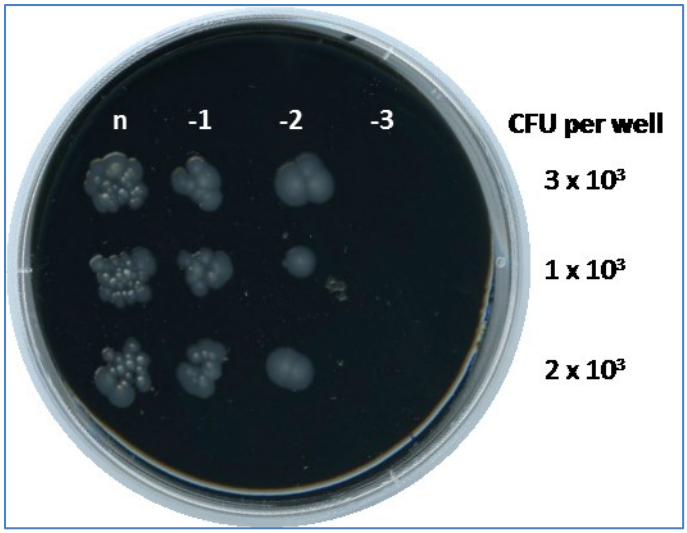

Figure 24 *Colonies recovered on BCYE agar from lysis of RAW 264.7 cells infected with L. pneumophila Paris (MOI = 1) at 24 hours post-infection. Plate shows 3 biological replicates. 10µl lysate (n) and tenfold serial dilutions in PBS (-1, -2, -3) from a total of 100µl lysate were plated from each well.*

Several aspects of the protocol were modified in an attempt to recover viable colonies from later time points. For example, the infected cells were lysed with Triton X-100, so the effect of this detergent on cell viability was assessed. A broth culture of *L. pneumophila* Paris at approximately 10^6 bacteria/ml was centrifuged in 1ml volumes at 13,000 x g for 1 minute. The resulting pellets were resuspended in 1ml of either 0%, 0.05% or 0.1% Triton X-100 in PBS. After incubation for 5 minutes at room temperature, each suspension was serially diluted in PBS, then 10µl of each tenfold dilution was plated on BCYE agar. The plates were incubated at 37°C until colonies were visible.

The results of this assay showed that 0.05% Triton X-100 does not inhibit the growth of colonies on BCYE agar (*Figure 25*). However, the bacteria used in this assay were taken from broth culture so may have been phenotypically different from intracellular bacteria.

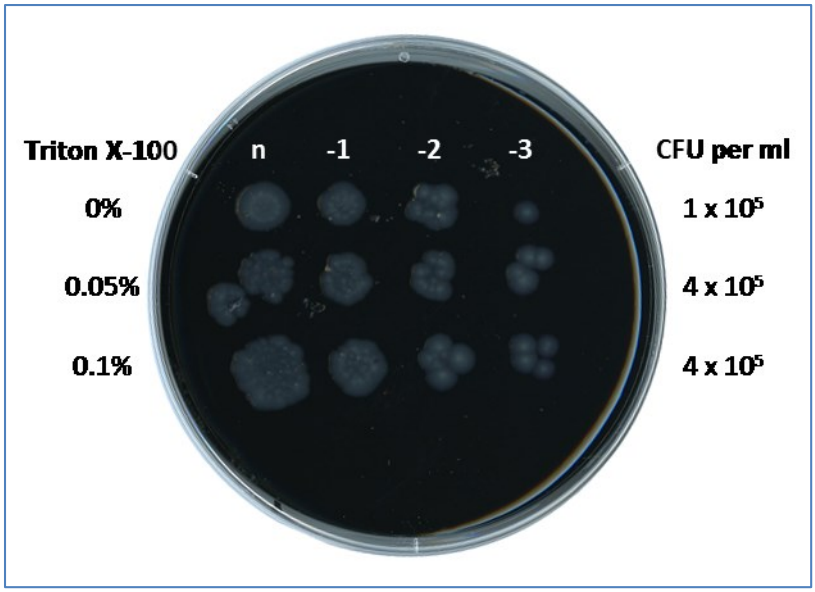

Figure 25 *L. pneumophila colonies recovered on BCYE agar after incubation in PBS with 0%, 0.05% or 0.1% Triton X-100 for 5 minutes prior to plating. 10µl (n) and tenfold serial dilutions in PBS (-1, -2, -3) of each suspension were plated.*

Due to the time and cost of these experiments, alternative approaches were used to compare the replication of representative *L. pneumophila* isolates of clades A, B C and D.

Growth curve of representative isolates in broth culture

One feature of the *L. pneumophila* isolates that could underlie the increased virulence of clade C and D isolates is their rate of replication. In order to compare the replication rate of each clade, a microplate reader was used to measure the OD_{600} of broth cultures of representative isolates. Each broth culture was diluted to a starting OD_{600} of 0.02 in either broth or DMEM, then 200µl of each diluted sample was added to a 96-well tissue culture plate. Growth was quantified hourly over 4 days by measuring OD_{600} using a microplate reader. No significant difference in replication rate was observed between representative isolates in broth culture, as determined by a student's 2-sample t-test (Figure 26 and *Figure 27*). In contrast, no replication was observed in DMEM (Figure 27). Therefore, any bacterial replication measured during gentamicin protection assays can be assumed to take place inside infected RAW 264.7 cells.

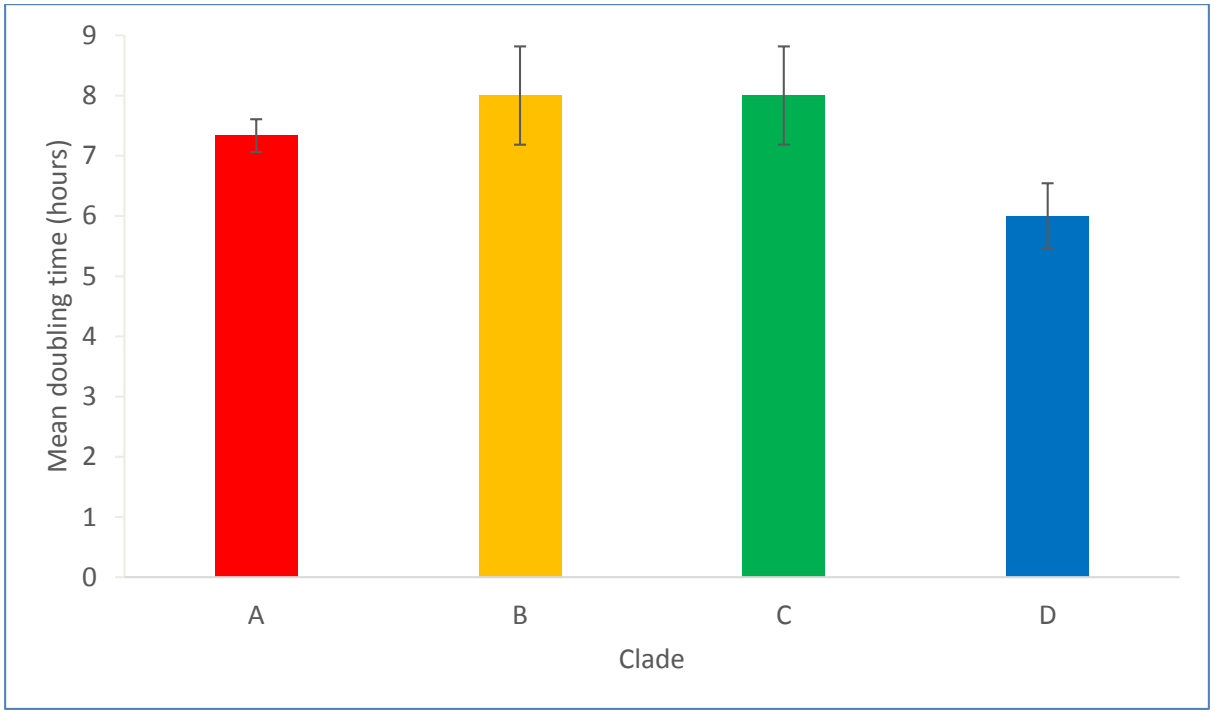

Figure 26 *Doubling time of representative L. pneumophila isolates in broth culture as measured by change in OD_{600} at exponential phase. Error bars indicate the standard error of the mean across three biological replicates.*

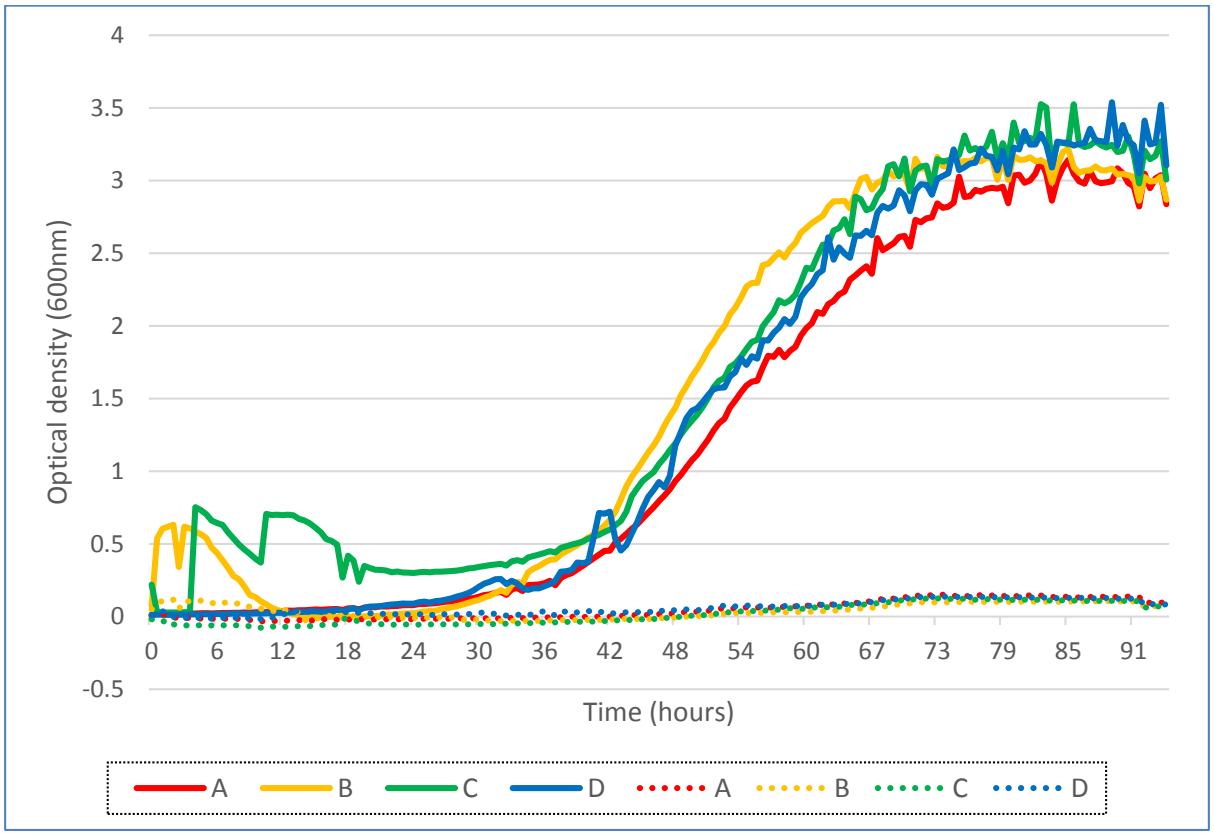

Figure 27 *Growth curve of representative L. pneumophila isolates in broth culture (solid lines) or DMEM (dotted lines) as measured by OD_{600} at 1 hour intervals using a microplate reader set at 37°C and shaking. Lines represent mean result from three biological replicates.*

Intracellular growth of representative *L. pneumophila* isolates

During infection, bacteria must replicate efficiently inside their host in order to spread to other cells (Finlay and Falkow, 1997). A higher rate of intracellular replication increases the number of bacterial cells available to infect new host cells, and may therefore increase the virulence of the bacteria. Therefore, representative isolates from each clade were compared to identify any differences in replication rate that could underlie the increased virulence of clade C and D isolates in the *Galleria* model.

Confocal microscopy was used to visualise any gross differences in the infection of RAW 264.7 cells with representative *L. pneumophila* isolates of each clade, listed in *Table 6*. At 30 minutes post-infection (MOI = 1), bacteria from each clade were visible inside RAW 264.7 cells, indicating no obvious difference in host cell invasion between the clades (*Figure 28*).

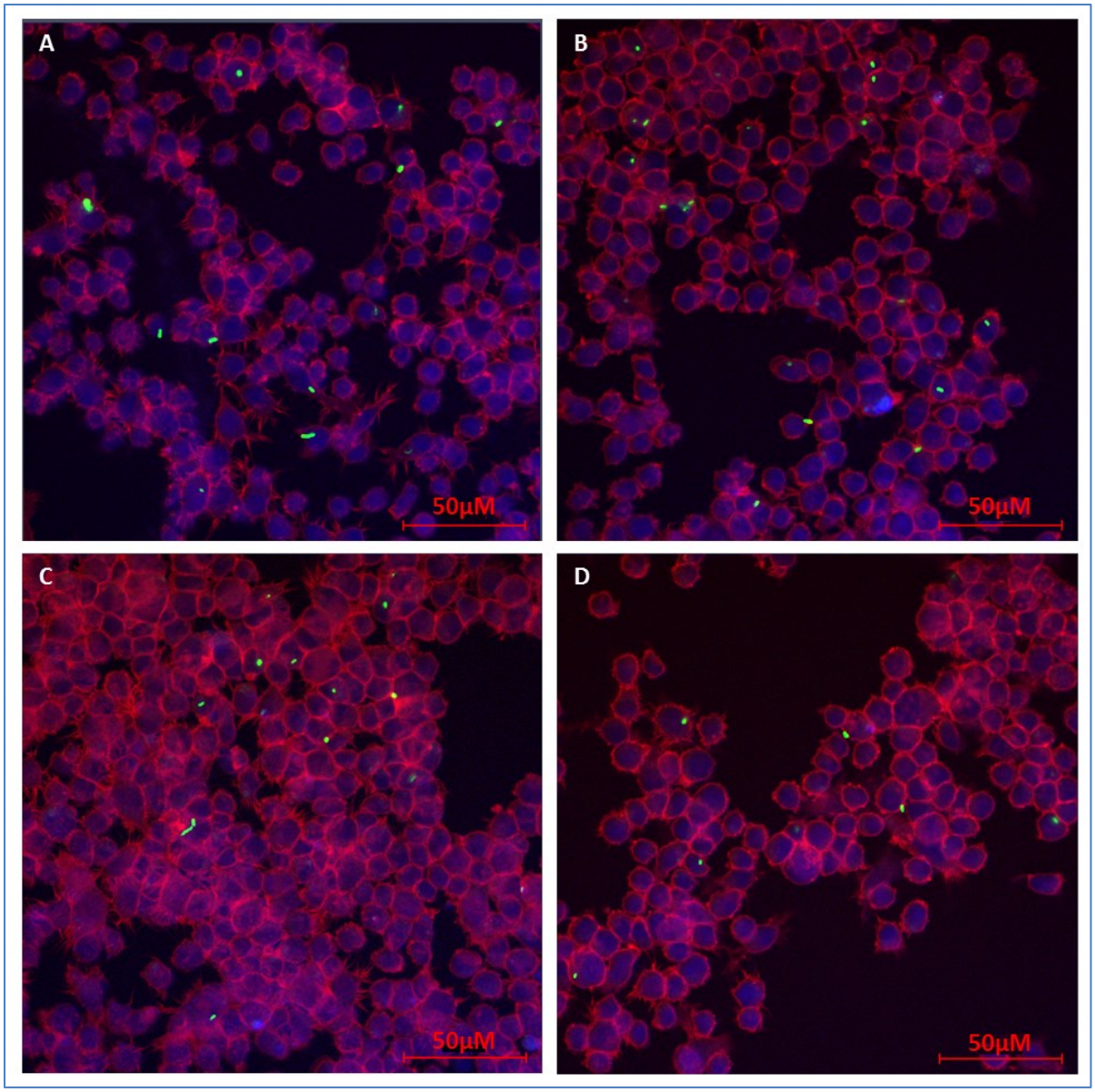

Figure 28 *Confocal microscopy images of RAW 264.7 cells infected with representative L. pneumophila isolates of each clade (labelled) at 30 minutes post-infection. RAW 264.7 cells seeded on 13mm poly-L-lysine glass coverslips were inoculated at an MOI of 1. After centrifugation at 500rpm for 5 minutes, the infected cells were incubated in antibiotic-free media at 37°C for 30 minutes. Media was then removed from the plate and each well was washed twice with PBS. Cells on the coverslips were fixed with PFA (4% paraformaldehyde in PBS; pH 7.4) for 20 minutes at room temperature. Cells were then permeabilised with 0.5% Triton X100 for 15 minutes at room temperature. Non-specific binding sites were blocked with BSA/PBS for 30 minutes at room temperature. Legionella were stained with FITC-conjugated anti-Legionella antibody (green), F-actin was visualised with Phalloidin 568 (red) and DNA was stained with DAPI (blue).*

Real-time quantitative PCR (qPCR) was used to quantify the number of *Legionella* inside infected RAW 264.7 cells over time. In this assay, multiple PCRs are monitored simultaneously in the thermal cycler, which detects the change in the fluorescent signal that is emitted by the dye SYBR Green I when it binds double-stranded DNA (Higuchi *et al.*, 1993). The number of cycles at which the fluorescence level becomes statistically significantly higher than the background level is known as the

threshold cycle (Ct). As the Ct is inversely proportional to the log of the initial copy number, it can be used to compare the number of copies of a gene of interest in multiple DNA samples (Dieffenbach and Dveksler, 1995).

For each reaction, an amplification plot is generated with tenfold serial dilutions of the amplification product. The Ct of each dilution is then plotted against the initial DNA quantity of each dilution, and the resulting gradient is used to calculate PCR efficiency (*E)* of one cycle during the exponential phase according the equation: $E = 10^{-1/\text{gradient}}$ (Rasmussen, 2001). The relative expression ratio (*R)* of a target gene is calculated using the Ct of an unknown sample versus a control, according to the equation: $R = E^{\Delta Ct(\text{control} - \text{unknown})}$ (Pfaffl, 2001).

DNA samples were prepared by infecting RAW 264.7 cells with representative isolates of each clade at an MOI of 1. The DNA samples were extracted at 30 minutes, 2 hours, 4 hours and 24 hours post-infection using the QIAamp® DNA Mini Kit (Qiagen). Primers were designed to probe the DNA samples for the *Legionella* gene *icmQ* and the RAW 264.7 cell gene *β-actin*. The primers were validated by PCR on genomic DNA extracted from RAW 264.7 cells infected with the representative *Legionella* isolate from clade A (*Figure 29*).

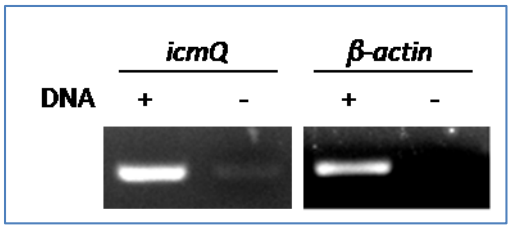

Figure 29 *PCR validation of primers for the genes icmQ and β-actin on genomic DNA extracted from RAW 264.7 cells infected with Legionella clade A isolate 12_5415 (MOI=1) at 2 hours post-infection. Negative controls (-) contain no DNA.*

Appropriate primer concentrations for qPCR were determined by amplification plots of the two genes with a range of primer concentrations (Figure 30). These plots showed that primer concentrations of 300nM and 200nM were sufficient for reactions with the primers for *icmQ* and *β-actin*, respectively. Dissociation curves were also generated for each pair of primers to determine the melting temperature of the amplification products (Figure 31). The single sharp peak present in each plot indicates the presence of a single amplification product and therefore high specificity of the primers and no primer dimer formation. Across three biological and technical replicates, the mean efficiency of the primers for *icmQ* and *β-actin* were 2.39 and 2.13, respectively (correlation coefficient $R^2 > 0.95$).

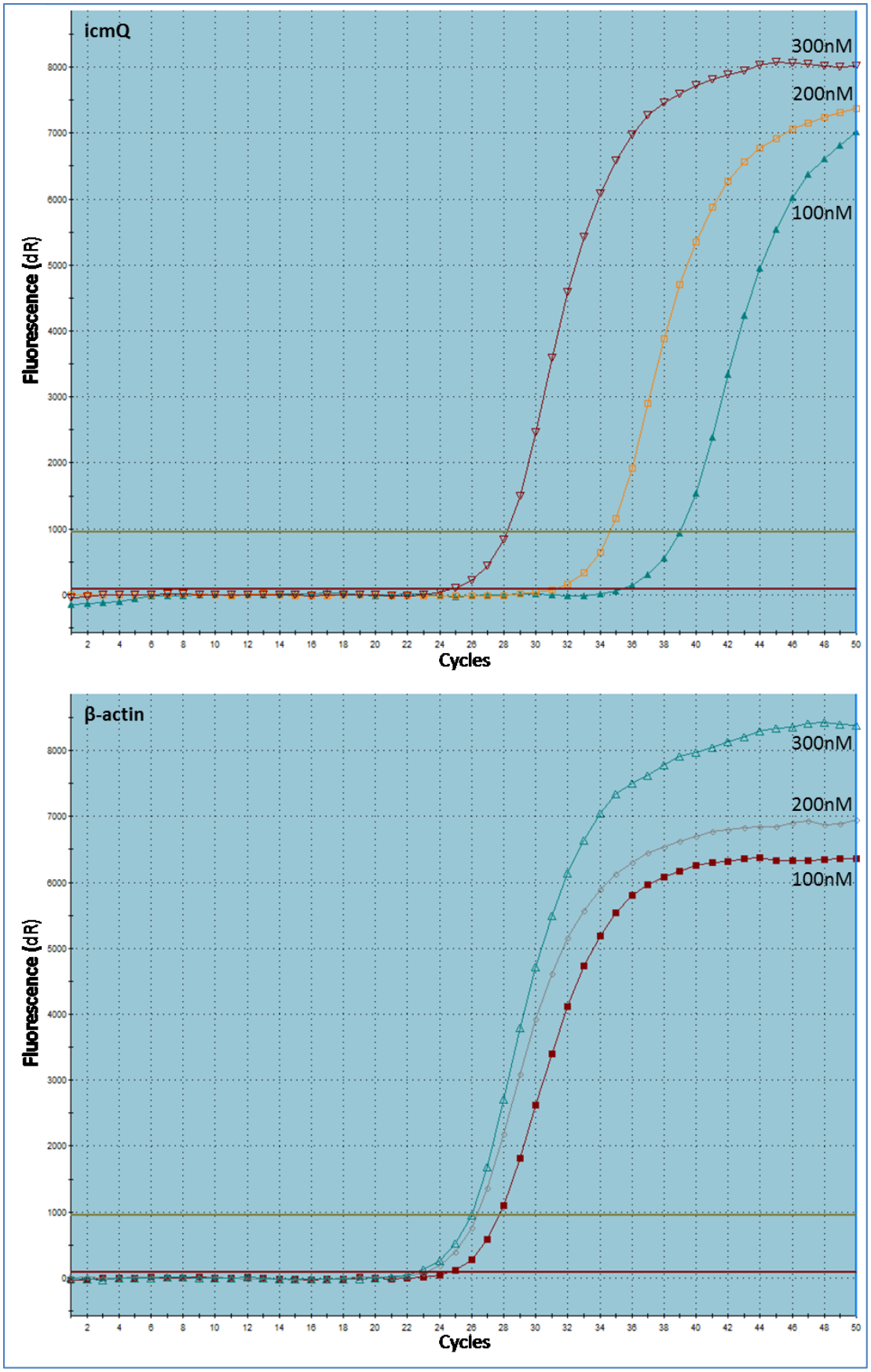

Figure 30 *Amplification plots with primers for icmQ and β-actin at 100nM, 200nM or 300nM. The genomic DNA sample used was extracted from RAW 264.7 cells infected with Legionella clade A isolate 12_5415 (MOI=1) at 2 hours post-infection.*

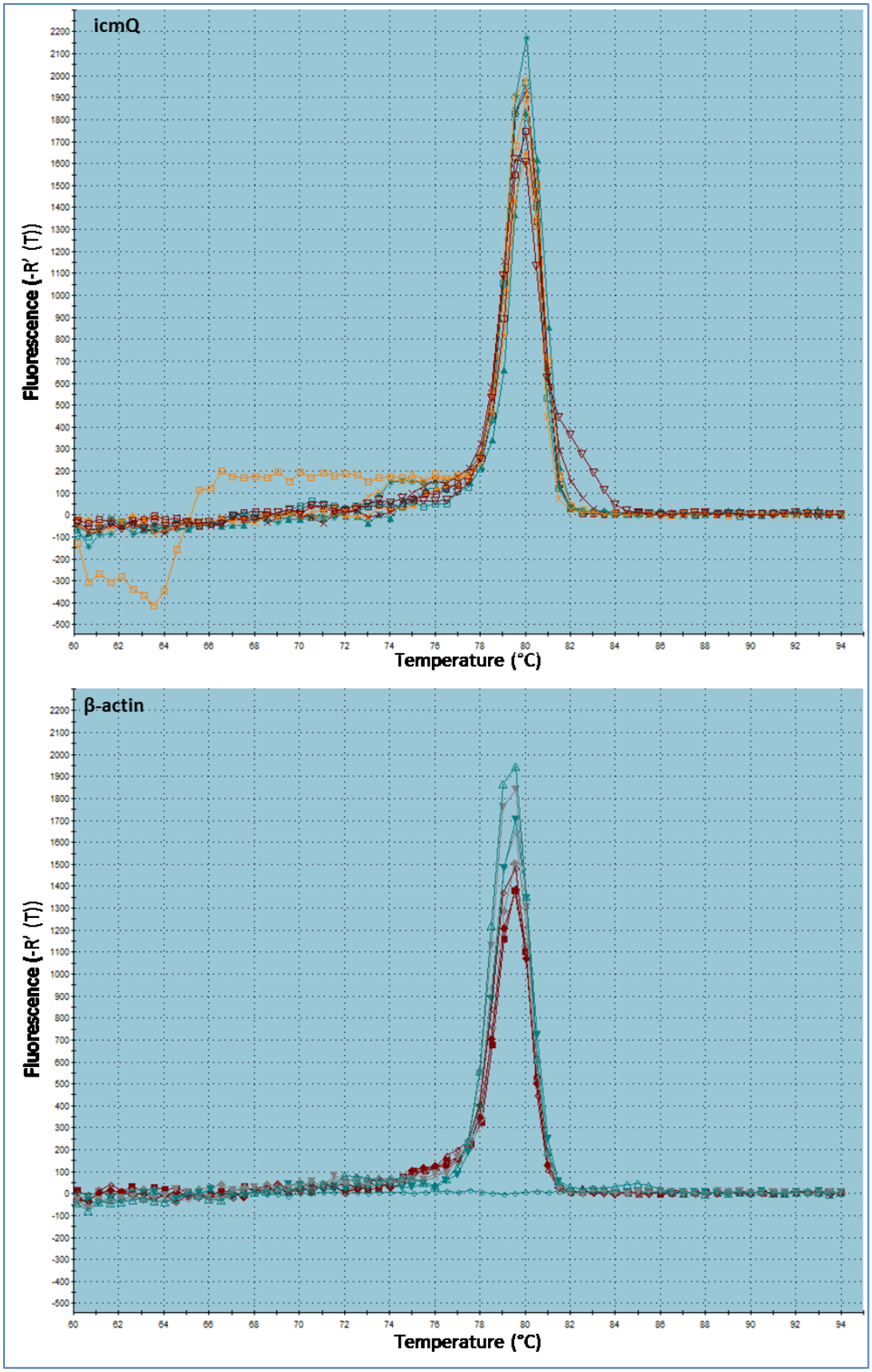

Figure 31 *Dissociation curve with forward and reverse primers for icmQ and β-actin at 100nM, 200nM or 300nM. The genomic DNA sample used was extracted from RAW 264.7 cells infected with Legionella clade A isolate 12_5415 (MOI=1) at 2 hours post-infection.*

This qPCR assay was used to compare the relative number of *Legionella* inside RAW 264.7 cells at 30 minutes after infection with representative isolates of each clade. In this assay, the relative quantity of *icmQ* and *β-actin* was compared between 10µg DNA samples from cells infected with each isolate. For each gene, the relative expression ratio was calculated relative to sample with the highest Ct (and therefore lowest initial copy number) of the four samples. The ratio of *Legionella* to RAW 264.7 cells was then calculated by dividing the relative expression ratio of *icmQ* by that of *β-actin* (*Figure 32*).

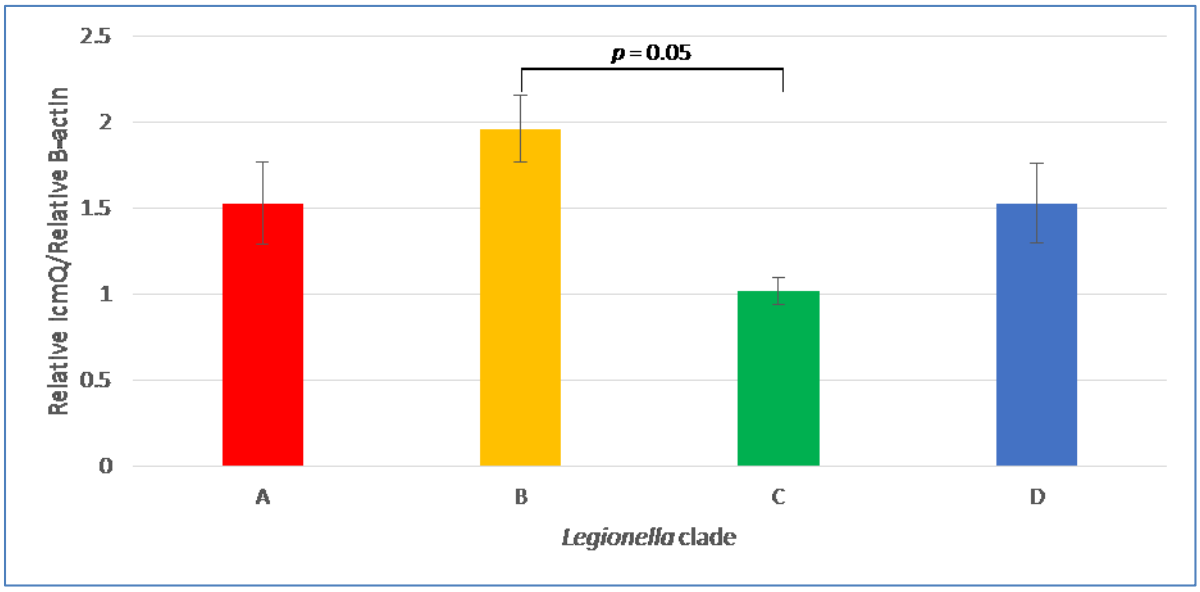

Figure 32 *Relative number of intracellular Legionella at 30 minutes post-infection as determined by real-time qPCR. Error bars show standard error across three biological and technical replicates.*

The results show a significant difference in the number of intracellular *Legionella* in RAW 264.7 cells infected with clade B and C isolates, as determined by a student's 2-sample t-test (*Figure 32*). As the infections were all carried out at an MOI of 1, verified by plating serial dilutions of the inoculum, this variation could be due to a difference in the efficiency of host cell invasion between the isolates. Therefore, when quantifying the intracellular replication of each isolate by qPCR, the relative expression ratios were calculated relative to the Ct at 30 minutes post-infection. The ratio of *Legionella* to RAW 264.7 cells was then calculated by dividing the relative expression ratio of *icmQ* by that of *β-actin* (Figure 33).

The results of the real-time qPCR experiment indicate that isolates from clades A and B showed higher net replication than those from clades C and D (Figure 33). The fold change was significantly higher in the clade A isolate than the clade D isolate. These results suggest an inverse

correlation between net intracellular replication and virulence in the *Galleria* infection model described by McAdam *et al.* (2014).

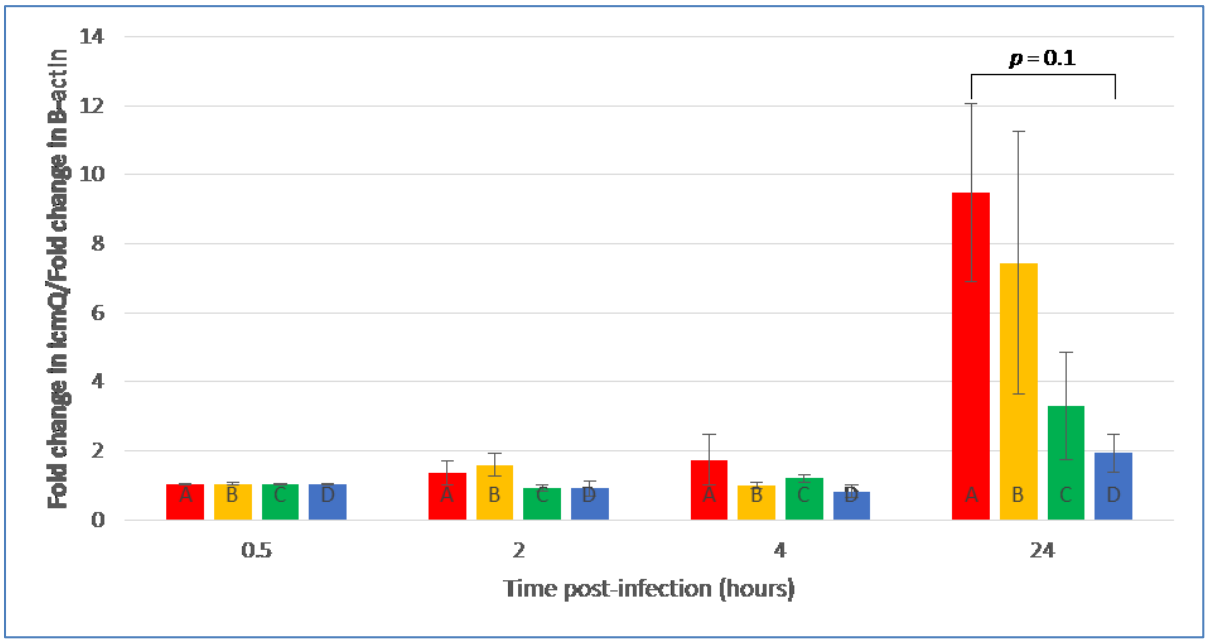

Figure 33 *Fold change in the number of intracellular Legionella as determined by real-time qPCR. Bar labels indicate the clade of each representative isolate. Error bars show standard error across three biological and technical replicates.*

Another example of this inverse correlation is found in the *Salmonella enterica* serovar Choleraesuis, which causes systemic disease with a high mortality rate in pigs (Paulin *et al.*, 2007). In contrast, the serovar Typhimurium causes acute enteritis but is rarely fatal. Typhimurium shows greater net replication than Choleraesuis in the intestinal mucosa, where it causes a greater induction of proinflammatory cytokines. It is thought that the rapid pro-inflammatory response triggered by Typhimurium may confine the infection to the intestine, whereas the slower replication of Choleraesuis may facilitate evasion from the host immune response and the resulting systemic disease. Furthermore, it has been suggested that the slow growth rate of *Mycobacterium tuberculosis* may prevent rapid death of the host and thereby promote dissemination of the bacteria (Ernst *et al.*, 2007).

Cell cytotoxicity assay

A cytotoxicity assay was used to compare the rate of host cell death during infection with representative isolates of each clade (Figure 34). The CytoTox 96® Non-Radioactive Cytotoxicity Assay (Promega) was used to measure the amount of lactate dehydrogenase (LDH) released by infected

RAW 264.7 cells into the supernatant at 2, 4 and 24 hours post-infection during a gentamicin protection assay (MOI =1). LDH release is used as a measure of cytotoxicity as this cytosolic enzyme is released from dead or damaged cells (Parhamifar *et al.*, 2013). In this assay, LDH catalyses the conversion of NAD^+ into NADH, which results in the conversion of a yellow tetrazolium salt into red formazan. This colour change is proportional to the amount of LDH and therefore the number of lysed cells, and can be measured by the absorbance of the supernatant at 490nm.

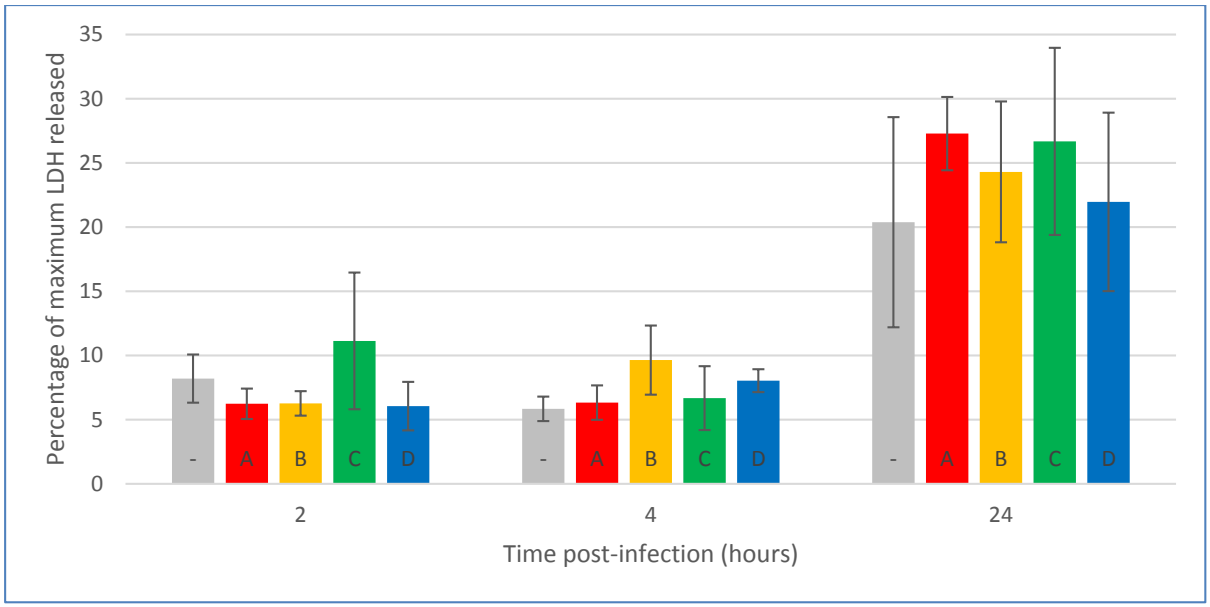

Figure 34 *Cell cytotoxicity assay. Bar labels indicate uninfected cells (-) or the clade of the representative isolate used for infection. Error bars show standard error across three biological replicates.*

In this assay, the absorbance at 490nm was measured using the FLUOstar Optima microplate reader (BMG LabTech). The percentage of lysed cells was calibrated using phenol red-free DMEM as the negative control (0%) and uninfected cells incubated with Lysis Solution (Promega) for 45 minutes as the positive control (100%). The assay was optimised by using phenol red-free DMEM during the infections to ensure that the colour change of the assay was not affected by the presence of phenol red in the supernatant. In addition, the supernatant samples were centrifuged at 300 x g for 4 minutes to remove any detached cells that may have been present. This step ensured that the supernatant samples did not contain any additional LDH released from the detached cells when the samples were frozen for storage before the assay was performed.

The results of the cytotoxicity assay show no significant difference in the rate of cell death during infection with isolates of each clade, as determined by a student's 2-sample t-test (Figure 34). Furthermore, no significant difference was observed between the rate of cell death in uninfected and infected cells. This evidence indicates that the isolates do not activate pyroptosis. This could be

verified by quantifying IL-1β and IL-18 released from the host cell as a measure of caspase-1 activation and pyroptosis (Case and Roy, 2013).

LC3 conversion assay

In order to survive inside the host cell, *L. pneumophila* escapes the autophagy pathway and thereby evades lysosomal degradation of the LCV (reviewed in Xu and Luo, 2013). Autophagy clears intracellular pathogens by packaging them into phagosomes, which then fuse with lysosomes to degrade the enclosed pathogens (Xie and Klionsky, 2007). The autophagy pathway of infected cells is inhibited by the *L. pneumophila* effector protein RavZ (Choy *et al.*, 2012). Although the gene encoding RavZ is present in all 4 of the clades, it is possible that one or more of the predicted novel effectors could also be involved in modulating host cell autophagy.

Therefore, the level of LC3 conversion was determined as a measure of autophagy in RAW 264.7 cells during infection with representative isolates of each clade. In mammalian cells, the microtubule-associated protein 1 light chain 3 (LC3) is found in two distinct forms, LC3-I and LC3-II (Kabeya *et al.*, 2000). LC3-I is present in the cytosol, whereas LC3-II is a lipidated form which specifically binds to autophagosome membranes (Tanida *et al.*, 2004). The conversion of LC3-I to LC3-II correlates with autophagosome formation and is therefore used as a marker of autophagy.

RAW 264.7 cells were inoculated with either representative *L. pneumophila* isolates (MOI = 1) or DMEM (uninfected control), then lysed with BugBuster™ Protein Extraction Reagent (Novagen) at 2, 4 or 24 hours post-infection. The resulting lysate samples were separated by SDS-PAGE, then visualised by western blotting with an antibody against LC3 (Figure 35). The intensities of LC3-I and LC3-II in each sample were quantified using the Li-Cor Odyssey infrared imager and Li-Cor Image Studio software. The ratio of LC3-II to total LC3 was then calculated as a measure of autophagy (Figure 36).

No significant difference was observed between cells infected with representative isolates, or between infected and uninfected cells, as determined by a student's 2-sample t-test. However, significant inhibition by the clade D isolate at 24 hours post-infection may be seen with further replicates of the assay.

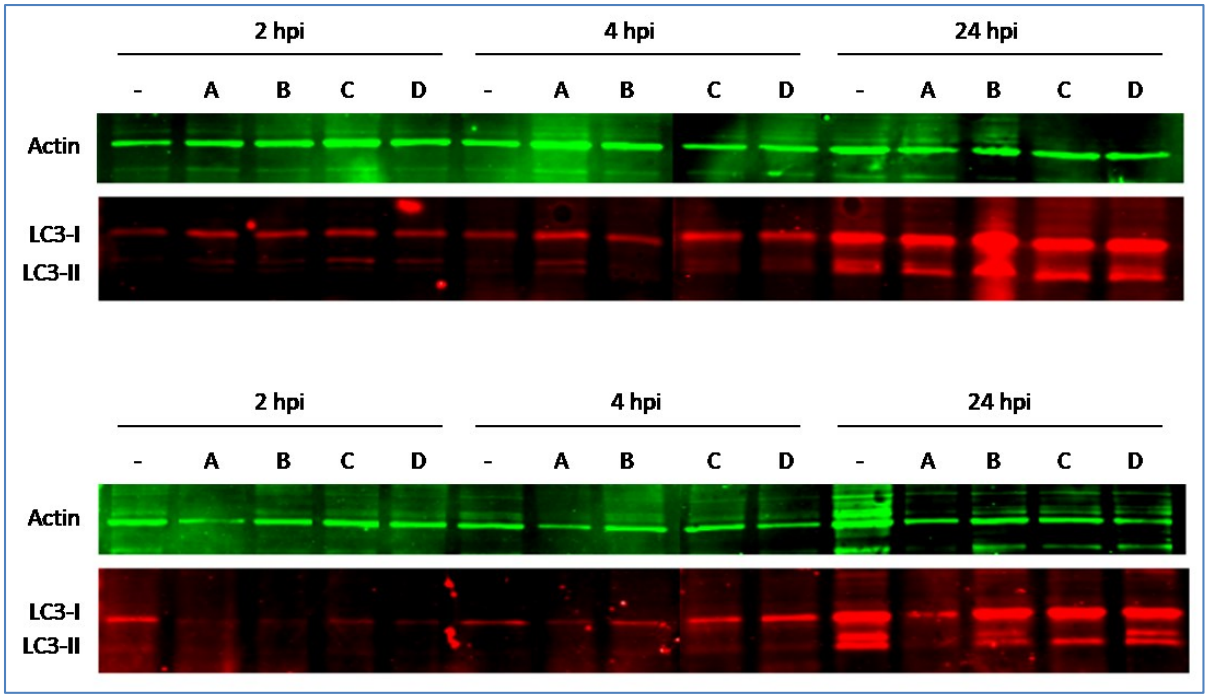

Figure 35 *LC3 conversion assay by western blot. Data from 2 biological replicates is shown. Each lane contains a lysate sample from either uninfected cells (-) or cells infected with a representative isolate (A, B, C, D) at 2, 4 or 24 hours post-infection (hpi). Actin was used as a loading control.*

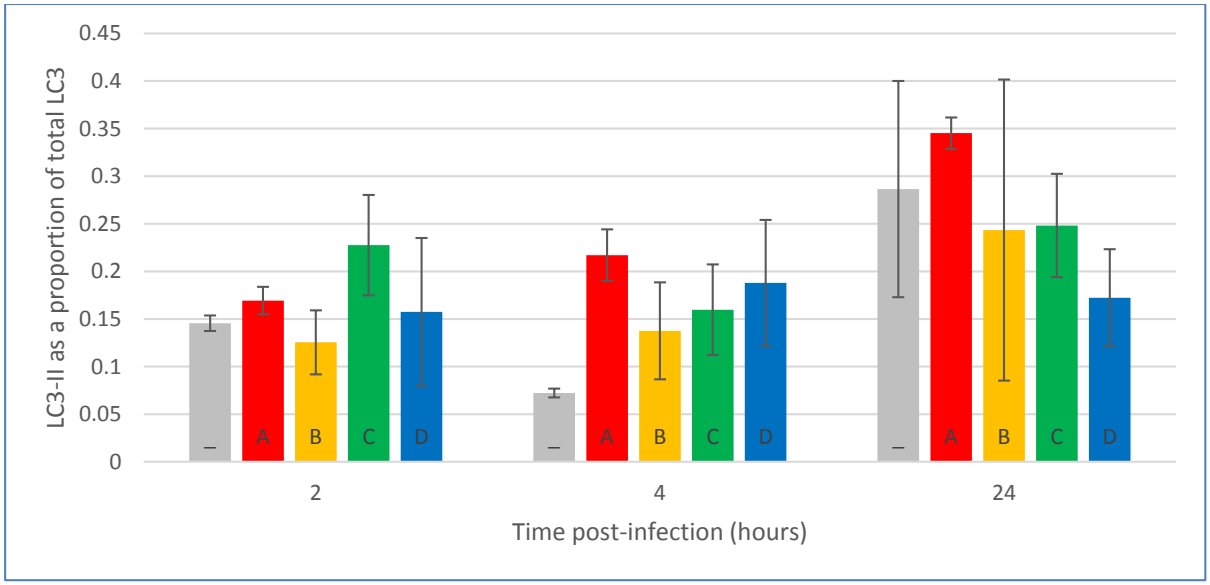

Figure 36 *LC3 conversion assay. Bar labels indicate uninfected cells (-) or the clade of the representative isolate used for infection. Error bars show standard error across two biological replicates.*

Summary

The replication rates of *L. pneumophila* isolates from each clade were compared in both broth culture and infected RAW 264.7 cells. No significant difference in replication was observed in broth culture. In contrast, the net intracellular replication of clades A and B was higher than that of clades C and D, suggesting an inverse correlation between intracellular replication rate and virulence. However, assays for cell cytotoxicity and autophagy showed no significant difference between cells infected with the representative isolates.

Chapter 5: General discussion

Identification of a novel T4SS-encoding pathogenicity island

Bioinformatic analysis has shown that the unique 39-kb region identified in clades C and D closely resembles a pathogenicity island. These islands carry one or more virulence genes, and therefore contribute to rapid changes in the virulence of a species (Dobrindt *et al*., 2004). Virulence genes previously found on other pathogenicity islands encode proteins with a range of different functions including adherence, iron uptake, capsule formation, entry into host cells and secretion systems. It is therefore possible that the 39-kb region also carries virulence genes, which could underlie the increased virulence of clade C and D isolates.

A 65-kb pathogenicity island found in 41 *L. pneumophila* strains has also been identified in three strains of *Legionella anisa*, indicating that the islands may be transferred between different *Legionella* species (*Cazalet et al*., 2008). This finding supports the hypothesis that the 39-kb region was transferred to some of the Edinburgh outbreak *L. pneumophila* strains from *L. longbeachae* in the environment.

The *Legionella* genomic island (LGI-2) identified in *L. pneumophila* Corby can be transferred by conjugation (Lautner *et al.*, 2013). LGI-2 is excised from the chromosome, generating a circular episomal form of the island, which can be transferred to another *L. pneumophila* strain. Lautner *et al.* (2013) used primers specific to either the circular or chromosomal form of the genomic island in order to determine the rate of excision by real-time qPCR. This technique could be used to determine whether or not the 39-kb region is excised and therefore a functional genomic island.

Acquisition of the pathogenicity island from *L. longbeachae*

The 39-kb region was found to share 94% nucleotide identity with the homologous region in a *L. longbeachae* isolate from a compost sample provided by a Legionnaires' disease patient. This patient was one of six people infected with *L. longbeachae* in Scotland between August and September 2013 (Potts *et al.*, 2013). All six of these patients required intensive care and notably, all were amateur gardeners who had been exposed to horticultural growing media during their incubation period. This finding has significance as commercial compost is thought to be the main source of human infection by this species (Health Protection Scotland, 2013).

L. longbeachae was detected in five samples of growing media linked to five of the patients. The same amplified fragment length polymorphism (AFLP) DNA profile was found in isolates from the

patients and isolates from the growing media that they had been working with (Health Protection Scotland, 2014). However, whole genome sequencing showed that there was no close relationship between isolates from the patients and the growing media linked to each case.

L. longbeachae causes around 50% of cases of Legionnaires' disease in Australia (NNDSS Annual Report Writing Group, 2015). Unfortunately, *L. longbeachae* infections test negative using routine *Legionella* urinary antigen tests, as these only detect *L. pneumophila* (Health Protection Scotland, 2013). Therefore *L. longbeachae* can only be identified by elevated antibody titre, PCR and culture.

The interaction between *L. longbeachae* and its host cells is thought to be distinct from that of *L. pneumophila,* as the *L. longbeachae* genome encodes a unique set of putative Dot/Icm T4BSS effectors and eukaryotic-like proteins (Cazalet *et al.*, 2010). Unlike *L. pneumophila, L. longbeachae* does not trigger caspase-1 activation in murine macrophages, and is therefore able to replicate inside the lungs of C57BL/6 and BALB/c mice (Asare *et al.*, 2007). Therefore, the acquisition of *L. longbeachae* genes could provide *L. pneumophila* with novel virulence determinants or survival mechanisms.

Predicted T4SS-secreted effector proteins

mRNA encoding the predicted effector protein 00662 was detected during the infection of RAW 264.7 cells with *L. pneumophila* isolates of clades C and D. However, expression of predicted effector mRNA was only studied at 18 hours post-infection, so it is possible that the other predicted effectors are expressed at either earlier or later stages of infection and were missed in this analysis. RNA samples could be taken at hourly time points to determine the time at which expression is induced.

Expression of the predicted effector protein 00662 could be validated by the construction of a fusion protein with a c-Myc tag, which could then be detected using an antibody against the c-Myc epitope. Secretion of this fusion protein by the newly identified LGI-T4SS could be verified by transfecting the plasmid encoding the fusion protein into isolates with and without the 39-kb region. Secretion of the protein during broth culture could then be determined by western blot analysis of the supernatant. Secretion and localisation of the protein during host cell infection could also be studied by immunohistochemistry.

Figure 37 shows the predicted eukaryotic-like linear motifs in the protein encoded by *00662*. The predicted functions of these motifs (discussed below) could be verified by assays such as an *in*

vitro actin polymerisation assay for the WH2 actin-binding motif. In addition, deletion mutants could be constructed to determine the requirement of each domain in intracellular replication or virulence. To determine the requirement of the LGI-T4SS, 00662 or other predicted effectors in the virulence of *Legionella*, knockout mutants could be constructed and compared with wild-type strains in infection models.

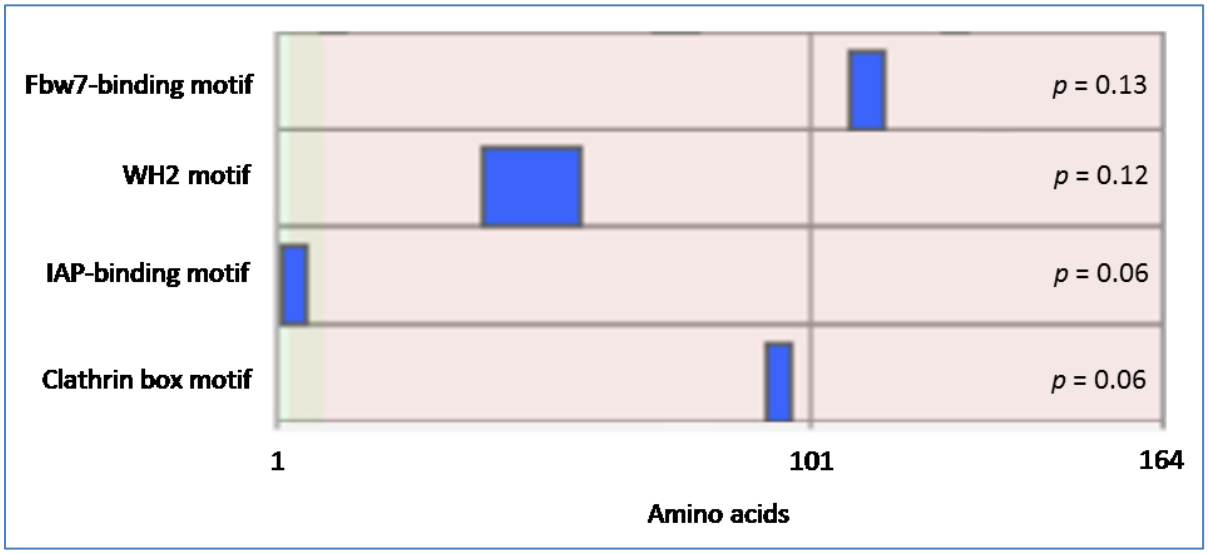

Figure 37 *Location and probability of predicted eukaryotic linear motifs in protein 00662 as determined by the eukaryotic linear motif resource ELM (http://elm.eu.org) (Dinkel et al., 2013).*

Fbw7-binding motif

Fbw7 (F-box and WD repeat domain-containing protein 7) is an F-box protein that acts as a substrate receptor for a class of E3 ubiquitin ligases called SCF (Skp1 Cullin-1 F-box) ligases (Davis *et al.*, 2014). E3 ubiquitin ligases facilitate the covalent attachment of ubiquitin to a specific protein (Schwartz and Ciechanover, 2009). This marks the protein for degradation by the 26S proteasome as part of the ubiquitin-proteasome system (UPS). The UPS is a major pathway for the degradation of regulatory proteins in the eukaryotic cell (Crusio *et al.*, 2010). Therefore, the UPS has far-reaching effects including the regulation of cell division, apoptosis and inflammation (Finley, 2009).

In an SCF E3 ubiquitin ligase, Skp1 links the complex to an interchangeable F-box protein via its F-box domain, thereby conferring substrate specificity (Welcker and Clurman, 2008) (Figure 38). The SCF-Fbw7 complex (SCF^{Fbw7}) is thought to target over twenty cellular proteins with roles in proliferation, apoptosis and metabolism (Davis *et al.*, 2014). The majority of Fbw7 substrates are transcriptional regulators involved in gene expression (Welcker and Clurman, 2008).

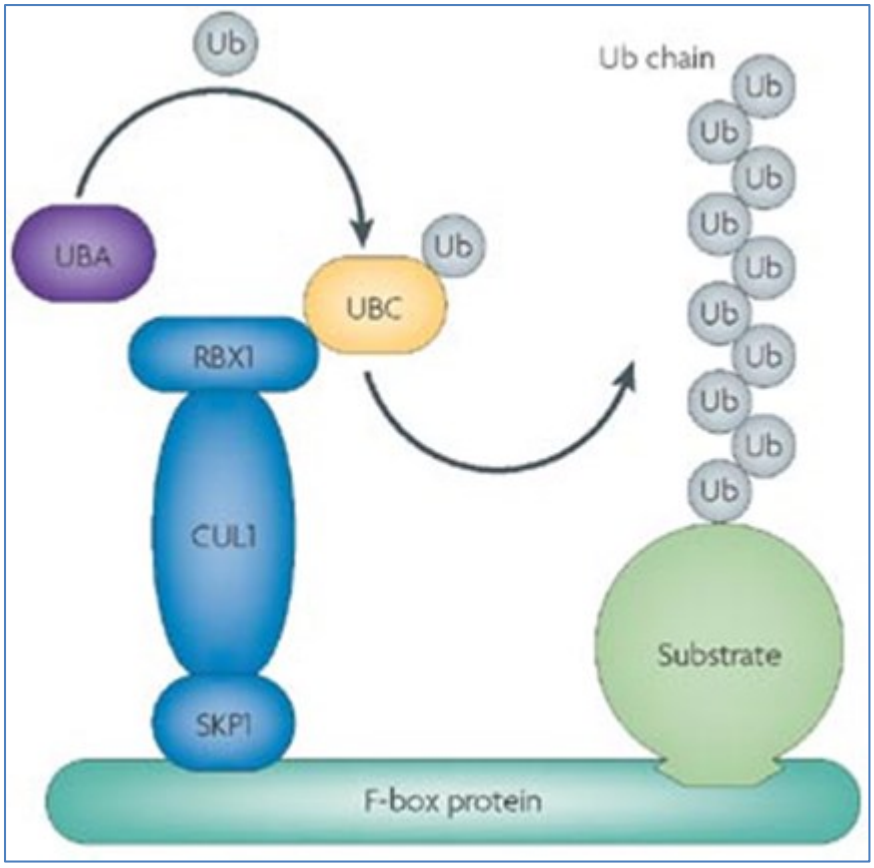

Figure 38 *SCF ubiquitin ligase complex (Welcker and Clurman, 2008). Cullin-1 (CUL1) links the RING protein RBX1 to SKP1 (Zheng et al., 2002). The RING subunit recruits an E2 ubiquitin-conjugating enzyme (UBC) and Skp1 binds an F-box protein, which binds the substrate (Petroski and Deshaies, 2005, Bai et al., 1996). The E1 ubiquitin-activating enzyme (UBA) transfers a ubiquitin molecule to the E2 ubiquitin-conjugating enzyme (UBC) (Alberts et al., 2008b). Next, the UBC forms a complex with the SCF E3 ubititin ligase, which binds the protein substrate. The UBC then assembles a polyubiquitin chain on the substrate protein.*

For example, one of the Fbw7 substrates is a transcription factor and proto-oncogene called c-Myc (Yada *et al.*, 2004). This protein is expressed transiently as cells enter the G_1 phase of the cell cycle and promotes cell proliferation. Depletion of Fbw7 by RNA interference has been shown to increase the abundance and activity of c-Myc. SCF^{Fbw7} also targets other proto-oncogenes such as cyclin E, Notch and Jun (Welcker and Clurman, 2008). Therefore, it can be considered to be a tumour suppressor. Notably, the *Fbw7* gene is one of the most frequently mutated genes in human cancers (Davis *et al.*, 2014).

The binding of Fbw7 by 00662 may inhibit its substrate receptor activity, thereby preventing the ubiquitination and degradation of host cell proteins by the UPS. The resulting accumulation of host cell proteins may increase proliferation or reduce apoptosis of the host cell, thereby protecting the replicative niche of *L. pneumophila* and facilitating intracellular replication.

WH2 motif

The WH2 domain (WASP homology domain 2) binds actin monomers and is present in many regulators of the actin cytoskeleton (Paunola *et al.*, 2002). Several species of bacteria secrete effector proteins containing WH2 domains via a Type III Secretion System (Yu *et al.*, 2011). For example, the *Vibrio cholerae* effector VopF disrupts the actin cytoskeleton of eukaryotic host cells via its WH2 domain (Tam *et al.*, 2007).

The actin cytoskeleton of the eukaryotic host cell is involved in many vital processes, including endocytosis, phagocytosis and cell division (Alto and Orth, 2012). Therefore, an actin-binding WH2 domain in 00662 could promote intracellular *L. pneumophila* survival via several different mechanisms. For example, disruption of the actin cytoskeleton may inhibit vesicle trafficking and thereby protect the LCV from lysosomal degradation. Alternatively, reorganisation of the actin cytoskeleton could lead to a loss of cell membrane integrity and cause lysis of the host cell (Ham *et al.*, 2011).

IAP-binding motif

Inhibitor of apoptosis proteins (IAPs) suppress apoptotic cell death (Salvesen and Duckett, 2002). IAPs contain baculoviral IAP repeat (BIR) domains, which bind to and inhibit active caspases (Prunell and Troy, 2004) (*Figure 39*). IAP antagonists act by displacing bound caspases from the BIR domains of IAPs (Orme and Meier, 2009).

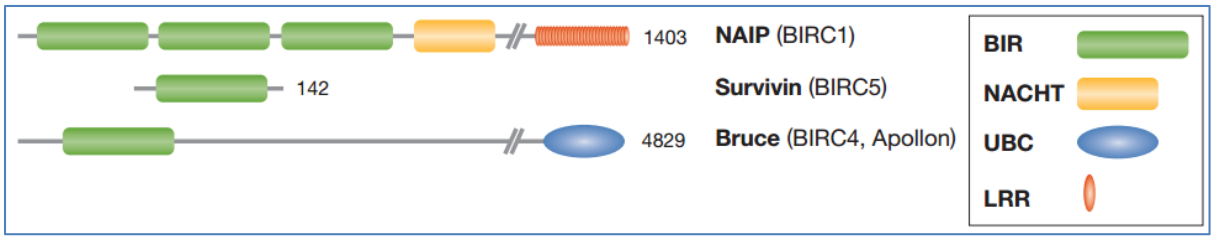

Figure 39 *The human IAP family contains BIR (baculoviral IAP repeat), NACHT (NAIP, C2TA, HET-E and TP1), UBC (ubiquitin conjugation) and LRR (leucine-rich repeat) domains (Eckelman et al., 2006).*

The predicted IAP-binding motif on 00662 binds specifically to Type II BIR domains, which are found in two mammalian proteins, Survivin and Bruce/Apollon (Lens *et al.*, 2006). Survivin plays an essential role in chromosome segregation and cytokinesis during cell division. In contrast, Bruce/Apollon is an IAP that prevents SMAC-induced apoptosis by facilitating the proteasomal

degradation of caspase-9 and the pro-apoptotic molecule SMAC via IAP-binding motifs (Hao *et al.*, 2004).

A type II BIR domain is present on the Naip5 protein, which is required for flagellin-induced caspase-1 activation in resistant macrophages (Eckelman *et al.*, 2006, Amer *et al.*, 2006). Therefore, inhibition of Naip5 by 00662 could prevent caspase-1 activation. This would inhibit fusion of the LCV with the lysosome, prevent host cell pyroptosis and promote survival of *L. pneumophila* inside the host cell.

Clathrin box motif

Clathrin-coated vesicles transport material between the plasma membrane, endosomes and Golgi compartments (Alberts *et al.*, 2008a). Clathrin protein subunits are comprised of three heavy and three light polypeptide chains, forming a triskelion structure. These assemble into a framework on the cytosolic surface of membranes. Adaptor proteins form a layer between the clathrin framework and the membrane, where they bind the clathrin to the membrane via lateral interactions.

The clathrin box motif on 00662 is found on adaptor proteins, and interacts with the clathrin heavy chain. This interaction may therefore inhibit the formation of clathrin-coated vesicles in the host cell and disrupt intracellular trafficking.

Measuring intracellular replication of *L. pneumophila*

During intracellular growth, *L. pneumophila* can differentiate into several different phenotypic forms (Garduno *et al.*, 2002). This introduces several limitations into the quantification of intracellular *Legionella* replication. For example, quantifying *L. pneumophila* colonies plated on CYE agar plates is skewed in favour of bacteria that are present in a particular phenotypic form that supports growth on agar (Tiaden *et al.*, 2013). The efficiency of DNA extraction is also affected by the presence of different phenotypic forms. For example, the mature intracellular form (MIF) is resistant to detergent-mediated lysis, thereby reducing the efficiency of DNA extraction (Garduno *et al.*, 2002). Therefore, DNA extraction also skews qPCR quantification of *L. pneumophila* in favour of those present in a particular phenotypic form.

Nevertheless, relative numbers of intracellular bacteria were measured by real-time qPCR. However, the growth curves recorded in broth culture show that *L. pneumophila* replication can take

several days. Therefore, it would be useful to extend the qPCR experiment to compare replication rates at later time points. In addition, it would be useful to validate the results in human cell lines, such as U937 macrophages, THP-1 monocytes or HL-60 promyelocytic cells.

An alternative method for quantifying intracellular replication is flow cytometry (Tiaden *et al.*, 2013). Bacteria that constitutively express green fluorescent protein (GFP) can be quantified by GFP fluorescence intensity, thereby providing a method for real-time analysis of intracellular replication that is sensitive, fast and accurate.

Measuring host cell responses and virulence

The LC3 conversion assay showed no significant difference in inhibition of autophagy between isolates of the four clades. However, this assay could be optimised by carrying out the infection of RAW 264.7 cells under starvation conditions using FCS-free media (Kabeya *et al.*, 2000). This would induce autophagy in the host cells and therefore provide more conclusive evidence of any inhibition by the *Legionella* isolates.

To determine the mechanism underlying the difference in virulence between the clades, other aspects of the host cell response could be studied. For example, pore formation during host cell pyroptosis could be measured by incubation with propidium iodide (Case and Roy, 2013). This molecule can pass through pores in the cell membrane and bind to nucleic acid. The fluorescence of propidium iodide increases when bound to nucleic acid, and can therefore be used as a measure of pore formation in real time using a multi-well fluorescence plate reader. Alternatively, the level of IL-1β and IL-18 released by the host cell can be quantified by ELISA as a measure of pyroptosis.

McAdam *et al.* (2014) used a *Galleria mellonella* infection model to compare the virulence of *L. pneumophila* isolates from each clade. Although this has been shown to be an effective model for human infection, an *in vivo* mammalian infection model could be used to validate these results (Harding *et al.*, 2012). For example, two well-studied models are the guinea pig and the A/J mouse (Hori and Zamboni, 2013, Edelstein, 2013).

Summary

The results of this report indicate that the novel T4SS identified in the *L. pneumophila* outbreak isolates is an LGI-T4SS that originated in *L. longbeachae.* The novel region also encodes at least one putative T4SS-secreted effector protein, which contains several eukaryotic-like motifs. These motifs could facilitate host cell interactions and thereby underlie the increased virulence of isolates containing the novel region. In addition, an inverse correlation was shown between the presence of the novel region and net intracellular replication. Future work could build on these findings to determine the precise role of the novel T4SS in infection.

References

AKHTER, A., GAVRILIN, M. A., FRANTZ, L., WASHINGTON, S., DITTY, C., LIMOLI, D., DAY, C., SARKAR, A., NEWLAND, C. & BUTCHAR, J. 2009. Caspase-7 activation by the Nlrc4/Ipaf inflammasome restricts Legionella pneumophila infection. *PLoS Pathog,* 5**,** e1000361.

AL-BANA, B. H., HADDAD, M. T. & GARDUÑO, R. A. 2014. Stationary phase and mature infectious forms of Legionella pneumophila produce distinct viable but non-culturable cells. *Environmental microbiology,* 16**,** 382-395.

ALBERTS, B., JOHNSON, A., LEWIS, J., RAFF, M., ROBERTS, K. & WALTER, P. 2008a. The Assembly of a Clathrin Coat Drives Vesicle Formation. *Molecular Biology of the Cell.* 5th ed. New York: Garland Science.

ALBERTS, B., JOHNSON, A., LEWIS, J., RAFF, M., ROBERTS, K. & WALTER, P. 2008b. An Elaborate Ubiquitin-Conjugating System Marks Proteins for Destruction. *Molecular Biology of the Cell.* 5th ed. New York: Garland Science.

ALLOMBERT, J., FUCHE, F., MICHARD, C. & DOUBLET, P. 2013. Molecular mimicry and original biochemical strategies for the biogenesis of a Legionella pneumophila replicative niche in phagocytic cells. *Microbes and Infection,* 15**,** 981-988.

ALTO, N. M. & ORTH, K. 2012. Subversion of cell signaling by pathogens. *Cold Spring Harbor perspectives in biology,* 4**,** a006114.

ALTSCHUL, S. F., GISH, W., MILLER, W., MYERS, E. W. & LIPMAN, D. J. 1990. Basic local alignment search tool. *Journal of molecular biology,* 215**,** 403-410.

ALVAREZ-MARTINEZ, C. E. & CHRISTIE, P. J. 2009. Biological diversity of prokaryotic type IV secretion systems. *Microbiology and Molecular Biology Reviews,* 73**,** 775-808.

AMER, A., FRANCHI, L., KANNEGANTI, T.-D., BODY-MALAPEL, M., ÖZÖREN, N., BRADY, G., MESHINCHI, S., JAGIRDAR, R., GEWIRTZ, A. & AKIRA, S. 2006. Regulation of Legionella phagosome maturation and infection through flagellin and host Ipaf. *Journal of Biological Chemistry,* 281**,** 35217-35223.

AMER, A. O. & SWANSON, M. S. 2005. Autophagy is an immediate macrophage response to Legionella pneumophila. *Cellular microbiology,* 7**,** 765-778.

ASARE, R., SANTIC, M., GOBIN, I., DORIC, M., SUTTLES, J., GRAHAM, J. E., PRICE, C. D. & KWAIK, Y. A. 2007. Genetic susceptibility and caspase activation in mouse and human macrophages are distinct for Legionella longbeachae and L. pneumophila. *Infection and immunity,* 75**,** 1933-1945.

BACKERT, S. & MEYER, T. F. 2006. Type IV secretion systems and their effectors in bacterial pathogenesis. *Current opinion in microbiology,* 9**,** 207-217.

BAI, C., SEN, P., HOFMANN, K., MA, L., GOEBL, M., HARPER, J. W. & ELLEDGE, S. J. 1996. SKP1 connects cell cycle regulators to the ubiquitin proteolysis machinery through a novel motif, the F-box. *Cell,* 86**,** 263-274.

BANDYOPADHYAY, P., LIU, S., GABBAI, C. B., VENITELLI, Z. & STEINMAN, H. M. 2007. Environmental mimics and the Lvh type IVA secretion system contribute to virulence-related phenotypes of Legionella pneumophila. *Infection and immunity,* 75**,** 723-735.

BANGA, S., GAO, P., SHEN, X., FISCUS, V., ZONG, W.-X., CHEN, L. & LUO, Z.-Q. 2007. Legionella pneumophila inhibits macrophage apoptosis by targeting pro-death members of the Bcl2 protein family. *Proceedings of the National Academy of Sciences,* 104**,** 5121-5126.

BARTRAM, J. 2007. *Legionella and the prevention of legionellosis*, World Health Organization.

BARYSHEVA, O. V., FUJII, J., TAKAESU, G. & YOSHIDA, S.-I. 2008. Application of unstable Gfp variants to the kinetic study of Legionella pneumophila icm gene expression during infection. *Microbiology,* 154**,** 1015-1025.

BASKERVILLE, A., CONLAN, J., ASHWORTH, L. & DOWSETT, A. 1986. Pulmonary damage caused by a protease from Legionella pneumophila. *British journal of experimental pathology,* 67**,** 527.

BERGER, K. H. & ISBERG, R. R. 1993. Two distinct defects in intracellular growth complemented by a single genetic locus in Legionella pneumophila. *Molecular microbiology,* 7**,** 7-19.

BERGSBAKEN, T., FINK, S. L. & COOKSON, B. T. 2009. Pyroptosis: host cell death and inflammation. *Nature Reviews Microbiology,* 7**,** 99-109.

BERRINGTON, W. R. & HAWN, T. R. 2013. Human Susceptibility to Legionnaires' Disease. *Legionella.* Springer.

BLANDER, S. J. & HORWITZ, M. A. 1991a. Vaccination with Legionella pneumophila membranes induces cell-mediated and protective immunity in a guinea pig model of Legionnaires' disease. Protective immunity independent of the major secretory protein of Legionella pneumophila. *Journal of Clinical Investigation,* 87**,** 1054.

BLANDER, S. J. & HORWITZ, M. A. 1991b. Vaccination with the major secretory protein of Legionella induces humoral and cell-mediated immune responses and protective immunity across different serogroups of Legionella pneumophila and different species of Legionella. *The Journal of Immunology,* 147**,** 285-291.

BRIELAND, J., FREEMAN, P., KUNKEL, R., CHRISP, C., HURLEY, M., FANTONE, J. & ENGLEBERG, C. 1994. Replicative Legionella pneumophila lung infection in intratracheally inoculated A/J mice. A murine model of human Legionnaires' disease. *The American journal of pathology,* 145**,** 1537.

BROMBACHER, E., URWYLER, S., RAGAZ, C., WEBER, S. S., KAMI, K., OVERDUIN, M. & HILBI, H. 2009. Rab1 guanine nucleotide exchange factor SidM is a major phosphatidylinositol 4-phosphate-binding effector protein of Legionella pneumophila. *Journal of Biological Chemistry,* 284**,** 4846-4856.

BRÜGGEMANN, H., HAGMAN, A., JULES, M., SISMEIRO, O., DILLIES, M. A., GOUYETTE, C., KUNST, F., STEINERT, M., HEUNER, K. & COPPÉE, J. Y. 2006. Virulence strategies for infecting phagocytes deduced from the in vivo transcriptional program of Legionella pneumophila. *Cellular microbiology,* 8**,** 1228-1240.

CARTER, M. Q., CHEN, J. & LORY, S. 2010. The Pseudomonas aeruginosa pathogenicity island PAPI-1 is transferred via a novel type IV pilus. *J Bacteriol,* 192**,** 3249-58.

CARVER, T., THOMSON, N., BLEASBY, A., BERRIMAN, M. & PARKHILL, J. 2009. DNAPlotter: circular and linear interactive genome visualization. *Bioinformatics,* 25**,** 119-120.

CASE, C. L. & ROY, C. R. 2013. Analyzing Caspase-1 Activation During Legionella pneumophila Infection in Macrophages. *Legionella.* Springer.

CAZALET, C., GOMEZ-VALERO, L., RUSNIOK, C., LOMMA, M., DERVINS-RAVAULT, D., NEWTON, H. J., SANSOM, F. M., JARRAUD, S., ZIDANE, N. & MA, L. 2010. Analysis of the Legionella longbeachae genome and transcriptome uncovers unique strategies to cause Legionnaires' disease. *PLoS genetics,* 6**,** e1000851.

CAZALET, C., JARRAUD, S., GHAVI-HELM, Y., KUNST, F., GLASER, P., ETIENNE, J. & BUCHRIESER, C. 2008. Multigenome analysis identifies a worldwide distributed epidemic Legionella pneumophila clone that emerged within a highly diverse species. *Genome research,* 18**,** 431-441.

CAZALET, C., RUSNIOK, C., BRÜGGEMANN, H., ZIDANE, N., MAGNIER, A., MA, L., TICHIT, M., JARRAUD, S., BOUCHIER, C. & VANDENESCH, F. 2004. Evidence in the Legionella pneumophila genome for exploitation of host cell functions and high genome plasticity. *Nature genetics,* 36**,** 1165-1173.

CHIEN, M., MOROZOVA, I., SHI, S., SHENG, H., CHEN, J., GOMEZ, S. M., ASAMANI, G., HILL, K., NUARA, J. & FEDER, M. 2004. The genomic sequence of the accidental pathogen Legionella pneumophila. *Science,* 305**,** 1966-1968.

CHOY, A., DANCOURT, J., MUGO, B., O'CONNOR, T. J., ISBERG, R. R., MELIA, T. J. & ROY, C. R. 2012. The Legionella effector RavZ inhibits host autophagy through irreversible Atg8 deconjugation. *Science,* 338**,** 1072-1076.

CHRISTIE, P. J. 2001. Type IV secretion: intercellular transfer of macromolecules by systems ancestrally related to conjugation machines. *Molecular microbiology,* 40**,** 294-305.
CHRISTIE, P. J., ATMAKURI, K., KRISHNAMOORTHY, V., JAKUBOWSKI, S. & CASCALES, E. 2005. Biogenesis, architecture, and function of bacterial type IV secretion systems. *Annual review of microbiology,* 59.
CIANCIOTTO, N., EISENSTEIN, B., MODY, C., TOEWS, G. & ENGLEBERG, N. 1989. A Legionella pneumophila gene encoding a species-specific surface protein potentiates initiation of intracellular infection. *Infection and Immunity,* 57**,** 1255-1262.
CIRILLO, S. L., BERMUDEZ, L. E., EL-ETR, S. H., DUHAMEL, G. E. & CIRILLO, J. D. 2001. Legionella pneumophila Entry GenertxA Is Involved in Virulence. *Infection and immunity,* 69**,** 508-517.
CRUSIO, K., KING, B., REAVIE, L. & AIFANTIS, I. 2010. The ubiquitous nature of cancer: the role of the SCFFbw7 complex in development and transformation. *Oncogene,* 29**,** 4865-4873.
DALEBROUX, Z. D., SVENSSON, S. L., GAYNOR, E. C. & SWANSON, M. S. 2010. ppGpp conjures bacterial virulence. *Microbiology and Molecular Biology Reviews,* 74**,** 171-199.
DAVIS, R. J., WELCKER, M. & CLURMAN, B. E. 2014. Tumor suppression by the Fbw7 ubiquitin ligase: mechanisms and opportunities. *Cancer cell,* 26**,** 455-464.
DE FELIPE, K. S., PAMPOU, S., JOVANOVIC, O. S., PERICONE, C. D., SENNA, F. Y., KALACHIKOV, S. & SHUMAN, H. A. 2005. Evidence for acquisition of Legionella type IV secretion substrates via interdomain horizontal gene transfer. *Journal of bacteriology,* 187**,** 7716-7726.
DIEFFENBACH, C. W. & DVEKSLER, G. 1995. PCR primer. *A laboratory manual. Cold Spring Harbor, NY*.
DIEZ, E., LEE, S.-H., GAUTHIER, S., YARAGHI, Z., TREMBLAY, M., VIDAL, S. & GROS, P. 2003. Birc1e is the gene within the Lgn1 locus associated with resistance to Legionella pneumophila. *Nature genetics,* 33**,** 55-60.
DINKEL, H., VAN ROEY, K., MICHAEL, S., DAVEY, N. E., WEATHERITT, R. J., BORN, D., SPECK, T., KRÜGER, D., GREBNEV, G. & KUBAŃ, M. 2013. The eukaryotic linear motif resource ELM: 10 years and counting. *Nucleic acids research***,** gkt1047.
DOBRINDT, U., HOCHHUT, B., HENTSCHEL, U. & HACKER, J. 2004. Genomic islands in pathogenic and environmental microorganisms. *Nat Rev Microbiol,* 2**,** 414-24.
DOLÉANS-JORDHEIM, A., AKERMI, M., GINEVRA, C., CAZALET, C., KAY, E., SCHNEIDER, D., BUCHRIESER, C., ATLAN, D., VANDENESCH, F. & ETIENNE, J. 2006. Growth-phase-dependent mobility of the lvh-encoding region in Legionella pneumophila strain Paris. *Microbiology,* 152**,** 3561-3568.
ECKELMAN, B. P., SALVESEN, G. S. & SCOTT, F. L. 2006. Human inhibitor of apoptosis proteins: why XIAP is the black sheep of the family. *EMBO reports,* 7**,** 988-994.
EDELSTEIN, P. H. 2013. The Guinea pig model of legionnaires' disease. *Legionella.* Springer.
EDELSTEIN, P. H., CALARCO, K. & YASUI, V. K. 1984. Antimicrobial Therapy of Experimentally Induced Legionnaires' Disease in Guinea Pigs 1–3. *American Review of Respiratory Disease,* 130**,** 849-856.
EDELSTEIN, P. H., HU, B., HIGA, F. & EDELSTEIN, M. A. 2003. lvgA, a novel Legionella pneumophila virulence factor. *Infection and immunity,* 71**,** 2394-2403.
ENSMINGER, A. W. & ISBERG, R. R. 2009. Legionella pneumophila Dot/Icm translocated substrates: a sum of parts. *Current opinion in microbiology,* 12**,** 67-73.
ERNST, J. D., TREVEJO-NUÑEZ, G. & BANAIEE, N. 2007. Genomics and the evolution, pathogenesis, and diagnosis of tuberculosis. *Journal of Clinical Investigation,* 117**,** 1738.
EUROPEAN CENTRE FOR DISEASE PREVENTION AND CONTROL 2015. Legionnaires' disease in Europe 2013. *ECDC Surveillance Report*.
FAUCHER, S. P., MUELLER, C. A. & SHUMAN, H. A. 2011. Legionella pneumophila transcriptome during intracellular multiplication in human macrophages. *Frontiers in Microbiology,* 2.
FIELDS, B. S. 1996. The molecular ecology of legionellae. *Trends in microbiology,* 4**,** 286-290.

FINLAY, B. B. & FALKOW, S. 1997. Common themes in microbial pathogenicity revisited. *Microbiology and Molecular Biology Reviews,* 61**,** 136-169.
FINLEY, D. 2009. Recognition and processing of ubiquitin-protein conjugates by the proteasome. *Annual review of biochemistry,* 78**,** 477.
FISCHER, G., BANG, H., LUDWIG, B., MANN, K. & HACKER, J. 1992. Mip protein of Legionella pneumophila exhibits peptidyl-prolyl-cis/trans isomerase (PPIase) activity. *Molecular microbiology,* 6**,** 1375-1383.
FRASER, D. W., TSAI, T. R., ORENSTEIN, W., PARKIN, W. E., BEECHAM, H. J., SHARRAR, R. G., HARRIS, J., MALLISON, G. F., MARTIN, S. M., MCDADE, J. E., SHEPARD, C. C. & BRACHMAN, P. S. 1977. Legionnaires' disease: description of an epidemic of pneumonia. *N Engl J Med,* 297**,** 1189-97.
FRONZES, R., CHRISTIE, P. J. & WAKSMAN, G. 2009. The structural biology of type IV secretion systems. *Nature Reviews Microbiology,* 7**,** 703-714.
FUCHE, F., VIANNEY, A., ANDREA, C., DOUBLET, P. & GILBERT, C. 2015. Functional type 1 secretion system involved in Legionella pneumophila virulence. *Journal of bacteriology,* 197**,** 563-571.
GARCÍA-FULGUEIRAS, A., NAVARRO, C., FENOLL, D., GARCÍA, J., GONZÁLEZ-DIEGO, P., JIMÉNEZ-BUÑUALES, T., RODRIGUEZ, M., LOPEZ, R., PACHECO, F. & RUIZ, J. 2003. Legionnaires' disease outbreak in Murcia, Spain. *Emerging infectious diseases,* 9**,** 915-921.
GARDUNO, R. A., GARDUNO, E., HILTZ, M. & HOFFMAN, P. S. 2002. Intracellular growth of Legionella pneumophila gives rise to a differentiated form dissimilar to stationary-phase forms. *Infection and immunity,* 70**,** 6273-6283.
GOMEZ-VALERO, L., RUSNIOK, C. & BUCHRIESER, C. 2009. Legionella pneumophila: population genetics, phylogeny and genomics. *Infection, genetics and evolution,* 9**,** 727-739.
GOMEZ-VALERO, L., RUSNIOK, C., JARRAUD, S., VACHERIE, B., ROUY, Z., BARBE, V., MEDIGUE, C., ETIENNE, J. & BUCHRIESER, C. 2011. Extensive recombination events and horizontal gene transfer shaped the Legionella pneumophila genomes. *BMC genomics,* 12**,** 536.
GOMEZ-VALERO, L., RUSNIOK, C., ROLANDO, M., NEOU, M., DERVINS-RAVAULT, D., DEMIRTAS, J., ROUY, Z., MOORE, R. J., CHEN, H., PETTY, N. K., JARRAUD, S., ETIENNE, J., STEINERT, M., HEUNER, K., GRIBALDO, S., MEDIGUE, C., GLOCKNER, G., HARTLAND, E. L. & BUCHRIESER, C. 2014. Comparative analyses of Legionella species identifies genetic features of strains causing Legionnaires' disease. *Genome Biol,* 15**,** 505.
HACKER, J., BLUM-OEHLER, G., MÜHLDORFER, I. & TSCHÄPE, H. 1997. Pathogenicity islands of virulent bacteria: structure, function and impact on microbial evolution. *Molecular microbiology,* 23**,** 1089-1097.
HAM, H., SREELATHA, A. & ORTH, K. 2011. Manipulation of host membranes by bacterial effectors. *Nature Reviews Microbiology,* 9.
HAO, Y., SEKINE, K., KAWABATA, A., NAKAMURA, H., ISHIOKA, T., OHATA, H., KATAYAMA, R., HASHIMOTO, C., ZHANG, X. & NODA, T. 2004. Apollon ubiquitinates SMAC and caspase-9, and has an essential cytoprotection function. *Nature cell biology,* 6**,** 849-860.
HARDING, C. R., MATTHEIS, C., MOUSNIER, A., OATES, C. V., HARTLAND, E. L., FRANKEL, G. & SCHROEDER, G. N. 2013. LtpD is a novel Legionella pneumophila effector that binds phosphatidylinositol 3-phosphate and inositol monophosphatase IMPA1. *Infect Immun,* 81**,** 4261-70.
HARDING, C. R., SCHROEDER, G. N., REYNOLDS, S., KOSTA, A., COLLINS, J. W., MOUSNIER, A. & FRANKEL, G. 2012. Legionella pneumophila pathogenesis in the Galleria mellonella infection model. *Infection and immunity,* 80**,** 2780-2790.
HARRISON, E. M., CARTER, M. E., LUCK, S., OU, H. Y., HE, X., DENG, Z., O'CALLAGHAN, C., KADIOGLU, A. & RAJAKUMAR, K. 2010. Pathogenicity islands PAPI-1 and PAPI-2 contribute individually and synergistically to the virulence of Pseudomonas aeruginosa strain PA14. *Infect Immun,* 78**,** 1437-46.
HEALTH PROTECTION SCOTLAND 2013. Increased incidence of Legionnaires' disease caused by Legionella longbeachae in Scotland. *Health Protection Scotland.*

HEALTH PROTECTION SCOTLAND 2014. Cluster of Legionella longbeachae cases in Scotland in September/October 2013. *Health Protection Scotland.*
HIGUCHI, R., FOCKLER, C., DOLLINGER, G. & WATSON, R. 1993. Kinetic PCR analysis: real-time monitoring of DNA amplification reactions. *Biotechnology,* 11**,** 1026-1030.
HILBI, H., SEGAL, G. & SHUMAN, H. A. 2001. Icm/Dot-dependent upregulation of phagocytosis by Legionella pneumophila. *Molecular microbiology,* 42**,** 603-617.
HORI, J. I. & ZAMBONI, D. S. 2013. The Mouse as a Model for Pulmonary Legionella Infection. *Legionella.* Springer.
HORWITZ, M. A. 1983a. Formation of a novel phagosome by the Legionnaires' disease bacterium (Legionella pneumophila) in human monocytes. *The Journal of experimental medicine,* 158**,** 1319-1331.
HORWITZ, M. A. 1983b. The Legionnaires' disease bacterium (Legionella pneumophila) inhibits phagosome-lysosome fusion in human monocytes. *The Journal of experimental medicine,* 158**,** 2108-2126.
HUBBER, A. & ROY, C. R. 2010. Modulation of host cell function by Legionella pneumophila type IV effectors. *Annual review of cell and developmental biology,* 26**,** 261-283.
HUNG, A. Y. & SHENG, M. 2002. PDZ domains: structural modules for protein complex assembly. *Journal of Biological Chemistry,* 277**,** 5699-5702.
ICHIMURA, Y., KIRISAKO, T., TAKAO, T., SATOMI, Y., SHIMONISHI, Y., ISHIHARA, N., MIZUSHIMA, N., TANIDA, I., KOMINAMI, E. & OHSUMI, M. 2000. A ubiquitin-like system mediates protein lipidation. *Nature,* 408**,** 488-492.
ISBERG, R. R., O'CONNOR, T. J. & HEIDTMAN, M. 2009. The Legionella pneumophila replication vacuole: making a cosy niche inside host cells. *Nature Reviews Microbiology,* 7**,** 13-24.
JARRAUD, S., DESCOURS, G., GINEVRA, C., LINA, G. & ETIENNE, J. 2013. Identification of Legionella in clinical samples. *Legionella.* Springer.
JENUWEIN, T., LAIBLE, G., DORN, R. & REUTER, G. 1998. SET domain proteins modulate chromatin domains in eu-and heterochromatin. *Cellular and Molecular Life Sciences CMLS,* 54**,** 80-93.
JOSEPH, C. & RICKETTS, K. 2010. Legionnaires disease in Europe 2007-2008. *Euro Surveillance: Bulletin europeen sur les maladies transmissibles= European communicable disease bulletin,* 15**,** 19493-19493.
JUHAS, M., CROOK, D. W., DIMOPOULOU, I. D., LUNTER, G., HARDING, R. M., FERGUSON, D. J. & HOOD, D. W. 2007. Novel type IV secretion system involved in propagation of genomic islands. *Journal of bacteriology,* 189**,** 761-771.
JUHAS, M., CROOK, D. W. & HOOD, D. W. 2008. Type IV secretion systems: tools of bacterial horizontal gene transfer and virulence. *Cellular microbiology,* 10**,** 2377-2386.
KABEYA, Y., MIZUSHIMA, N., UENO, T., YAMAMOTO, A., KIRISAKO, T., NODA, T., KOMINAMI, E., OHSUMI, Y. & YOSHIMORI, T. 2000. LC3, a mammalian homologue of yeast Apg8p, is localized in autophagosome membranes after processing. *The EMBO journal,* 19**,** 5720-5728.
KLOCKGETHER, J., REVA, O., LARBIG, K. & TUMMLER, B. 2004. Sequence analysis of the mobile genome island pKLC102 of Pseudomonas aeruginosa C. *J Bacteriol,* 186**,** 518-34.
KOCH, C. A., ANDERSON, D., MORAN, M. F., ELLIS, C. & PAWSON, T. 1991. SH2 and SH3 domains: elements that control interactions of cytoplasmic signaling proteins. *Science,* 252**,** 668-674.
KOZAK, N. A., LUCAS, C. E. & WINCHELL, J. M. 2013. Identification of Legionella in the environment. *Legionella.* Springer.
LAUTNER, M., SCHUNDER, E., HERRMANN, V. & HEUNER, K. 2013. Regulation, integrase-dependent excision, and horizontal transfer of genomic islands in Legionella pneumophila. *Journal of bacteriology,* 195**,** 1583-1597.
LAWLEY, T., KLIMKE, W., GUBBINS, M. & FROST, L. 2003. F factor conjugation is a true type IV secretion system. *FEMS microbiology letters,* 224**,** 1-15.
LENS, S. M., VADER, G. & MEDEMA, R. H. 2006. The case for Survivin as mitotic regulator. *Current opinion in cell biology,* 18**,** 616-622.

LI, L., STOECKERT, C. J. & ROOS, D. S. 2003. OrthoMCL: identification of ortholog groups for eukaryotic genomes. *Genome research,* 13**,** 2178-2189.
LI, T., LU, Q., WANG, G., XU, H., HUANG, H., CAI, T., KAN, B., GE, J. & SHAO, F. 2013. SET-domain bacterial effectors target heterochromatin protein 1 to activate host rDNA transcription. *EMBO reports,* 14**,** 733-740.
LIGHTFIELD, K. L., PERSSON, J., BRUBAKER, S. W., WITTE, C. E., VON MOLTKE, J., DUNIPACE, E. A., HENRY, T., SUN, Y.-H., CADO, D. & DIETRICH, W. F. 2008. Critical function for Naip5 in inflammasome activation by a conserved carboxy-terminal domain of flagellin. *Nature immunology,* 9**,** 1171-1178.
LOCHT, C., COUTTE, L. & MIELCAREK, N. 2011. The ins and outs of pertussis toxin. *FEBS Journal,* 278**,** 4668-4682.
LOMMA, M., GOMEZ VALERO, L., RUSNIOK, C. & BUCHRIESER, C. 2009. Legionella pneumophila–host interactions: insights gained from comparative genomics and cell biology.
LOSICK, V. P. & ISBERG, R. R. 2006. NF-κB translocation prevents host cell death after low-dose challenge by Legionella pneumophila. *The Journal of experimental medicine,* 203**,** 2177-2189.
MANDELL, L. A., WUNDERINK, R. G., ANZUETO, A., BARTLETT, J. G., CAMPBELL, G. D., DEAN, N. C., DOWELL, S. F., FILE, T. M., MUSHER, D. M. & NIEDERMAN, M. S. 2007. Infectious Diseases Society of America/American Thoracic Society consensus guidelines on the management of community-acquired pneumonia in adults. *Clinical infectious diseases,* 44**,** S27-S72.
MARCOTRIGIANO, J., GINGRAS, A.-C., SONENBERG, N. & BURLEY, S. K. 1999. Cap-dependent translation initiation in eukaryotes is regulated by a molecular mimic of eIF4G. *Molecular cell,* 3**,** 707-716.
MARRA, A., BLANDER, S. J., HORWITZ, M. A. & SHUMAN, H. A. 1992. Identification of a Legionella pneumophila locus required for intracellular multiplication in human macrophages. *Proceedings of the National Academy of Sciences,* 89**,** 9607-9611.
MCADAM, P., VAN DER BROEK, C., LINDSAY, D., WARD, M., HANSON, M., GILLIES, M., WATSON, M., STEVENS, J., EDWARDS, G. & FITZGERALD, R. 2014. Gene flow in environmental Legionella pneumophila leads to genetic and pathogenic heterogeneity within a Legionnaires' disease outbreak. *Genome Biol,* 15**,** 504.
MCCORMICK, D., THORN, S., MILNE, D., EVANS, C., STEVENSON, J., LLANO, M. & DONAGHY, M. 2012. Public health response to an outbreak of Legionnaires' disease in Edinburgh, United Kingdom, June 2012. *Euro Surveill,* 17.
MCCOY-SIMANDLE, K., STEWART, C. R., DAO, J., DEBROY, S., ROSSIER, O., BRYCE, P. J. & CIANCIOTTO, N. P. 2011. Legionella pneumophila type II secretion dampens the cytokine response of infected macrophages and epithelia. *Infection and immunity,* 79**,** 1984-1997.
MCDADE, J. E., SHEPARD, C. C., FRASER, D. W., TSAI, T. R., REDUS, M. A. & DOWDLE, W. R. 1977. Legionnaires' disease: isolation of a bacterium and demonstration of its role in other respiratory disease. *New England Journal of Medicine,* 297**,** 1197-1203.
MIYAMOTO, H., YOSHIDA, S.-I., TANIGUCHI, H. & SHUMAN, H. A. 2003. Virulence conversion of Legionella pneumophila by conjugal transfer of chromosomal DNA. *Journal of bacteriology,* 185**,** 6712-6718.
MOLOFSKY, A. B. & SWANSON, M. S. 2003. Legionella pneumophila CsrA is a pivotal repressor of transmission traits and activator of replication. *Molecular microbiology,* 50**,** 445-461.
NEWTON, H. J., ANG, D. K., VAN DRIEL, I. R. & HARTLAND, E. L. 2010. Molecular pathogenesis of infections caused by Legionella pneumophila. *Clinical microbiology reviews,* 23**,** 274-298.
NINIO, S. & ROY, C. R. 2007. Effector proteins translocated by Legionella pneumophila: strength in numbers. *Trends in Microbiology,* 15**,** 372-380.
OLIVER, J. D. 2010. Recent findings on the viable but nonculturable state in pathogenic bacteria. *FEMS microbiology reviews,* 34**,** 415-425.
ORME, M. & MEIER, P. 2009. Inhibitor of apoptosis proteins in Drosophila: gatekeepers of death. *Apoptosis,* 14**,** 950-960.

PARHAMIFAR, L., ANDERSEN, H. & MOGHIMI, S. M. 2013. Lactate dehydrogenase assay for assessment of polycation cytotoxicity. *Nanotechnology for Nucleic Acid Delivery.* Springer.

PAULIN, S. M., JAGANNATHAN, A., CAMPBELL, J., WALLIS, T. S. & STEVENS, M. P. 2007. Net replication of Salmonella enterica serovars Typhimurium and Choleraesuis in porcine intestinal mucosa and nodes is associated with their differential virulence. *Infection and immunity,* 75**,** 3950-3960.

PAUNOLA, E., MATTILA, P. K. & LAPPALAINEN, P. 2002. WH2 domain: a small, versatile adapter for actin monomers. *FEBS letters,* 513**,** 92-97.

PETROSKI, M. D. & DESHAIES, R. J. 2005. Function and regulation of cullin–RING ubiquitin ligases. *Nature reviews Molecular cell biology,* 6**,** 9-20.

PFAFFL, M. W. 2001. A new mathematical model for relative quantification in real-time RT–PCR. *Nucleic acids research,* 29**,** e45-e45.

POTTS, A., DONAGHY, M., MARLEY, M., OTHIENO, R., STEVENSON, J., HYLAND, J., POLLOCK, K., LINDSAY, D., EDWARDS, G. & HANSON, M. 2013. Cluster of Legionnaires disease cases caused by Legionella longbeachae serogroup 1, Scotland, August to September 2013. *Euro Surveill,* 18**,** 20656.

PRASHAR, A. & TEREBIZNIK, M. R. 2015. Legionella pneumophila: homeward bound away from the phagosome. *Current opinion in microbiology,* 23**,** 86-93.

PRICE, C. T., AL-KHODOR, S., AL-QUADAN, T., SANTIC, M., HABYARIMANA, F., KALIA, A. & KWAIK, Y. A. 2009. Molecular mimicry by an F-box effector of Legionella pneumophila hijacks a conserved polyubiquitination machinery within macrophages and protozoa. *PLoS Pathog,* 5**,** e1000704-e1000704.

PRICE, C. T., AL-QUADAN, T., SANTIC, M., JONES, S. C. & KWAIK, Y. A. 2010. Exploitation of conserved eukaryotic host cell farnesylation machinery by an F-box effector of Legionella pneumophila. *The Journal of experimental medicine,* 207**,** 1713-1726.

PRICE, C. T., AL-QUADAN, T., SANTIC, M., ROSENSHINE, I. & KWAIK, Y. A. 2011. Host proteasomal degradation generates amino acids essential for intracellular bacterial growth. *Science,* 334**,** 1553-1557.

PRUNELL, G. F. & TROY, C. M. 2004. Balancing neuronal death. *Journal of neuroscience research,* 78**,** 1-6.

RASMUSSEN, R. 2001. Quantification on the LightCycler. *Rapid cycle real-time PCR.* Springer.

RECHNITZER, C. & KHARAZMI, A. 1992. Effect of Legionella pneumophila cytotoxic protease on human neutrophil and monocyte function. *Microbial pathogenesis,* 12**,** 115-125.

ROLANDO, M. & BUCHRIESER, C. 2014. Legionella pneumophila type IV effectors hijack the transcription and translation machinery of the host cell. *Trends in cell biology,* 24**,** 771-778.

ROLANDO, M., SANULLI, S., RUSNIOK, C., GOMEZ-VALERO, L., BERTHOLET, C., SAHR, T., MARGUERON, R. & BUCHRIESER, C. 2013. Legionella pneumophila effector RomA uniquely modifies host chromatin to repress gene expression and promote intracellular bacterial replication. *Cell host & microbe,* 13**,** 395-405.

SALVESEN, G. S. & DUCKETT, C. S. 2002. IAP proteins: blocking the road to death's door. *Nature reviews Molecular cell biology,* 3**,** 401-410.

SAMRAKANDI, M. M., CIRILLO, S. L., RIDENOUR, D. A., BERMUDEZ, L. E. & CIRILLO, J. D. 2002. Genetic and phenotypic differences between Legionella pneumophila strains. *Journal of clinical microbiology,* 40**,** 1352-1362.

SANTIC, M., MOLMERET, M. & KWAIK, Y. A. 2005. Maturation of the Legionella pneumophila-containing phagosome into a phagolysosome within gamma interferon-activated macrophages. *Infection and immunity,* 73**,** 3166-3171.

SCHROEDER, G. N., PETTY, N. K., MOUSNIER, A., HARDING, C. R., VOGRIN, A. J., WEE, B., FRY, N. K., HARRISON, T. G., NEWTON, H. J. & THOMSON, N. R. 2010. Legionella pneumophila strain 130b possesses a unique combination of type IV secretion systems and novel Dot/Icm secretion system effector proteins. *Journal of bacteriology,* 192**,** 6001-6016.

SCHWARTZ, A. L. & CIECHANOVER, A. 2009. Targeting proteins for destruction by the ubiquitin system: implications for human pathobiology. *Annual review of pharmacology and toxicology,* 49**,** 73-96.

SEEMANN, T. 2014. Prokka: rapid prokaryotic genome annotation. *Bioinformatics***,** btu153.

SEGAL, E., CHA, J., LO, J., FALKOW, S. & TOMPKINS, L. 1999a. Altered states: involvement of phosphorylated CagA in the induction of host cellular growth changes by Helicobacter pylori. *Proceedings of the National Academy of Sciences,* 96**,** 14559-14564.

SEGAL, G., RUSSO, J. J. & SHUMAN, H. A. 1999b. Relationships between a new type IV secretion system and the icm/dot virulence system of Legionella pneumophila. *Molecular microbiology,* 34**,** 799-809.

SETH-SMITH, H. M., FOOKES, M. C., OKORO, C. K., BAKER, S., HARRIS, S. R., SCOTT, P., PICKARD, D., QUAIL, M. A., CHURCHER, C. & SANDERS, M. 2012. Structure, diversity, and mobility of the Salmonella pathogenicity island 7 family of integrative and conjugative elements within Enterobacteriaceae. *Journal of bacteriology,* 194**,** 1494-1504.

SILVEIRA, T. N. & ZAMBONI, D. S. 2010. Pore formation triggered by Legionella spp. is an Nlrc4 inflammasome-dependent host cell response that precedes pyroptosis. *Infection and immunity,* 78**,** 1403-1413.

STONE, B. J. & KWAIK, Y. A. 1999. Natural competence for DNA transformation by Legionella pneumophila and its association with expression of type IV pili. *Journal of bacteriology,* 181**,** 1395-1402.

SULLIVAN, M. J., PETTY, N. K. & BEATSON, S. A. 2011. Easyfig: a genome comparison visualizer. *Bioinformatics,* 27**,** 1009-1010.

SWANSON, M. & HAMMER, B. 2000. Legionella pneumophila pathogenesis: a fateful journey from amoebae to macrophages. *Annual Reviews in Microbiology,* 54**,** 567-613.

SZETO, L. & SHUMAN, H. A. 1990. The Legionella pneumophila major secretory protein, a protease, is not required for intracellular growth or cell killing. *Infect Immun,* 58**,** 2585-92.

TAM, V. C., SERRUTO, D., DZIEJMAN, M., BRIEHER, W. & MEKALANOS, J. J. 2007. A type III secretion system in Vibrio cholerae translocates a formin/spire hybrid-like actin nucleator to promote intestinal colonization. *Cell host & microbe,* 1**,** 95-107.

TANIDA, I., UENO, T. & KOMINAMI, E. 2004. LC3 conjugation system in mammalian autophagy. *The international journal of biochemistry & cell biology,* 36**,** 2503-2518.

TIADEN, A. N., KESSLER, A. & HILBI, H. 2013. Analysis of Legionella infection by flow cytometry. *Legionella.* Springer.

TILNEY, L. G., HARB, O. S., CONNELLY, P. S., ROBINSON, C. G. & ROY, C. R. 2001. How the parasitic bacterium Legionella pneumophila modifies its phagosome and transforms it into rough ER: implications for conversion of plasma membrane to the ER membrane. *Journal of Cell Science,* 114**,** 4637-4650.

TSAI, T. F., FINN, D. R., PLIKAYTIS, B. D., MCCAULEY, W., MARTIN, S. M. & FRASER, D. W. 1979. Legionnaires' disease: clinical features of the epidemic in Philadelphia. *Annals of internal medicine,* 90**,** 509-517.

TYSON, J. Y., PEARCE, M. M., VARGAS, P., BAGCHI, S., MULHERN, B. J. & CIANCIOTTO, N. P. 2013. Multiple Legionella pneumophila type II secretion substrates, including a novel protein, contribute to differential infection of the amoebae Acanthamoeba castellanii, Hartmannella vermiformis, and Naegleria lovaniensis. *Infection and immunity,* 81**,** 1399-1410.

VENKATARAMAN, C., HAACK, B. J., BONDADA, S. & KWAIK, Y. A. 1997. Identification of a Gal/GalNAc lectin in the protozoan Hartmannella vermiformis as a potential receptor for attachment and invasion by the Legionnaires' disease bacterium. *The Journal of experimental medicine,* 186**,** 537-547.

VERGUNST, A. C., SCHRAMMEIJER, B., DEN DULK-RAS, A., DE VLAAM, C. M., REGENSBURG-TUıNK, T. J. & HOOYKAAS, P. J. 2000. VirB/D4-dependent protein translocation from Agrobacterium into plant cells. *Science,* 290**,** 979-982.

VUCIC, D. & FAIRBROTHER, W. J. 2007. The inhibitor of apoptosis proteins as therapeutic targets in cancer. *Clinical Cancer Research,* 13**,** 5995-6000.

WAGNER, C., KHAN, A. S., KAMPHAUSEN, T., SCHMAUSSER, B., ÜNAL, C., LORENZ, U., FISCHER, G., HACKER, J. & STEINERT, M. 2007. Collagen binding protein Mip enables Legionella pneumophila to transmigrate through a barrier of NCI-H292 lung epithelial cells and extracellular matrix. *Cellular microbiology,* 9**,** 450-462.

WEE, B. A., WOOLFIT, M., BEATSON, S. A. & PETTY, N. K. 2013. A distinct and divergent lineage of genomic island-associated type IV Secretion Systems in Legionella. *PloS one,* 8**,** e82221.

WELCKER, M. & CLURMAN, B. E. 2008. FBW7 ubiquitin ligase: a tumour suppressor at the crossroads of cell division, growth and differentiation. *Nature Reviews Cancer,* 8**,** 83-93.

XIE, Z. & KLIONSKY, D. J. 2007. Autophagosome formation: core machinery and adaptations. *Nature cell biology,* 9**,** 1102-1109.

XU, J.-N., YANG, Z.-W., CHEN, J.-P., CHEN, D.-L., WANG, T., LIU, M.-J., ZHANG, L. & YANG, B.-B. 2012. Protective immunity against Legionnaires' disease in an A/J mouse model using a DNA vaccine composed of an outer membrane protein (29 kDa) and the PilE fusion protein. *Diagnostic microbiology and infectious disease,* 73**,** 9-15.

XU, L. & LUO, Z.-Q. 2013. Cell biology of infection by Legionella pneumophila. *Microbes and Infection,* 15**,** 157-167.

XU, L., SHEN, X., BRYAN, A., BANGA, S., SWANSON, M. S. & LUO, Z.-Q. 2010. Inhibition of host vacuolar H+-ATPase activity by a Legionella pneumophila effector. *PLoS pathogens,* 6**,** e1000822.

YADA, M., HATAKEYAMA, S., KAMURA, T., NISHIYAMA, M., TSUNEMATSU, R., IMAKI, H., ISHIDA, N., OKUMURA, F., NAKAYAMA, K. & NAKAYAMA, K. I. 2004. Phosphorylation-dependent degradation of c-Myc is mediated by the F-box protein Fbw7. *The EMBO journal,* 23**,** 2116-2125.

YU, B., CHENG, H.-C., BRAUTIGAM, C. A., TOMCHICK, D. R. & ROSEN, M. K. 2011. Mechanism of actin filament nucleation by the bacterial effector VopL. *Nature structural & molecular biology,* 18**,** 1068-1074.

ZHANG, X. L., TSUI, I. S., YIP, C. M., FUNG, A. W., WONG, D. K., DAI, X., YANG, Y., HACKETT, J. & MORRIS, C. 2000. Salmonella enterica serovar typhi uses type IVB pili to enter human intestinal epithelial cells. *Infect Immun,* 68**,** 3067-73.

ZHENG, N., SCHULMAN, B. A., SONG, L., MILLER, J. J., JEFFREY, P. D., WANG, P., CHU, C., KOEPP, D. M., ELLEDGE, S. J. & PAGANO, M. 2002. Structure of the Cul1–Rbx1–Skp1–F boxSkp2 SCF ubiquitin ligase complex. *Nature,* 416**,** 703-709.

ZOU, L., NAN, C. & HU, F. 2013. Accurate prediction of bacterial type IV secreted effectors using amino acid composition and PSSM profiles. *Bioinformatics,* 29**,** 3135-3142.